Multiscale isogeometric fracture simulation

XFEM, IGA, Embedded interfaces, digital twins

Stéphane P.A. Bordas, Lars Beex, Pierre Kerfriden, Elena Atroshchenko, Xuan Peng, Haojie Lian, Ahmad Akbari, Olivier Goury, Hussein Rappel

Computational mechanics & computational materials sciences Multiscale/field interface problems

COMPETENCES

DISCRETISATION
discrete and continuum approaches

MULTI-SCALE FRACTURE
aerospace composites, polycrystalline materials

COUPLED PROBLEMS
biofilms, liquid crystals, fluid-structure, batteries

QUALITY & ERROR CONTROL
optimise computational time given an accuracy level

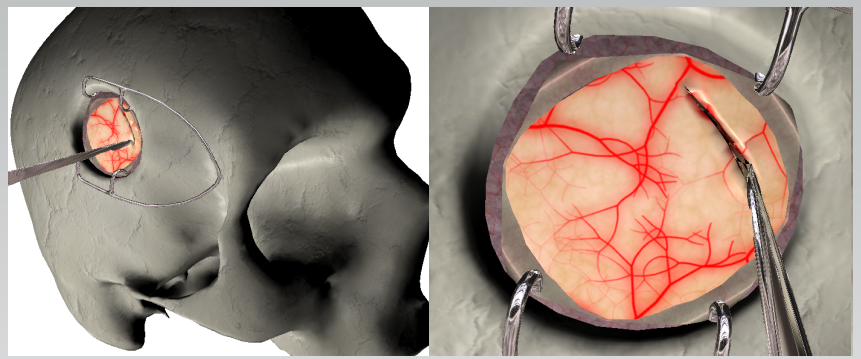

Real-time simulation of cutting during brain surgery

INTERACTIVITY
Reduce computational costs by several orders of magnitude

APPLICATIONS

PERSONALISED MEDICINE

Computer-aided surgery

Computer-aided diagnostics

ENGINEERING

Durability & Sustainability

Energy

Aerospace

http://legato-team.eu — stephane.bordas@uni.lu S. Bordas, B. Peters, A. Zilian and S. Belouettar (LIST)

Discretisation

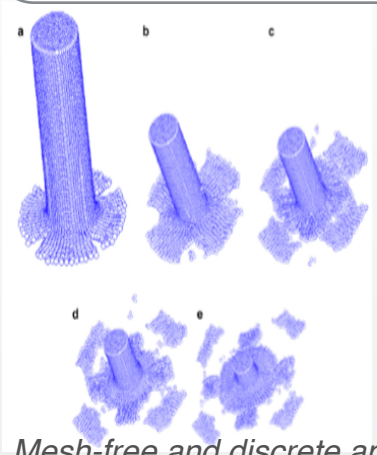

Mesh-free and discrete approaches to fracture

Fracture over multiple scales

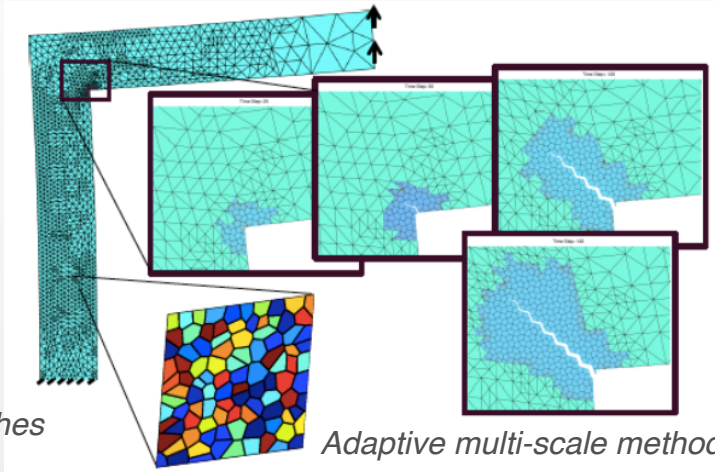

Adaptive multi-scale methods

Coupled problems

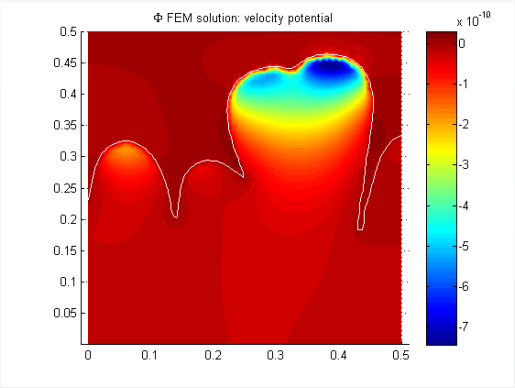

Biofilm growth

Quality and error control

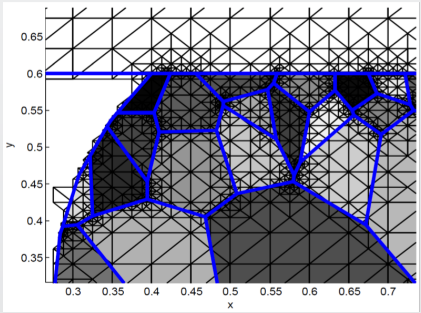

Durability of Pb-free solders

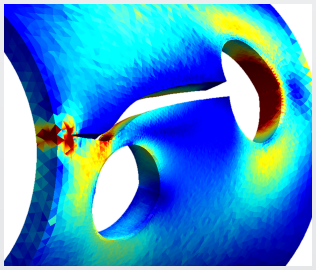

Error estimates for fracture

Interactivity and model order reduction

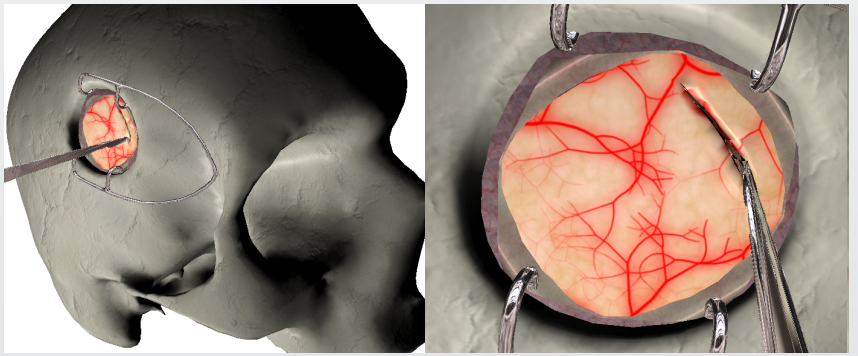

APPLICATIONS

Personalised Medicine

Computer-aided surgery

Computer-aided diagnostics

Engineering

Durability & Sustainability

Energy

Aerospace

Motivation: fracture of engineering structures and materials

- **Limerick**: unidirectional composites

thesis L. Cahill, 2014

- **China/USA**: hydraulic fracturing (shale gas)

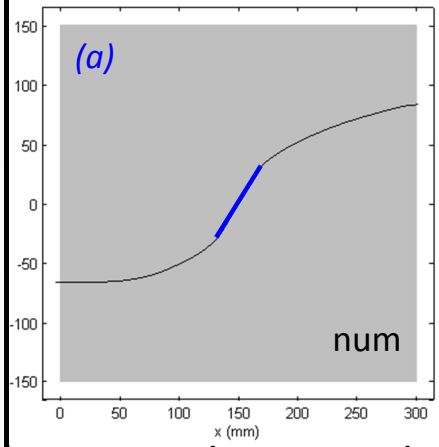

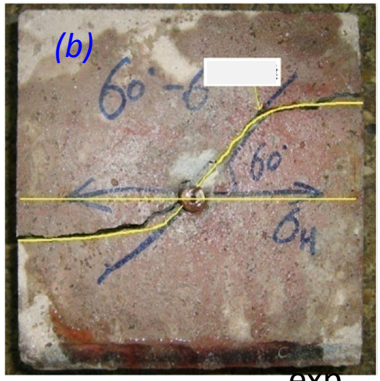

thesis M. Sheng, USA, China, 2016

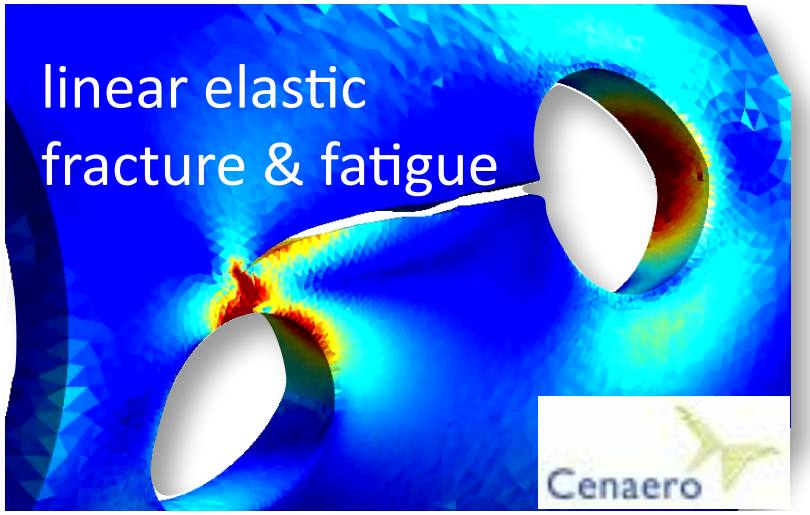

dynamics ductile

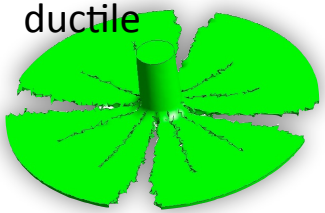

dynamics/brittle

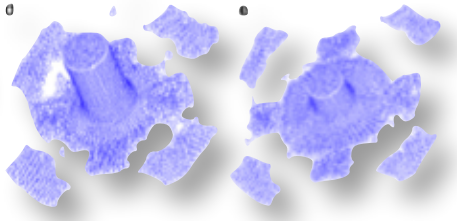

Motivation: multiscale fracture of engineering structures and materials

Solder joint durability (microelectronics), Bosch GmbH

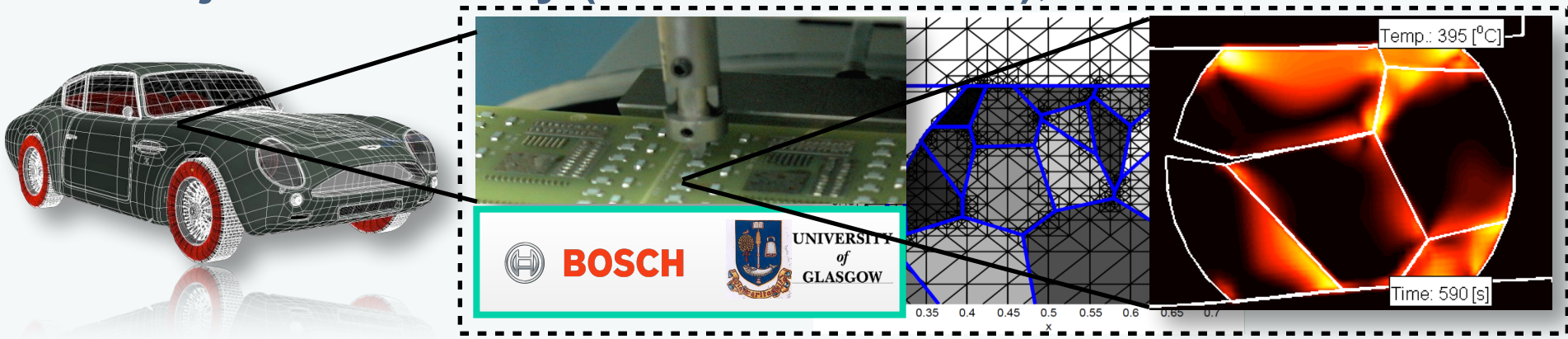

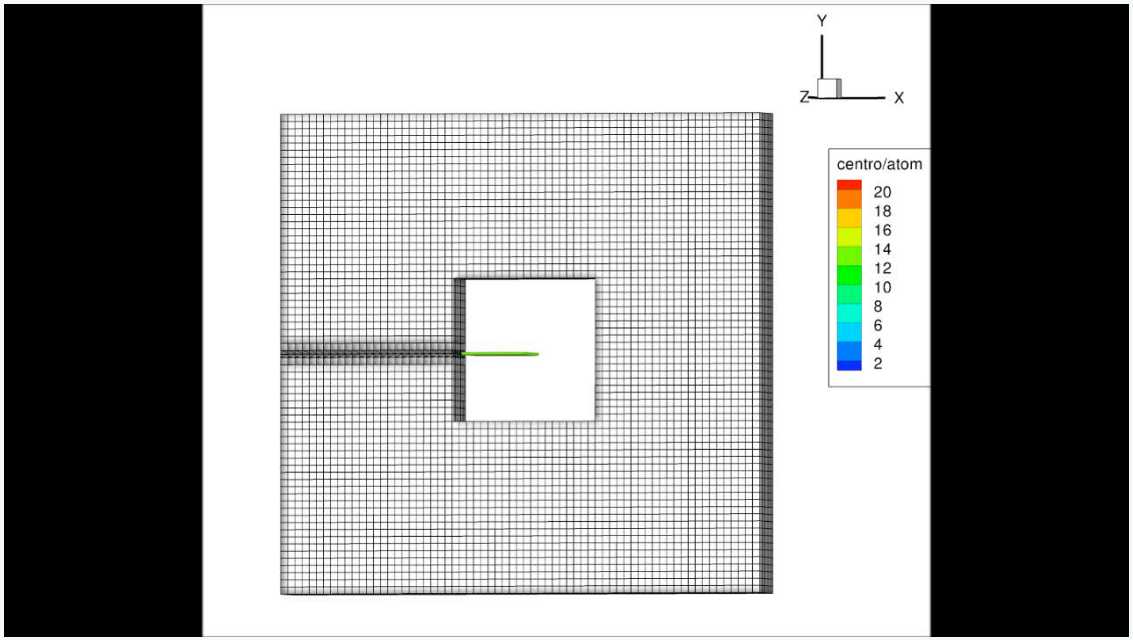

Motivation: multiscale fracture of engineering structures and materials

Practical early-stage design simulations (interactive)

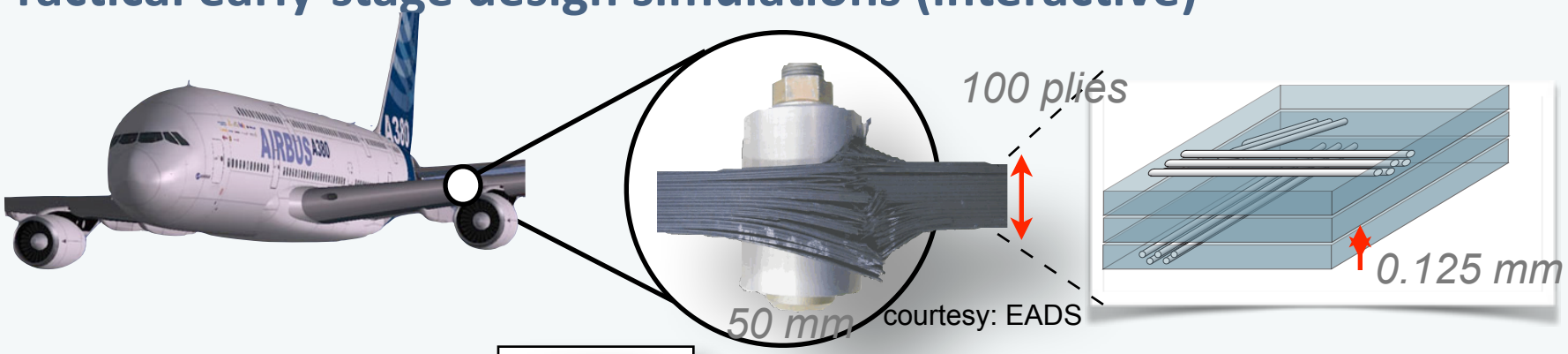

Discretise

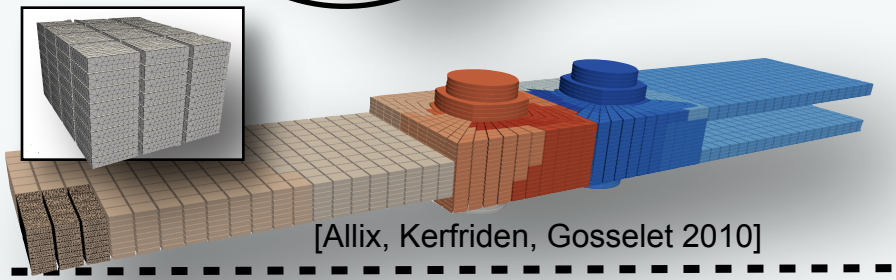

[Allix, Kerfriden, Gosselet 2010]

Surgical simulation

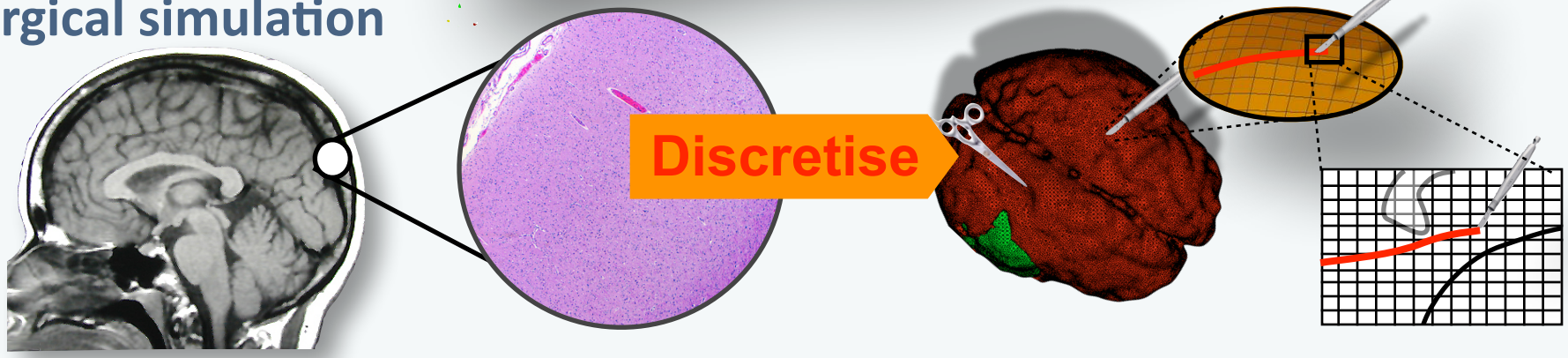

- Reduce the problem size while controlling the error (in QoI) when solving very large (multiscale) mechanics problems

GEOMETRICAL MODEL

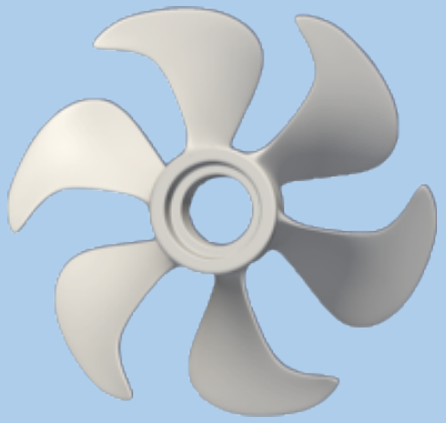

DISCRETISATION

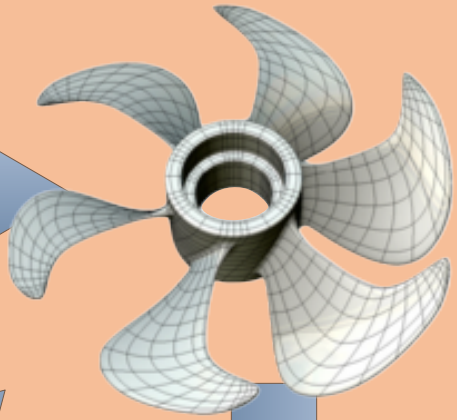

Verification

A POSTERIORI ERROR

MATERIAL MODELS

Phenomenological

Elasticity/Plasticity

Crack growth law (Paris…)

Fracture energy

Maximum tensile strength

Multi-scale

Debonding,Fibre pull-out

Fibre breakage, interface

fracture, grains,

NUMERICAL SOLUTION

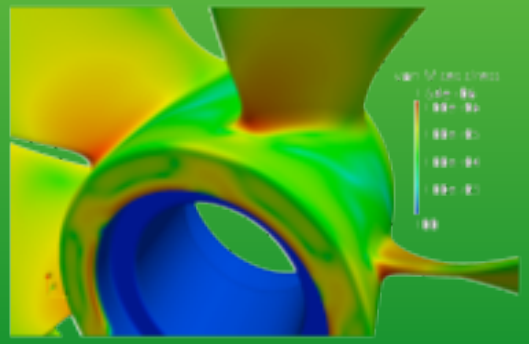

Validation & parameter identification

EXPERIMENTS

CONVENTIONAL APPROACH

When the material model is not known, this conventional approach is inadequate

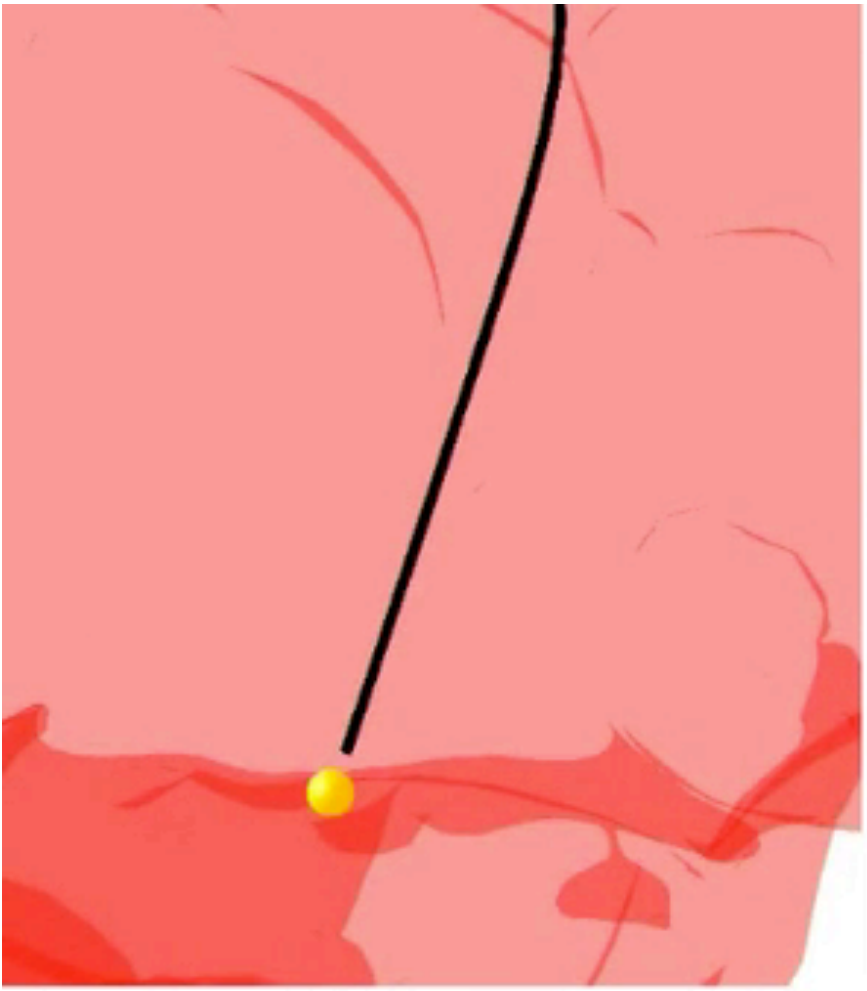

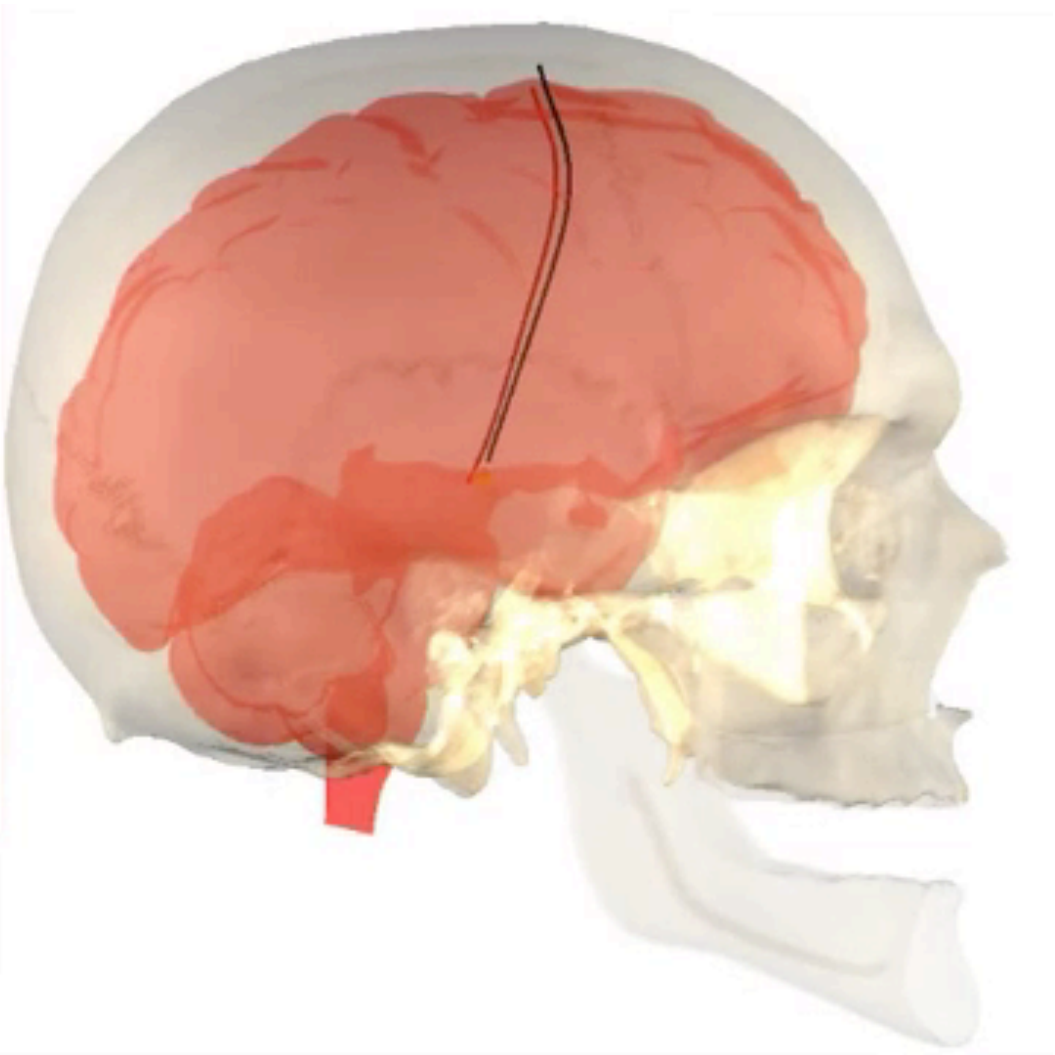

Deep-brain stimulation

Courtesy Alexandre Bilger, PhD thesis, Inria, 2014

Worst load combination

Scales of interest

Crack growth rate

INFORMATION

Inspection interval

Mission ?

DIGITAL TWIN OF THE SYSTEM

GEOMETRICAL MODEL

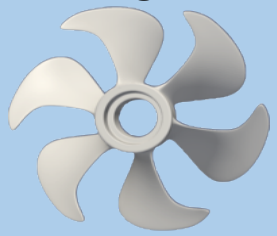

DISCRETISATION

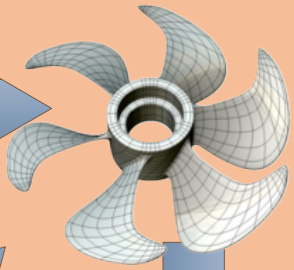

A POSTERIORI

LEARN MATERIAL MODELS

which scales?
what models?
what parameters?
what scale transition?
what data is missing?

NUMERICAL SOLUTION

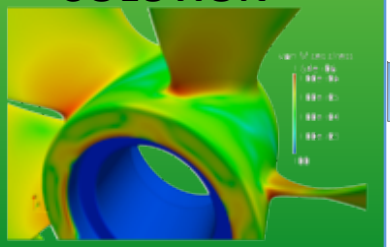

REAL SYSTEM

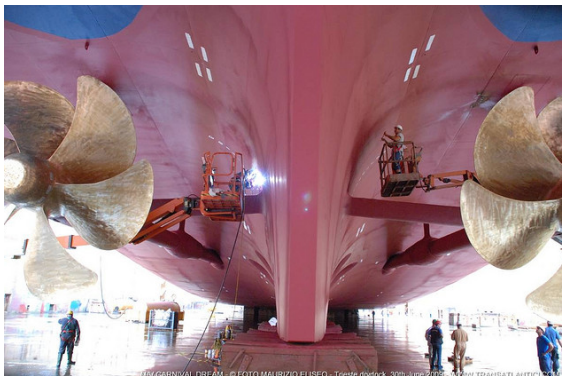

DATA

Strain

Environment Conditions

Cracks

Structural Health

Discretization

➡ partition of unity enrichment
✓ ~~(enriched) meshless~~ methods
✓ level sets

➡ isogeometric analysis
➡ implicit boundaries

Model reduction

✓ multi-scale & homogenisation
✓ algebraic model reduction (using POD
✓ Newton-Krylov, "local/global", domai
decomposition

Error control

✓ XFEM: goal-oriented error estimates
▸ used by CENAERO (Morfeo XFEM)
✓ meshless methods for fracture
✓ error estimation for reduced models

Ways to reduce the models

- Homogenisation (FE^2, etc.) - Hierarchical
- Concurrent and hybrid (bridging domain, ARLEQUIN, etc.)
- Enrichment (PUFEM, XFEM, GFEM)
- Model reduction (algebraic)

Reduction methods based on homogenisation

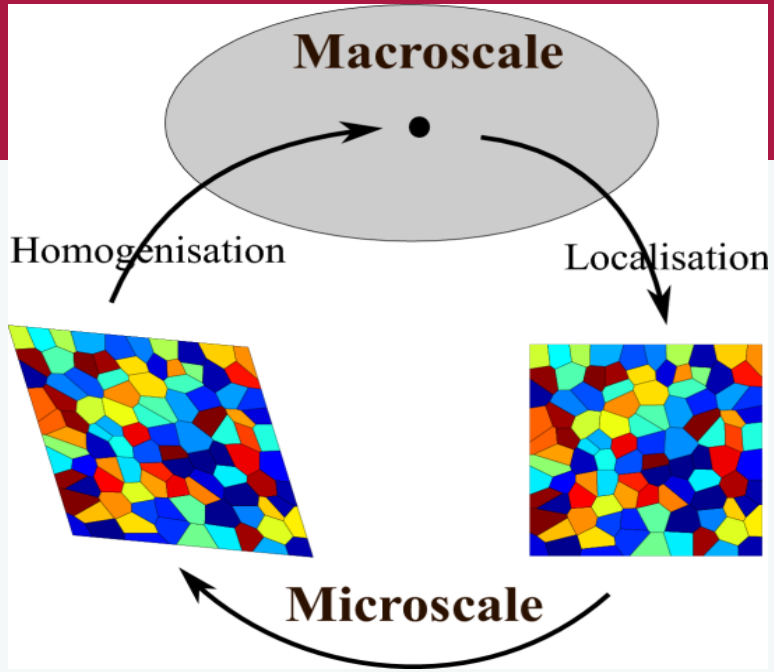

Definition of an RVE

$$l^c \gg l^f \gg l^g$$

Coupling of macroscopic and microscopic levels

The volume averaging theorem is postulated for:

1) Strain tensor:

$$\boldsymbol{\epsilon}^c = \frac{1}{|\Omega(\mathbf{x}^c)|} \int_{\partial\Omega(\mathbf{x}^c)} \mathbf{u}^f \otimes_s \mathbf{n}\, d\Gamma$$

2) Virtual work (Hill-Mandel condition):

$$\boldsymbol{\sigma}^c : \boldsymbol{\delta\epsilon}^c = \frac{1}{|\Omega(\mathbf{x}^c)|} \int_{\partial\Omega(\mathbf{x}^c)} \mathbf{t}^f \cdot \delta\mathbf{u}^f \, d\Gamma$$

3) Stress tensor:

$$\boldsymbol{\sigma}^c = \frac{1}{|\Omega(\mathbf{x}^c)|} \int_{\partial\Omega(\mathbf{x}^c)} \mathbf{t}^f \otimes \mathbf{x}^f \, d\Gamma$$

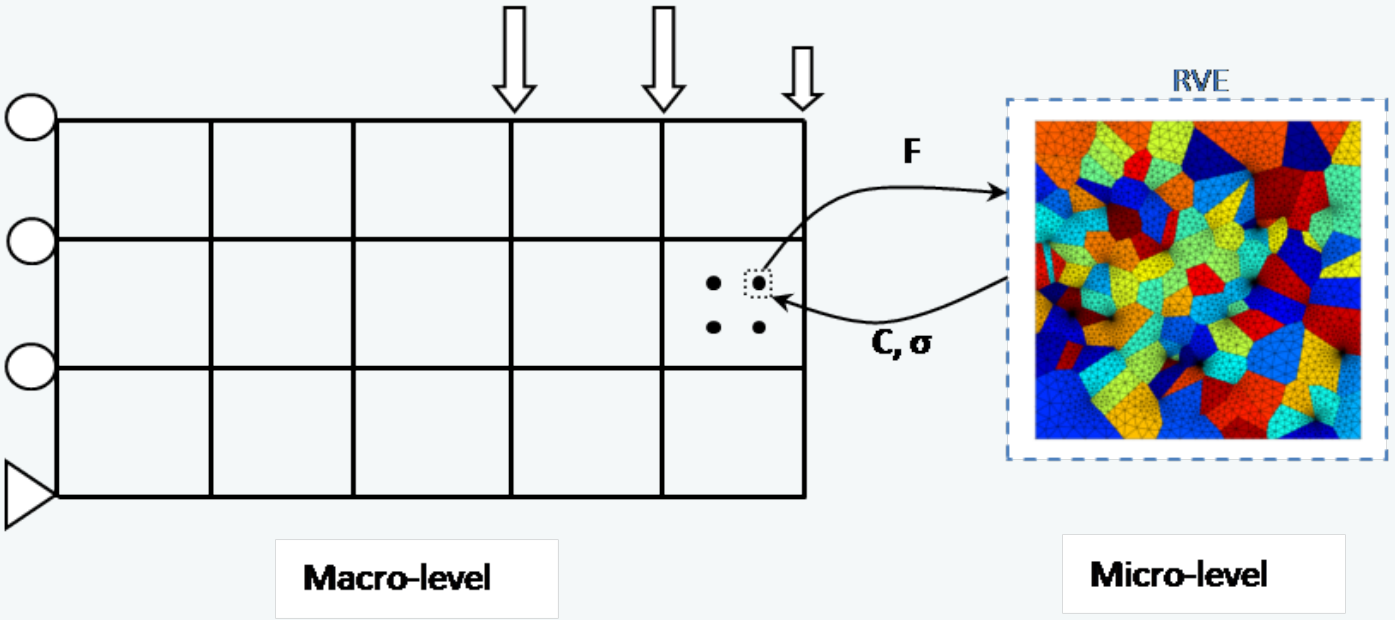

Advantages and abilities:

The macroscopic constitutive law is not required
Non-linear material behaviour can be simulated
Microscale behaviour of material is monitored at each load step

Drawbacks:

In softening regime:

- Lack of scale separation
- Macroscale mesh dependence

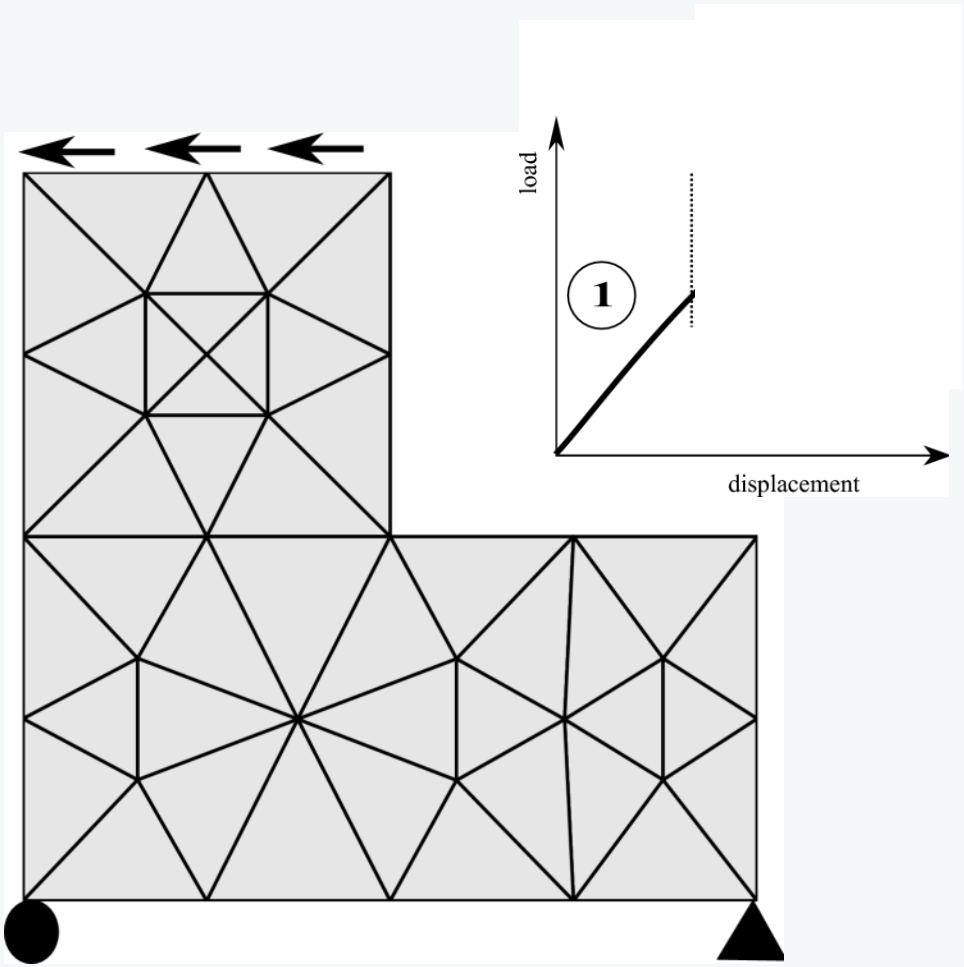
load
1
displacement

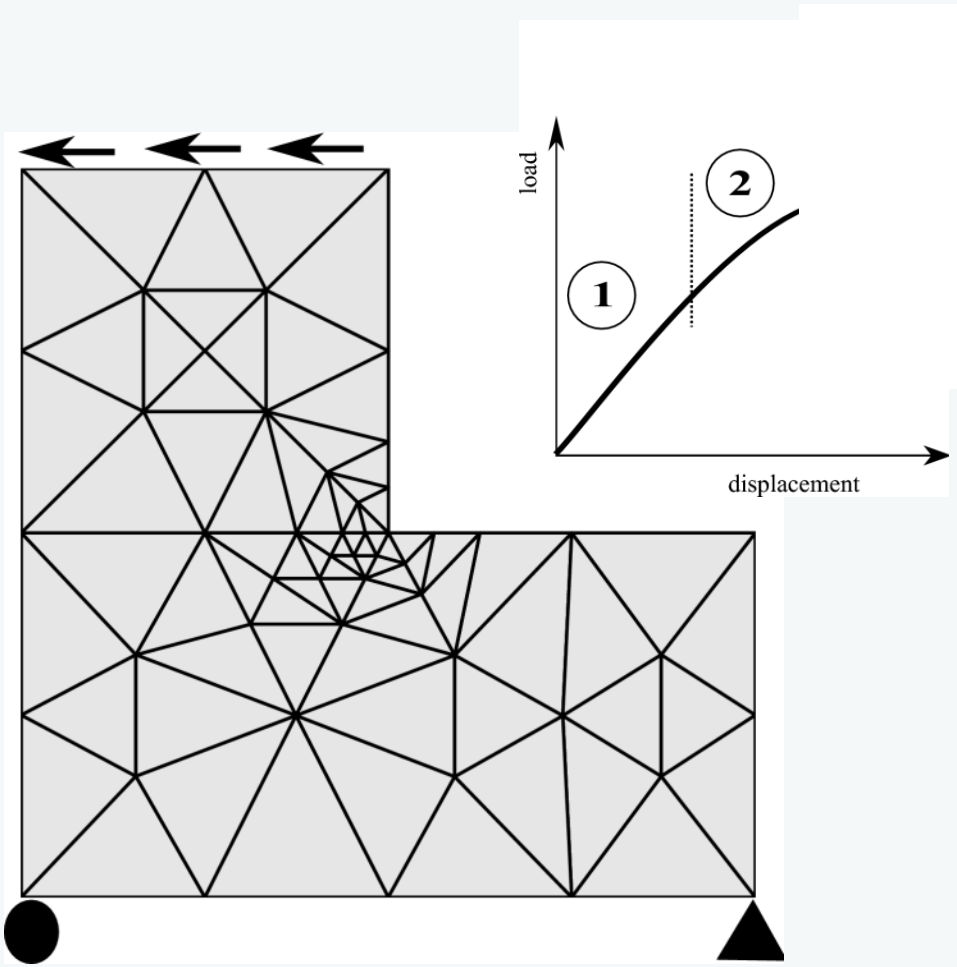
load
2
1
displacement

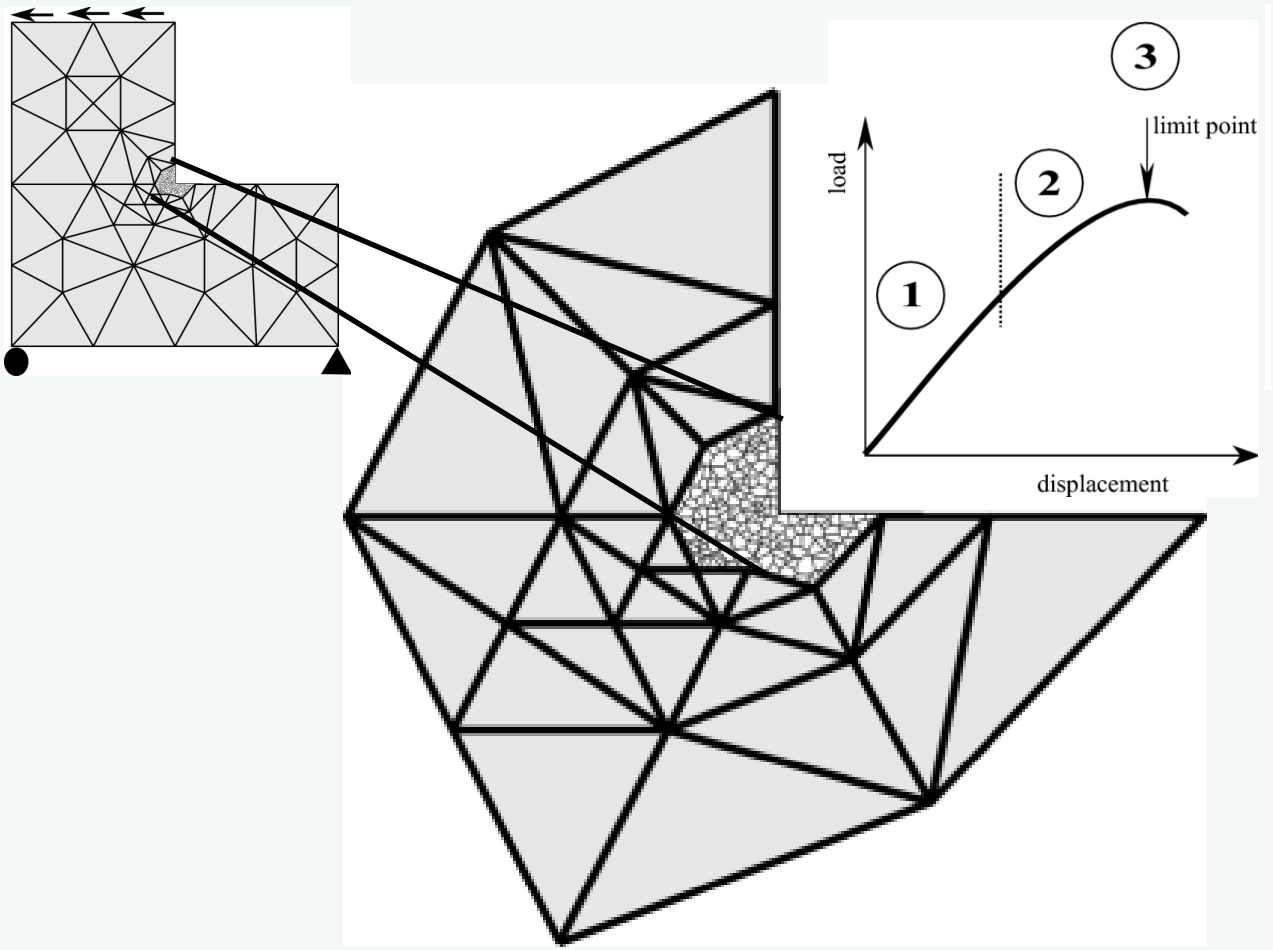

Details in Phil. Magazine, 2015, Akbari, Kerfriden, Bordas

Reduction methods based on algebraic reduction

Illustration of the method of separated representation

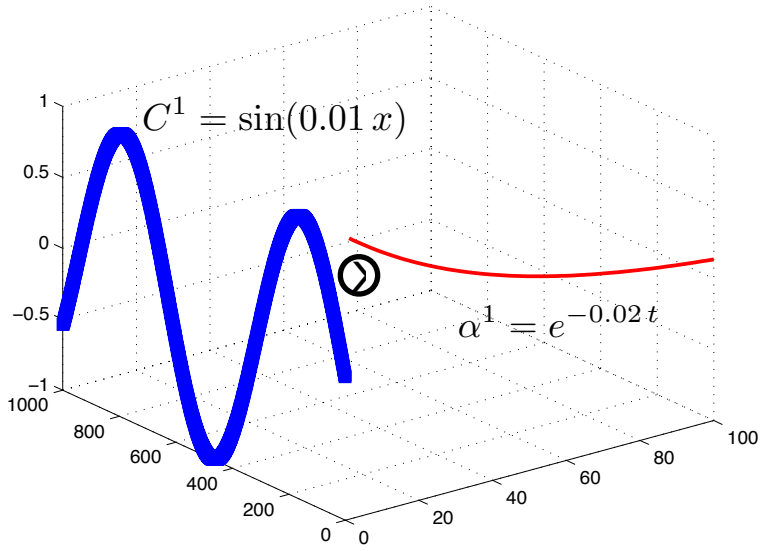

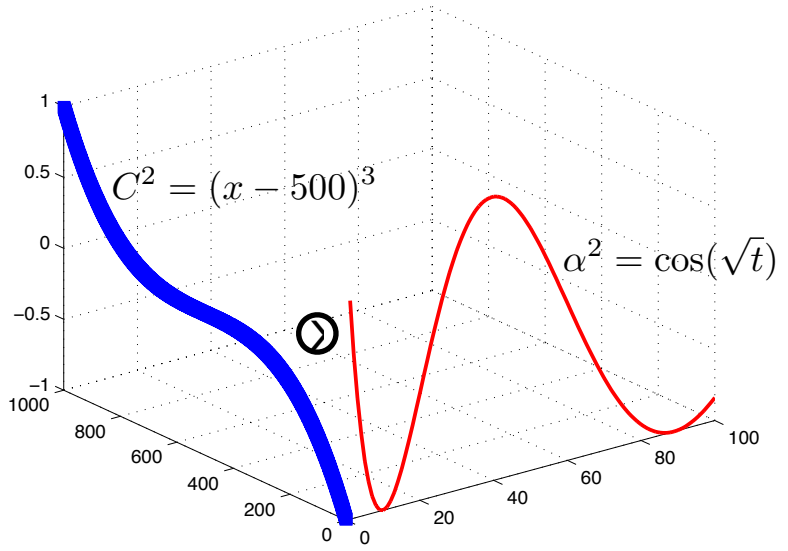

Illustration of the method of separated representation

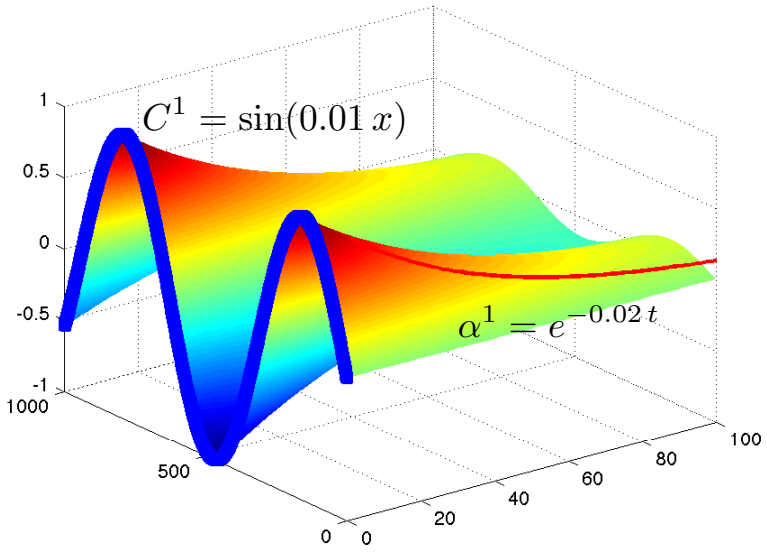

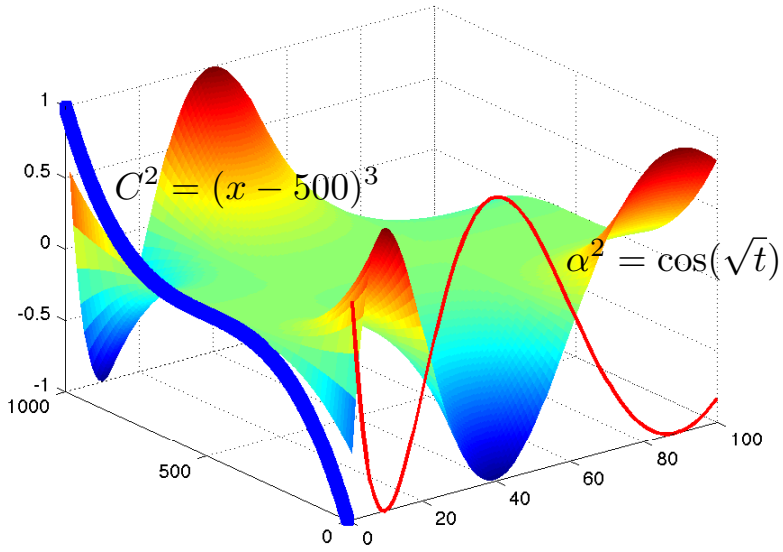

Illustration of the method of separated representation

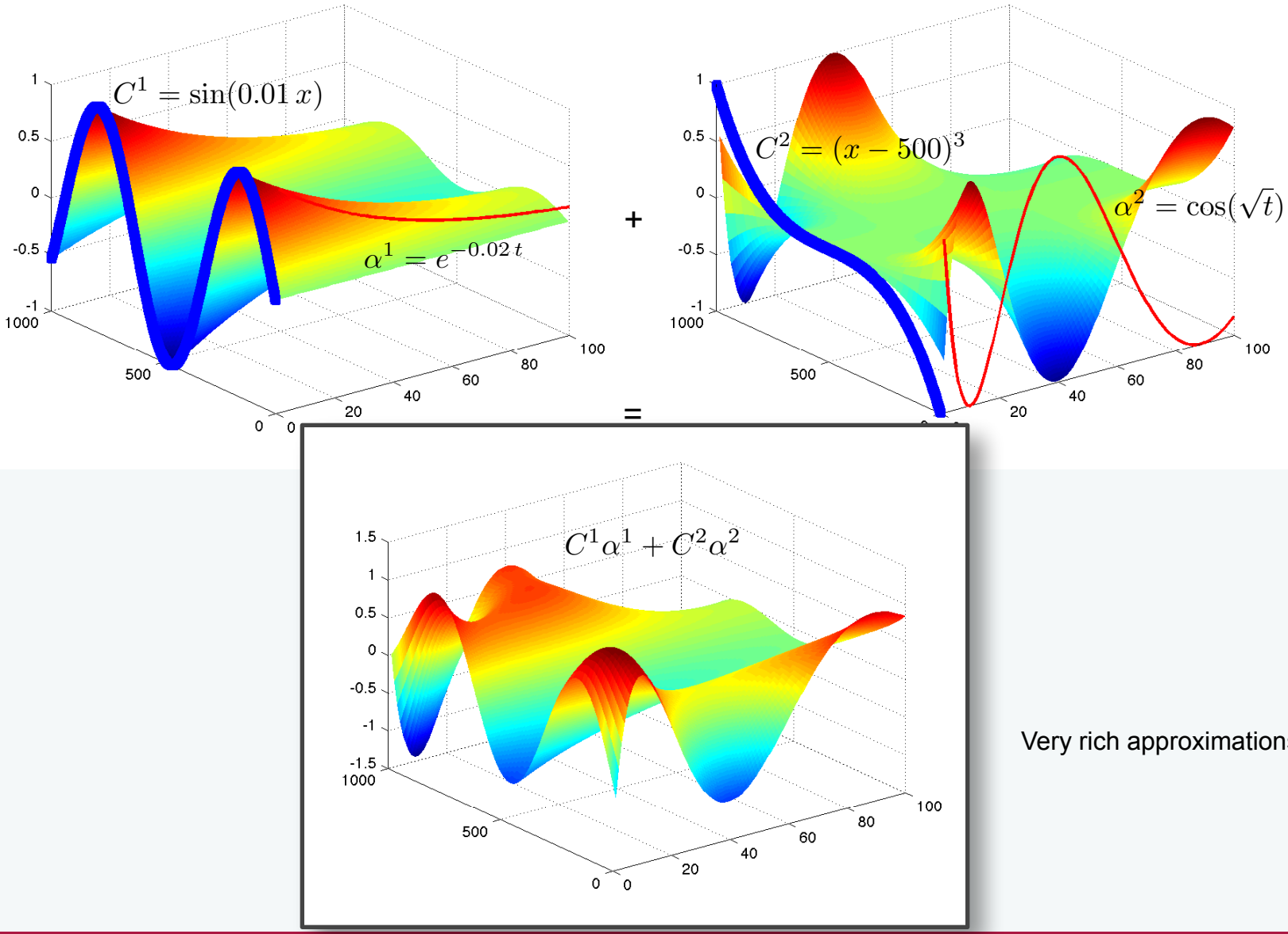

Very rich approximations!

Data compression: get the nose with the POD!

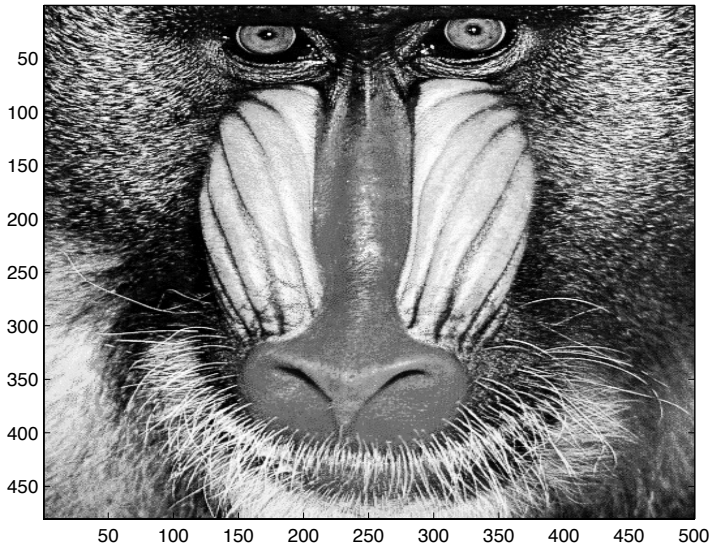

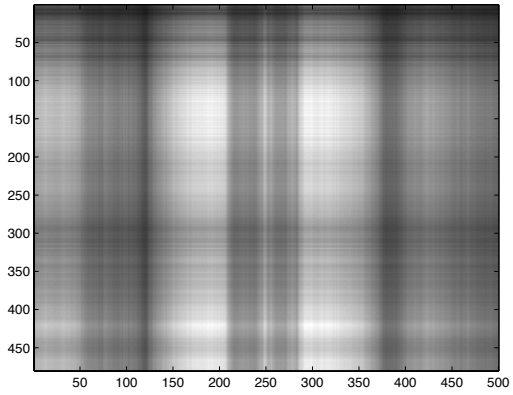

$n_c = 1$

$$\bar{u}(x_i, y_i) = \sum_{i=1}^{n_c} \underline{C}_x^i(x_i)\, \underline{C}_y^i(y_i)$$

$$(C_x^i, C_y^i)_{i \in [\![1, n_c]\!]} = \operatorname{argmin} \sum_{x_i} \sum_{y_j} (u(x_i, y_j) - \bar{u}(x_i, y_j))^2$$

Data compression: get the nose with the POD!

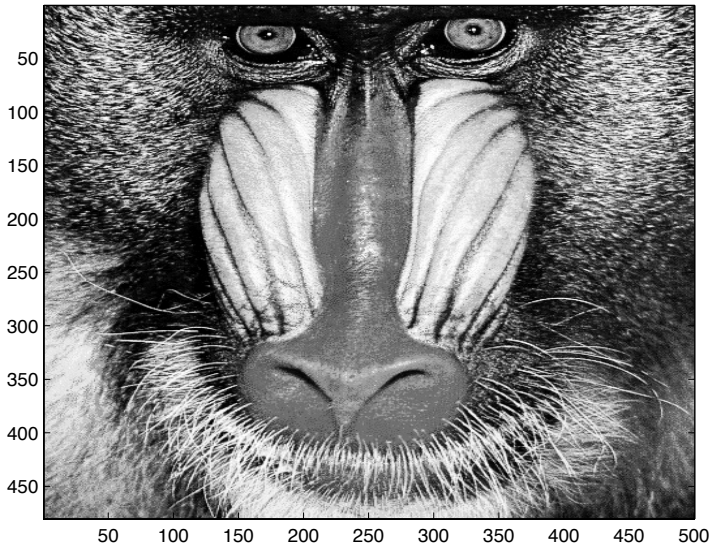

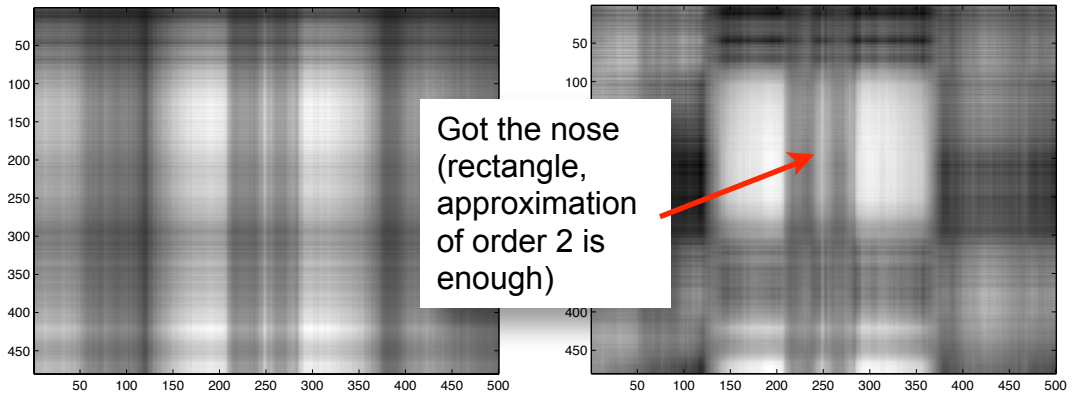

$n_c = 1$ $n_c = 2$

$$\bar{u}(x_i, y_i) = \sum_{i=1}^{n_c} \underline{C}_x^i(x_i)\, \underline{C}_y^i(y_i)$$

$$(C_x^i, C_y^i)_{i \in [\![1, n_c]\!]} = \operatorname{argmin} \sum_{x_i} \sum_{y_j} (u(x_i, y_j) - \bar{u}(x_i, y_j))^2$$

Data compression: get the nose with the POD!

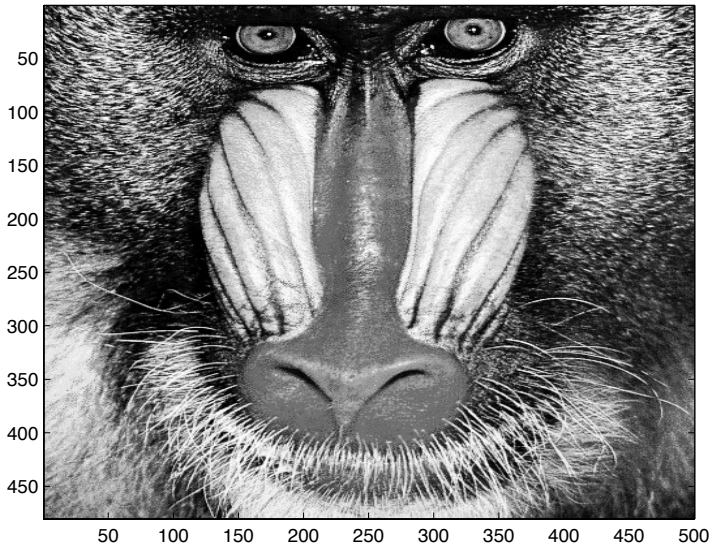

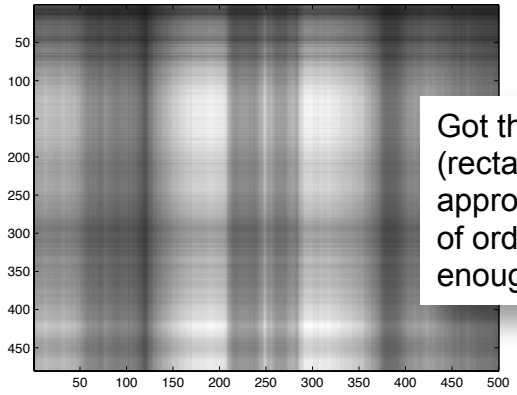

$n_c = 1$

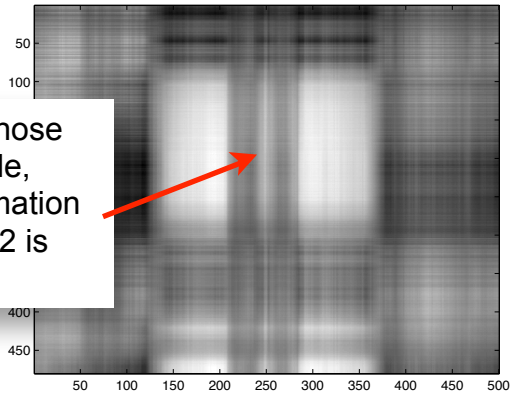

$n_c = 2$

Got the nose (rectangle, approximation of order 2 is enough)

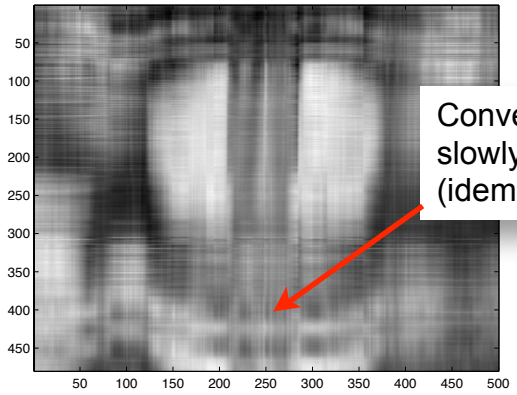

$n_c = 5$

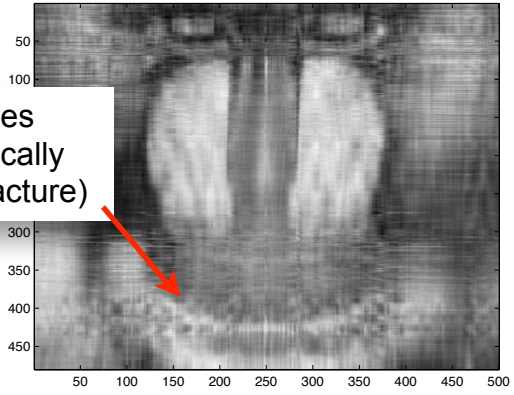

$n_c = 10$

Converges slowly locally (idem fracture)

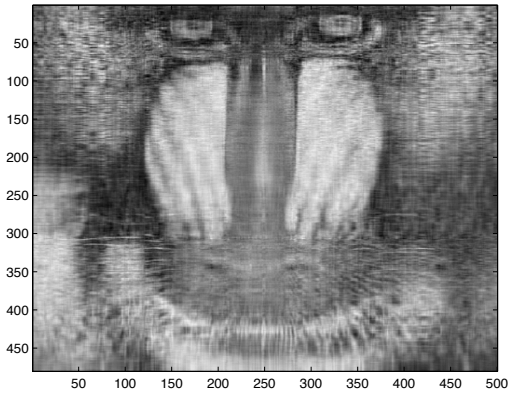

$n_c = 20$

$$\bar{u}(x_i, y_i) = \sum_{i=1}^{n_c} \underline{C}_x^i(x_i)\, \underline{C}_y^i(y_i)$$

$$(C_x^i, C_y^i)_{i \in [\![1, n_c]\!]} = \operatorname{argmin} \sum_{x_i} \sum_{y_j} (u(x_i, y_j) - \bar{u}(x_i, y_j))^2$$

Method of separated representation

- Search for the solution in space / time / parameter in a product space:

$$\underline{\bar{\mathbf{U}}}: \quad \mathcal{U}_{\text{sep}} = \mathbb{R}^n \times \mathcal{T} \times \mathcal{P} \to \mathbb{R}^n$$
$$\underline{\bar{\mathbf{U}}}(t,\mu) = \sum_{i=1}^{n_C} \underline{\mathbf{C}}_i \, \beta_i(t)\gamma_i(\mu)\,,$$

$$\underline{\mathbf{C}}^i \in \mathbb{R}^n$$
$$\beta^i : \mathcal{T} \to \mathbb{R}, \quad \forall i \in [\![1, n_C]\!]\,,$$
$$\gamma^i : \mathcal{P} \to \mathbb{R}, \quad \forall i \in [\![1, n_C]\!]\,,$$

- Optimality of an expansion of order n_c with respect to a particular metric defined on $\mathcal{U}_{\text{sep}}$

  ➡ different metrics lead to different methods, which have their pro/cons

  ➡ Choice strongly dependent on the context

  - Data compression: **POD** (Proper Orthogonal Decomposition) is a classical choice in dimension 2
  - Data compression in many dimensions: **multilinear POD**
  - Solver in many dimensions without *a priori* knowledge of the solution: **PGD**
  - Model order reduction: **Snapshot POD, Snapshot PGD**
  - Initialiser, preconditioners: **low-order POD**, **low-order PGD**, **Snapshot POD**

Proper Orthogonal Decomposition (POD)

- One writes the classical POD problem:

find an orthonormal basis $\underline{\underline{\mathbf{C}}} \in \mathbb{R}^{n \times n_c}$, $\underline{\underline{\mathbf{C}}}^T \, \underline{\underline{\mathbf{C}}} = \underline{\underline{\mathbf{I}}}_d$ *minimising the POD functional:*

$$J_{\mathrm{POD}}(\underline{\underline{\mathbf{C}}}) = \int_{t \in \mathcal{T}} \| \underline{\mathbf{U}}(t) - \underline{\underline{\mathbf{C}}} \, \underline{\underline{\mathbf{C}}}^T \underline{\mathbf{U}}(t) \|_2^2 \, dt$$

- Equivalently, look for a maximum of $\bar{J}_{\mathrm{POD}}(\underline{\underline{\mathbf{C}}}) = \int_{t \in \mathcal{T}} \underline{\mathbf{U}}(t)^T \underline{\underline{\mathbf{C}}} \, \underline{\underline{\mathbf{C}}}^T \underline{\mathbf{U}}(t) \, dt = \mathrm{Tr}(\underline{\underline{\mathbf{C}}}^T \underline{\underline{\mathbf{K}}} \, \underline{\underline{\mathbf{C}}})$
  - Correlation operator: $\underline{\underline{\mathbf{K}}} = \int_{t \in \mathcal{T}} \underline{\mathbf{U}}(t) \, \underline{\mathbf{U}}(t) \, dt$
- Solution: eigenvalue problem $\underline{\underline{\mathbf{K}}} \, \underline{\phi}^k = \lambda^k \underline{\phi}^k$ where $(\lambda^k)_{k \in [\![0,n]\!]}$ in decreasing order
  - $\underline{\underline{\mathbf{C}}} = (\, \underline{\phi}^1 \quad \underline{\phi}^2 \quad \dots \quad \underline{\phi}^{n_c} \,)$
  - $\int_{t \in \mathcal{T}} \alpha^i \, \alpha^j \, dt = \delta_{ij} \, \lambda^i$
- Error $J_{\mathrm{POD}}(\underline{\underline{\mathbf{C}}}) = \sum_{k=n_c+1}^{n} \lambda^k$

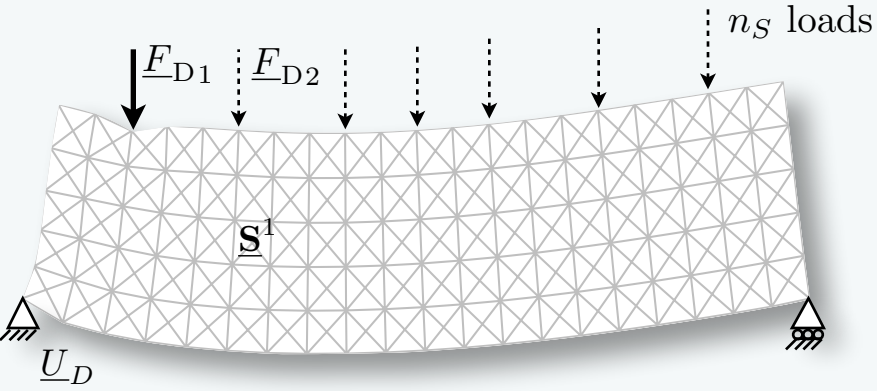

(1) Solve FINE for n_S parameters (EXPENSIVE!)

$$\underline{\mathbf{S}} = \left(\underline{\mathbf{S}}^1 \quad \underline{\mathbf{S}}^2 \quad \dots \quad \underline{\mathbf{S}}^{n_S} \right)$$

(2) Singular value decomposition

$$\underline{\mathbf{S}} = \underline{\mathbf{U}}\,\underline{\underline{\mathbf{\Sigma}}}\,\underline{\mathbf{V}}^T = \sum_{k=1}^{n_S} \Sigma^k \underline{\mathbf{U}}^k \underline{\mathbf{V}}^{kT}$$

n_S solutions, sorted by relevance

where $(\Sigma^k)_{k \in [\![1 \; n_S]\!]}$ in decreasing order

(3) Truncation

Reduced basis: family of representative solutions

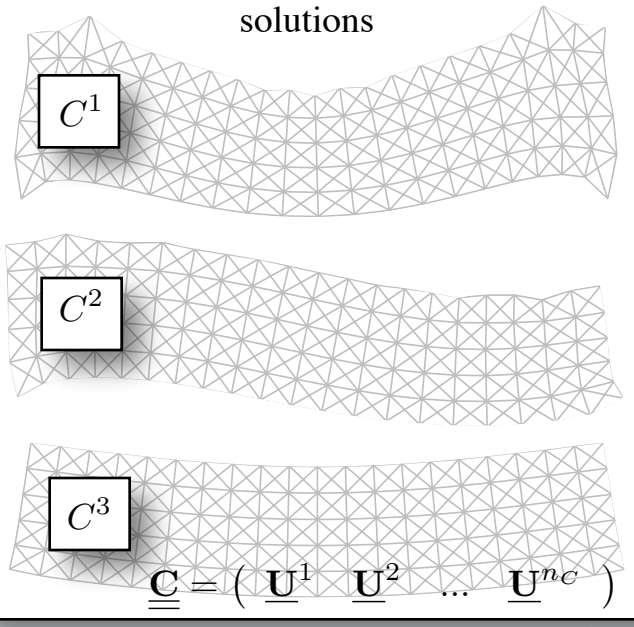

Family of representative solutions

$$\underline{\mathbf{U}} = \underline{\mathbf{C}}\,\boldsymbol{\alpha}$$

Solution — Coefficients

Initial set of equations

$$\underline{\mathbf{F}}_{\text{Int}}(\underline{\mathbf{U}}) + \underline{\mathbf{F}}_{\text{Ext}} = 0$$

(4) Galerkin orthogonality

$$\underline{\mathbf{C}}^T \underline{\mathbf{F}}_{\text{int}}(\underline{\mathbf{C}}\,\boldsymbol{\alpha}) + \underline{\mathbf{C}}^T \underline{\mathbf{F}}_{\text{ext}} = 0$$

Approximation of the solution in a space of small dimension (n_c)

Limitations: case of highly non-linear fracture mechanics

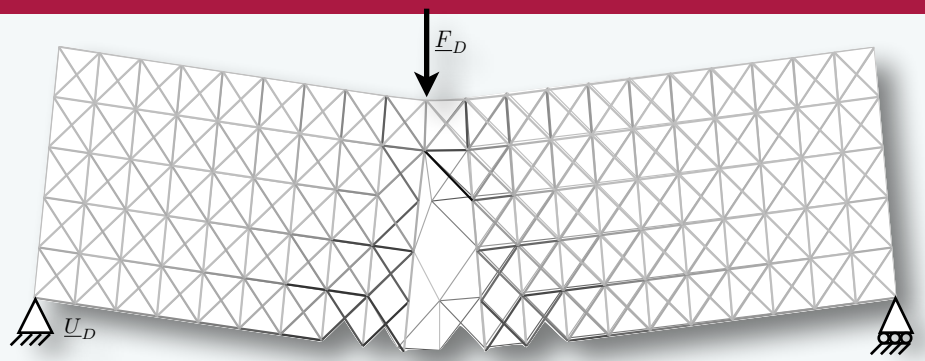

This solution is not in the snapshot !

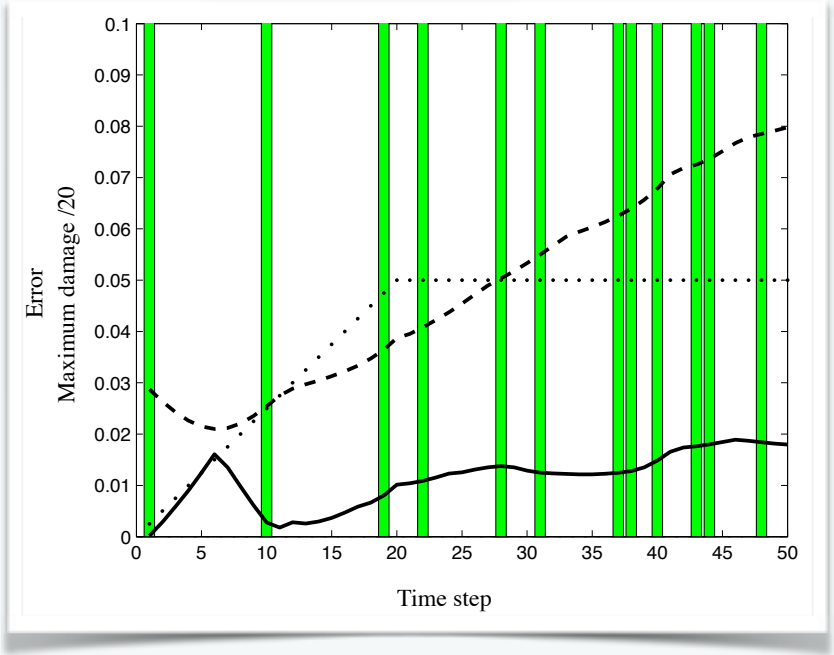

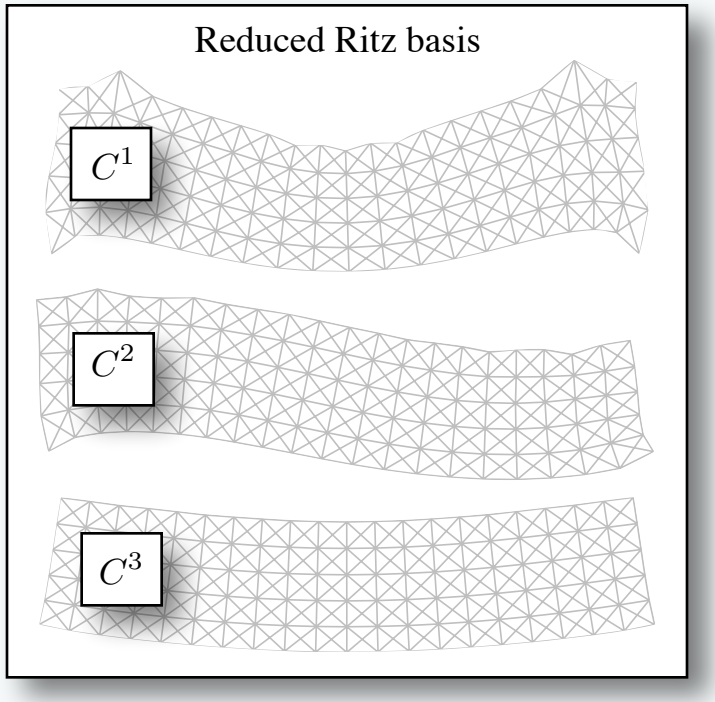

- P. Kerfriden, P. Gosselet, S. Adhikari, and S. Bordas. *Bridging proper orthogonal decomposition methods and augmented Newton-Krylov algorithms: an adaptive model order reduction for highly nonlinear mechanical problems*. Computer Methods in Applied Mechanics and Engineering, 200(5-8): 850-866, 2011.

Application to a parametric fracture problem

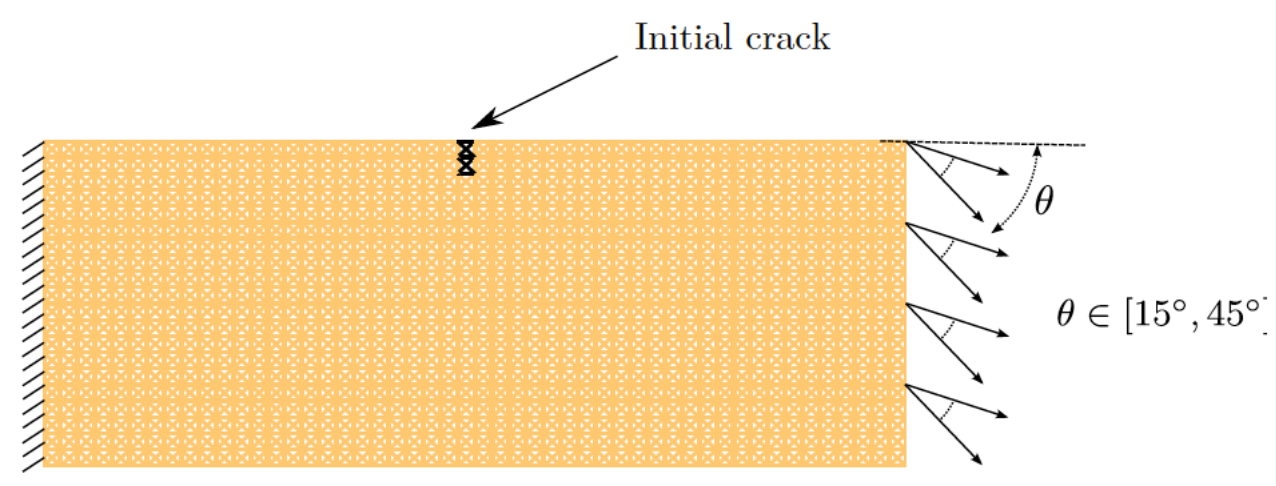

Application to a parametric fracture problem

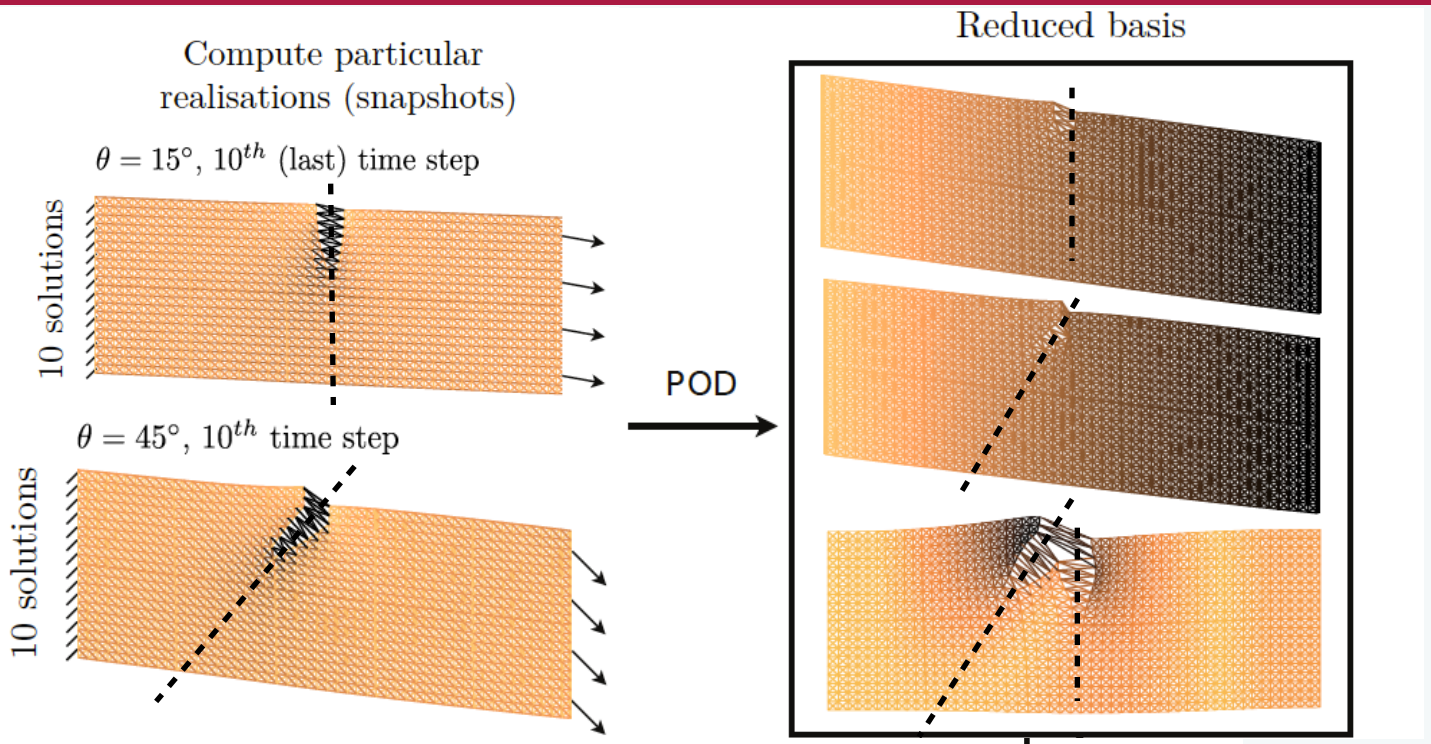

Solution at arbitrary angle using the reduced model

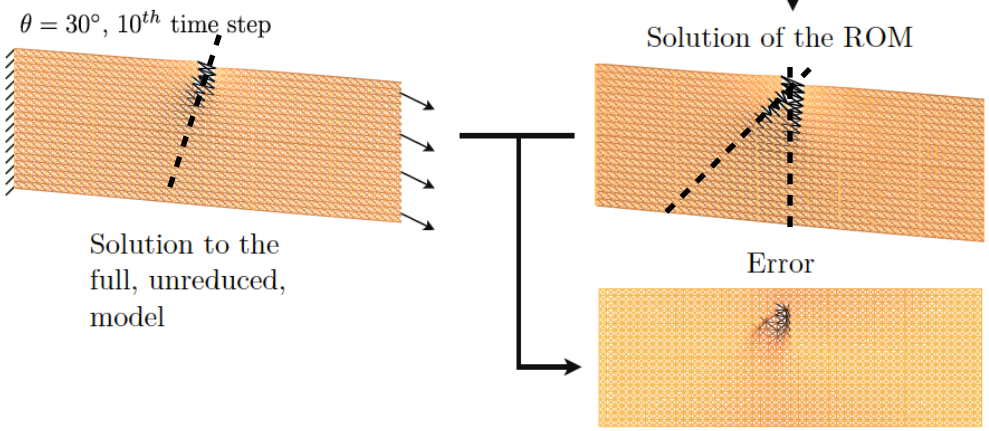

- The POD solution is not able to reproduce the solution in the cracked area
- Due to lack of correlation introduced by crack growth
- Leads to a local projection error

Parametric / stochastic multiscale fracture mechanics

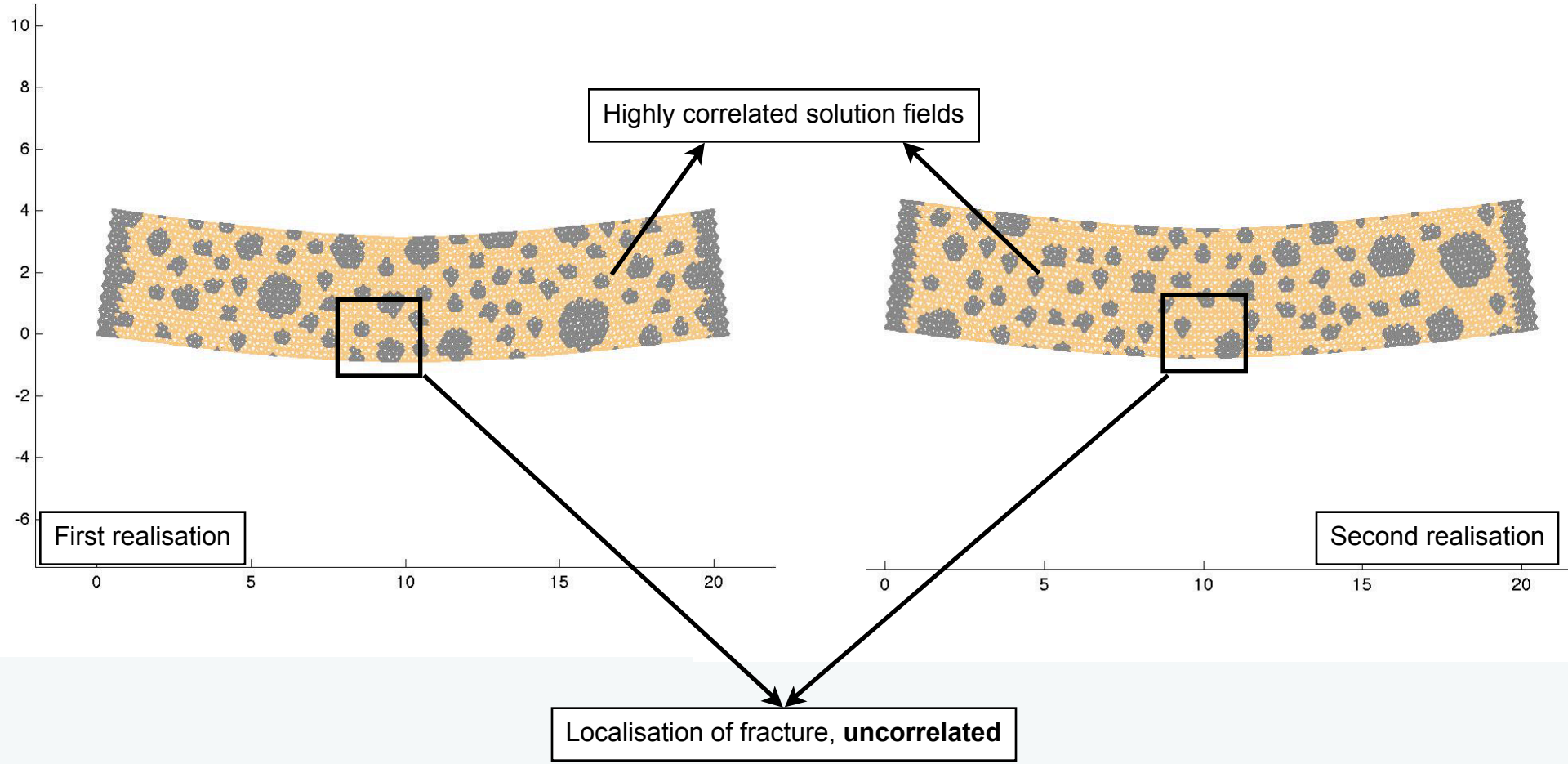

- Direct numerical simulation: efficient preconditioner?
- Reduced order modelling?
- Adaptive coupling?

CARDIFF UNIVERSITY
PRIFYSGOL CAERDYDD

UNIVERSITÉ DU LUXEMBOURG

THE RETURN OF THE MONKEY!

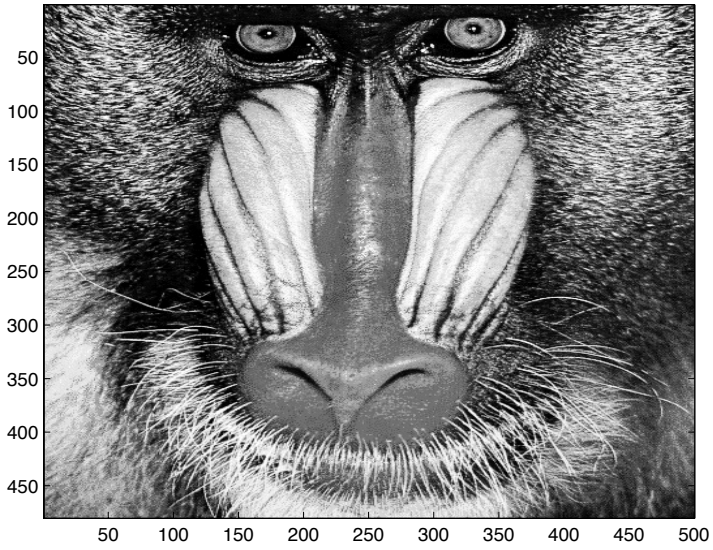

What can we do to address this lack of separation of scales/reducibility?

How we got to this point...

P. Kerfriden, P. Gosselet, S. Adhikari, and S. Bordas. Bridging proper orthogonal decomposition methods and augmented Newton-Krylov algorithms: an adaptive model order reduction for highly nonlinear mechanical problems. *Computer Methods in Applied Mechanics and Engineering*, 200(5-8):850–866, 2011.

P. Kerfriden, J.C. Passieux, and S. Bordas. Local/global model order reduction strategy for the simulation of quasi-brittle fracture. *International Journal for Numerical Methods in Engineering*, 89(2):154–179, 2011.

P. Kerfriden, K.M. Schmidt, T. Rabczuk, and Bordas S.P.A. Statistical extraction of process zones and representative subspaces in fracture of random composites. *Accepted for publication in International Journal for Multiscale Computational Engineering, arXiv:1203.2487v2*, 2012.

Data compression: fracture

Snapshot POD (snapshot space is spanned by the ensemble of solutions at all time steps)

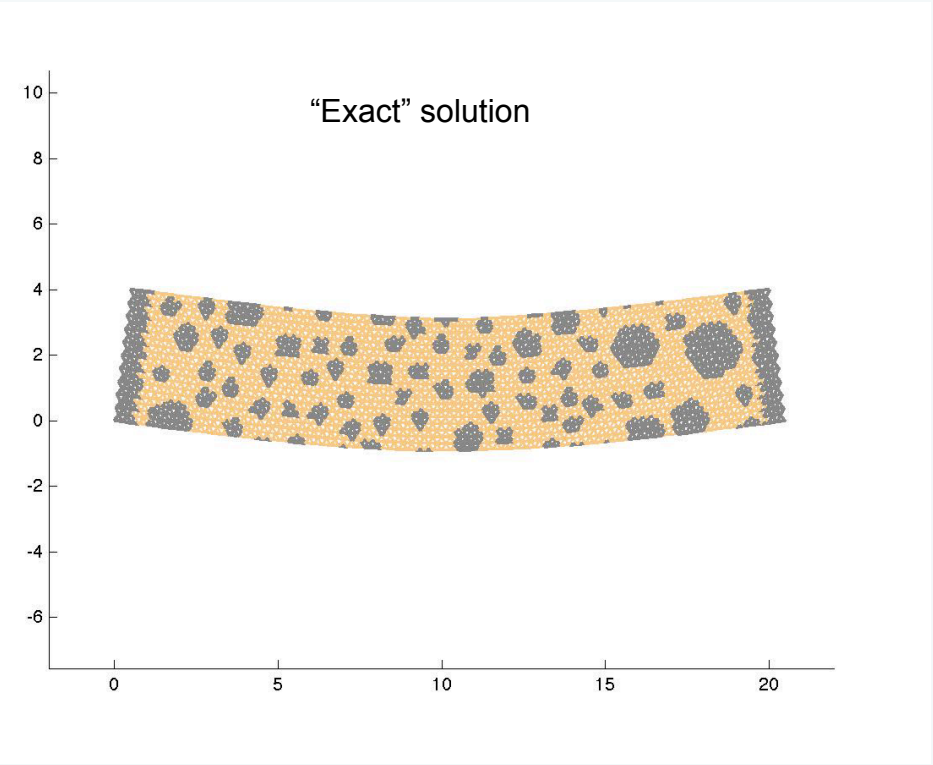

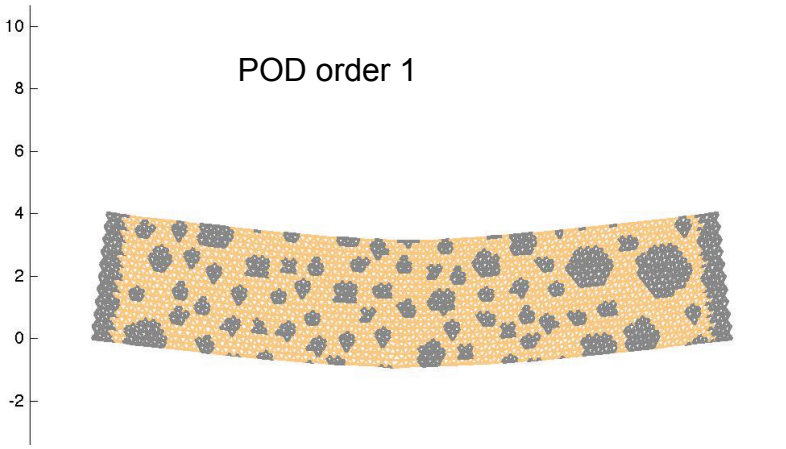

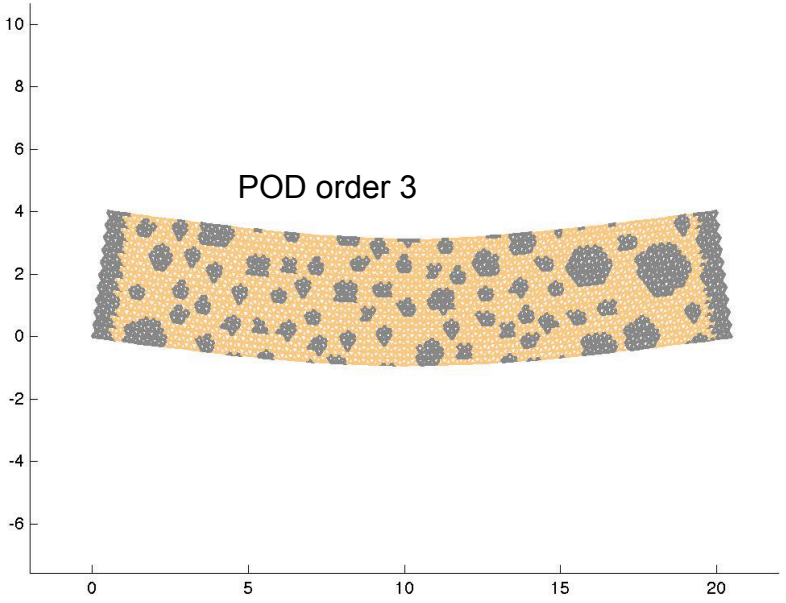

Partitioned POD/DDM

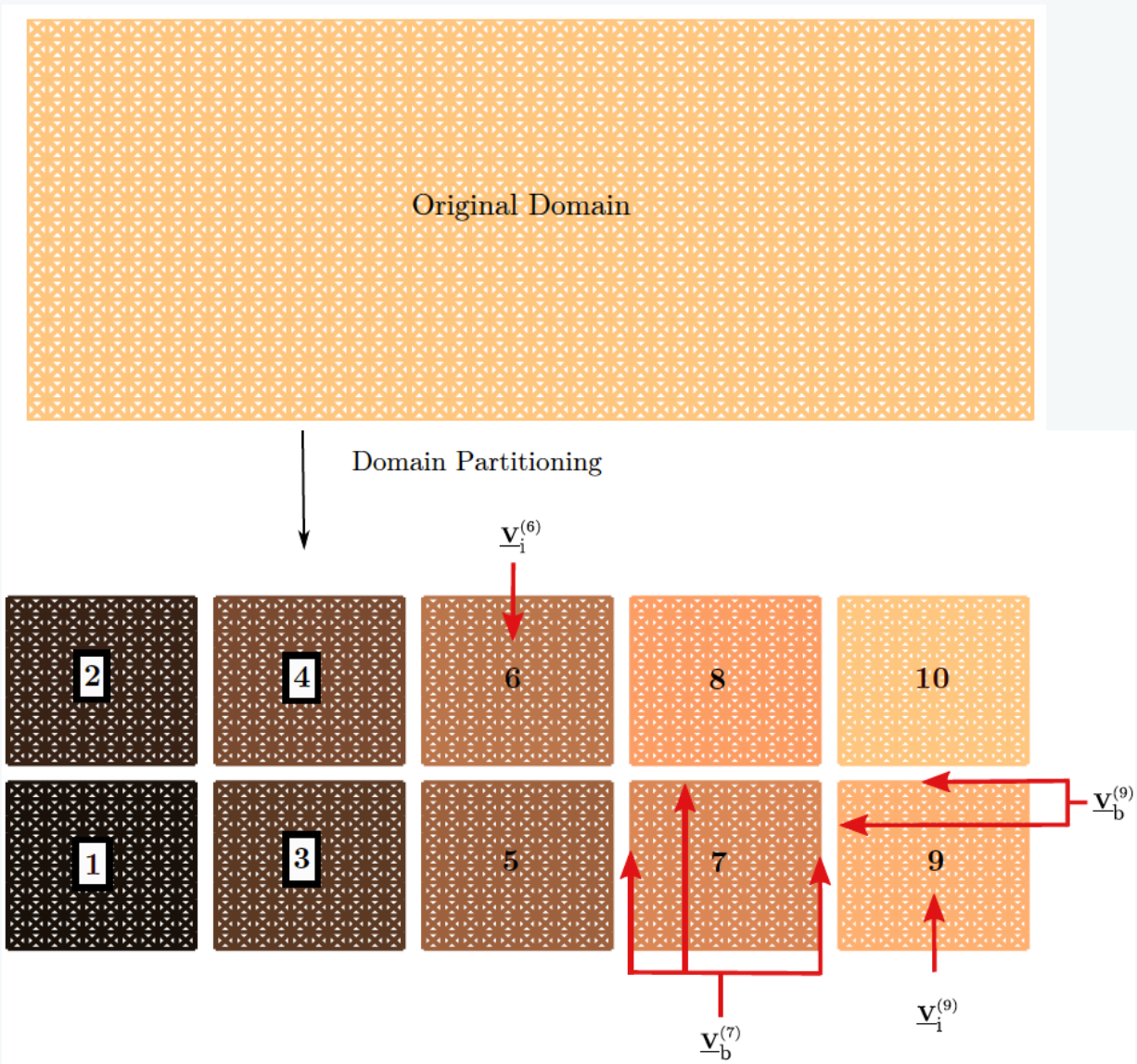

Reduced DDM-POD

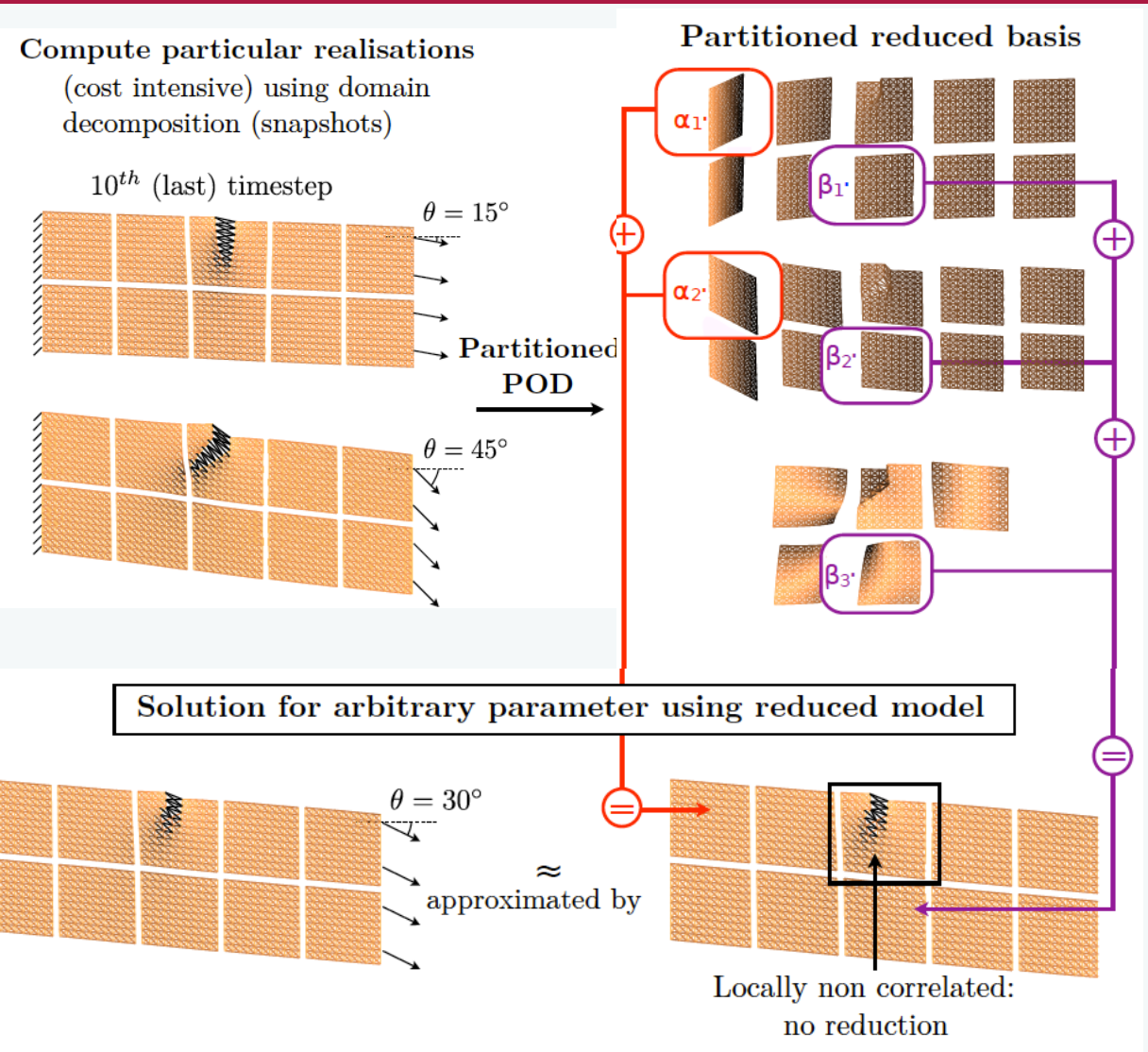

- Decompose the structure into subdomains
- Perform a reduction in the highly correlated region
- Couple the reduced to the non-reduced region by a primal Schur complement

Choice of the reduced subdomains: local error estimation by "leave one out cross-validation" (LOOCV)

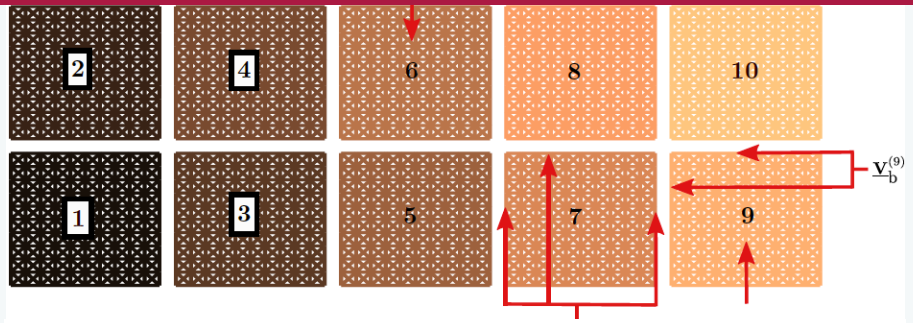

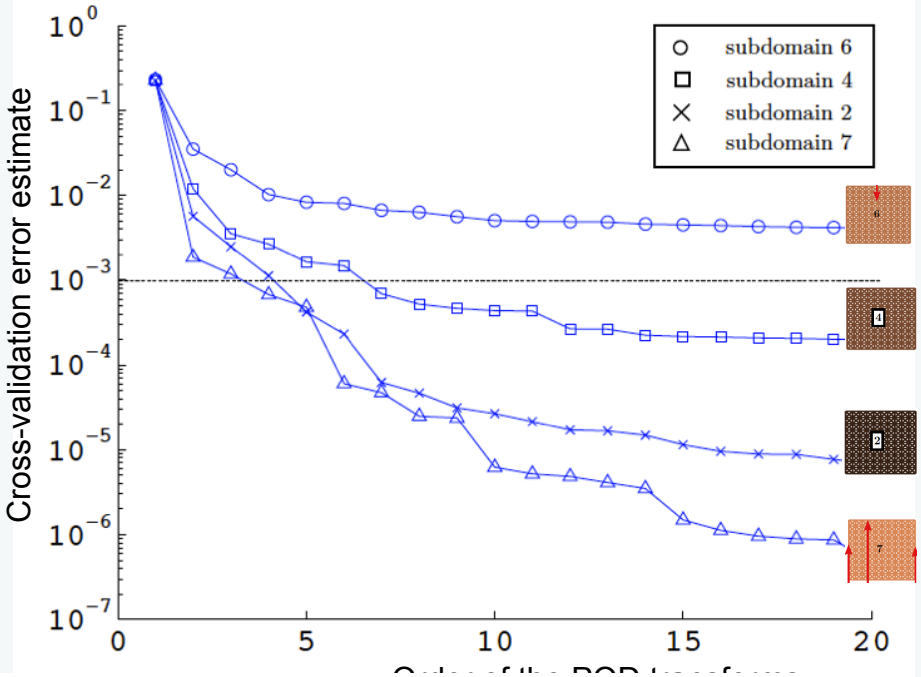

$$\left(\tilde{\nu}_{\text{snap}}^{(e)}\right)^2 = \frac{\sum_{\mu\in\mathcal{P}^{\text{s}}}\sum_{t_n\in\mathcal{T}^{\text{h}}}\left\|\underline{\mathbf{U}}_{\text{i}}(t_n,\mu) - \sum_{j=1}^{n_{\text{c}}^{(e)}}\left(\tilde{\underline{\mathbf{C}}}_{\text{i},j}^{(e),(\mu)\,T}\,\underline{\mathbf{U}}_{\text{i}}(t_n,\mu)\right)\tilde{\underline{\mathbf{C}}}_{\text{i},j}^{(e),(\mu)}\right\|_2^2}{\sum_{t_n\in\mathcal{T}^{\text{h}}}\sum_{\mu\in\mathcal{P}^{\text{s}}}\|\underline{\mathbf{U}}_{\text{i}}(t_n,\mu)\|_2^2}$$

- Reduced subspaces are independent and we assume a snapshot is *a priori* available
  - (1) Dimension of the local space for each subdomain?
  - (2) Is a given subdomain is reducible?
- (1) and (2) will be treated by cross-validation (e.g. W. J. Krzanowski. Cross-validation in principal component analysis. Biometrics, 43(3):575-584, 1987.)
  - **Training set**: snapshot
  - **Validation set**: set of additional finescale solutions
  - Independent training/validation avoids overfitting
  - Cross validation **emulates independence**. Error calculated using the local reduced basis obtained by a snapshot POD transform of all the available snapshot solutions except the one corresponding to the value of the summation variable.
- **NOTE:** If the snapshot is not assumed *a priori* then
  - Assess whether the snapshot contains sufficient information, and generate additional, suitable, data if required
  - Most analysis (mostly by statisticians) assume the snapshot is known *a priori*. Recent review: Hervé Abdi and Lynne J. Williams. Principal component analysis. Wiley Interdisciplinary Reviews: Computational Statistics, 2(4):433{459, 2010.

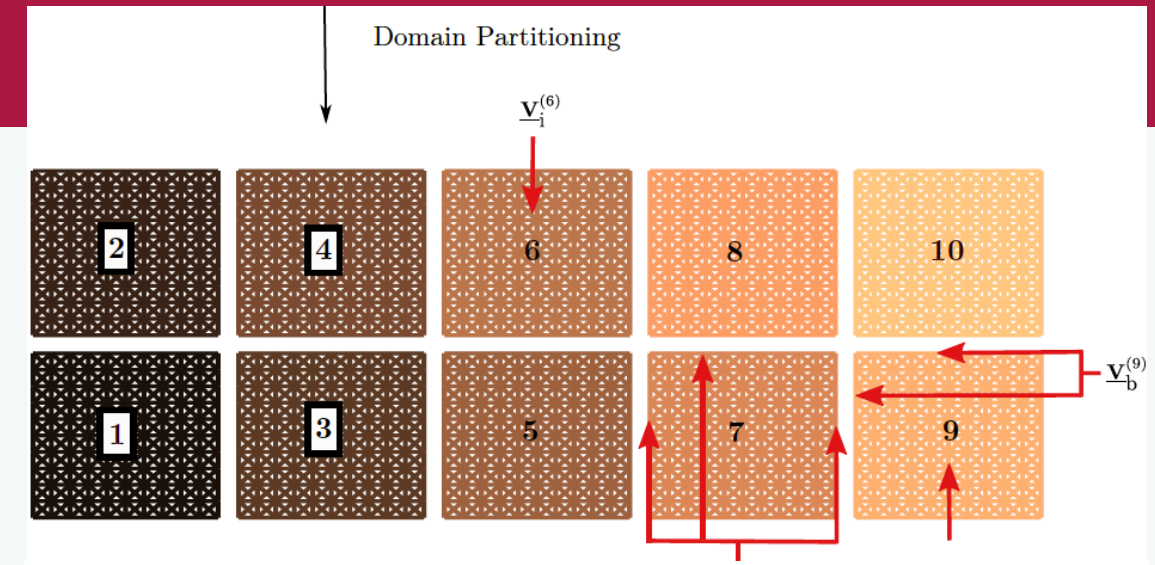
Domain Partitioning
$\underline{\mathbf{v}}_{\mathrm{i}}^{(6)}$
2
4
6
8
10
1
3
5
7
9
$\underline{\mathbf{v}}_{\mathrm{b}}^{(9)}$

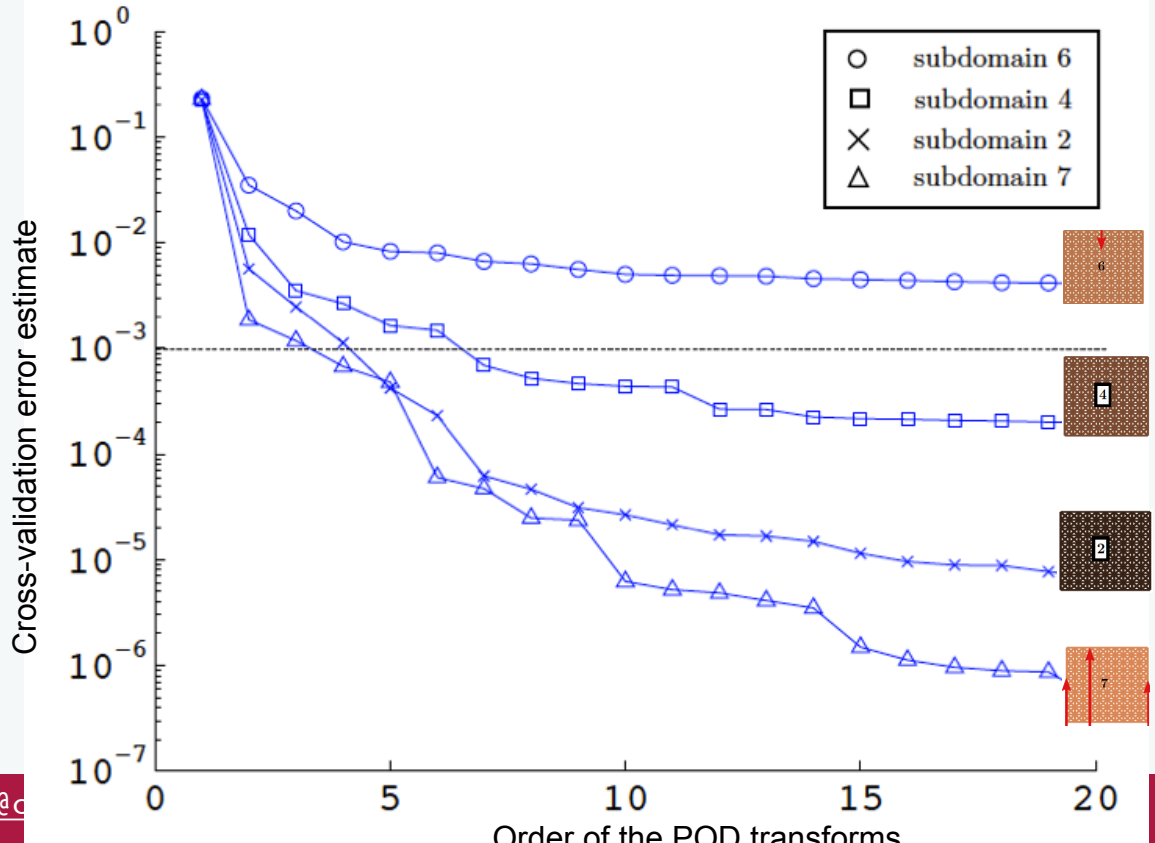
subdomain 6
subdomain 4
subdomain 2
subdomain 7
Cross-validation error estimate
10^{0}
10^{-1}
10^{-2}
10^{-3}
10^{-4}
10^{-5}
10^{-6}
10^{-7}
0
5
10
15
20
Order of the POD transforms

Performance: load angle 40 | 27 - 121 nodes

- Relative error

$$\nu^{\mathrm{app},(\mu)}\left(\underline{\mathbf{U}}^{\mathrm{app}}\right)^2 = \frac{\sum_{t_n \in \mathcal{T}^h} \|\underline{\mathbf{U}}^{\mathrm{app}}(t_n,\mu) - \underline{\mathbf{U}}^{\mathrm{ex}}(t_n,\mu)\|_2^2}{\sum_{t_n \in \mathcal{T}^h} \|\underline{\mathbf{U}}^{\mathrm{ex}}(t_n,\mu)\|_2^2}$$

40^o

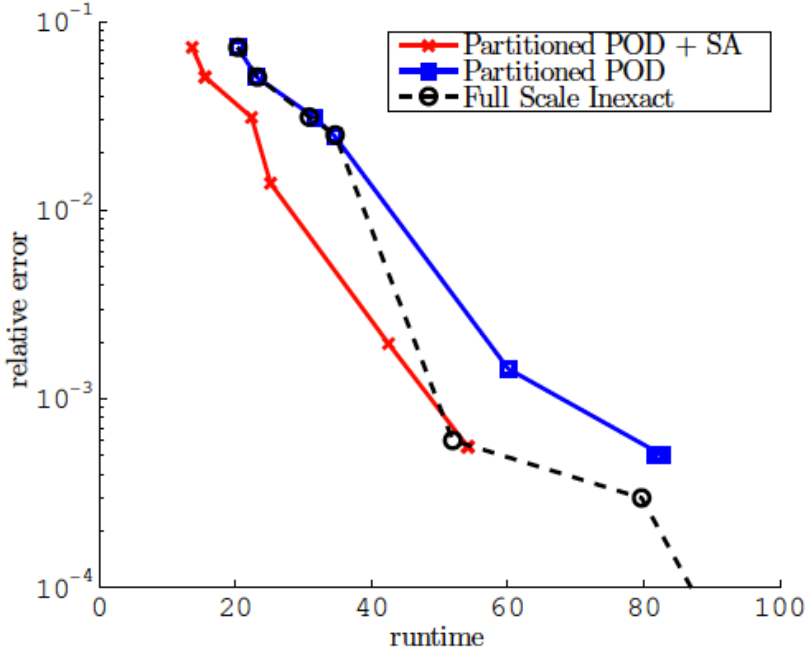

(a) Relative error for the different models using 121 nodes per subdomain

27^o

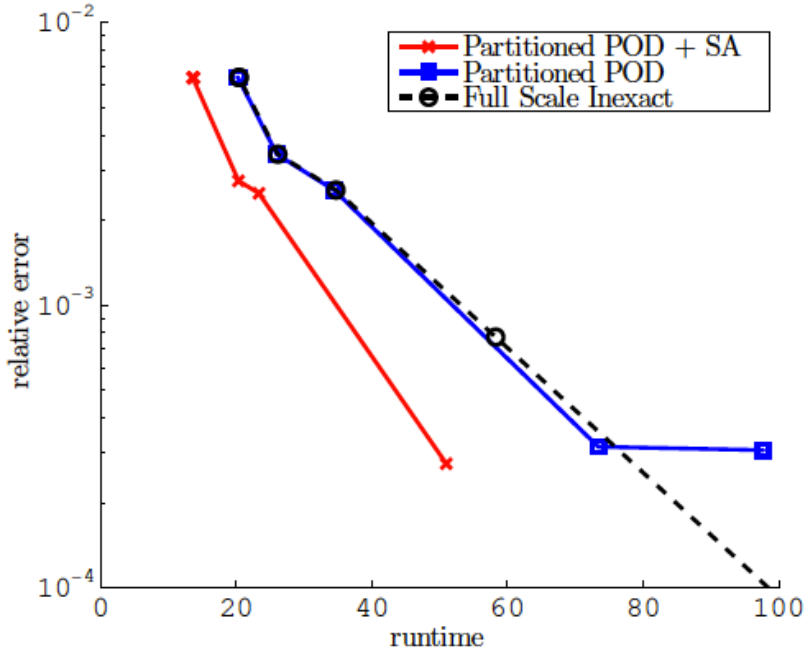

(a) Relative error for the different models using 121 no per subdomain

Performance: load angle 40 | 27 - 256 nodes

- Relative error

$$\nu^{\mathrm{app},(\mu)}\left(\underline{\mathbf{U}}^{\mathrm{app}}\right)^2 = \frac{\sum_{t_n \in \mathcal{T}^h} \|\underline{\mathbf{U}}^{\mathrm{app}}(t_n,\mu) - \underline{\mathbf{U}}^{\mathrm{ex}}(t_n,\mu)\|_2^2}{\sum_{t_n \in \mathcal{T}^h} \|\underline{\mathbf{U}}^{\mathrm{ex}}(t_n,\mu)\|_2^2}$$

40^o

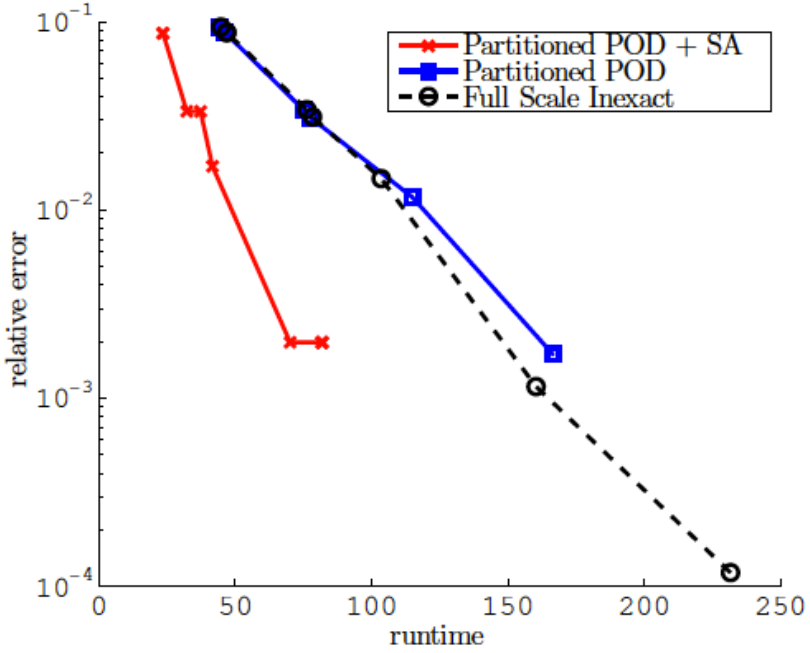

(b) Relative error for the different models using 256 nodes per subdomain

27^o

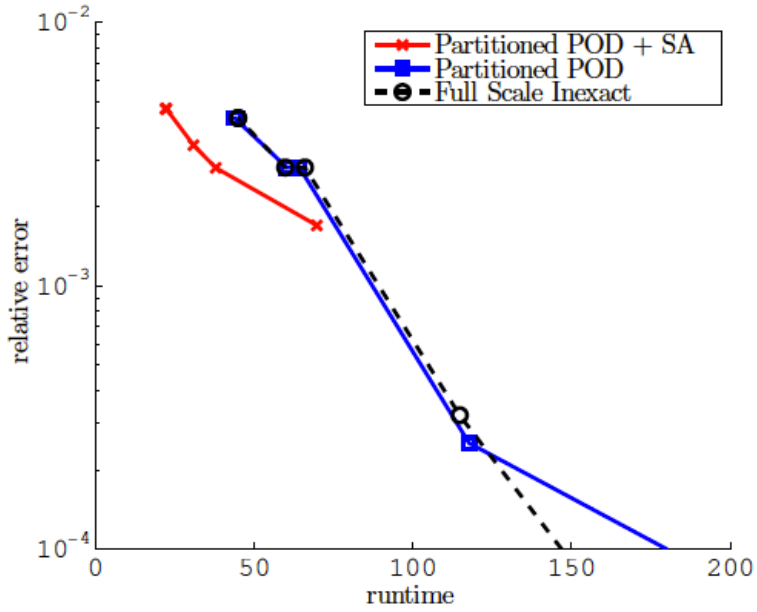

(b) Relative error for the different models using 256 nodes per subdomain

Performance: load angle 40 | 27 - 441 nodes

- Relative error

$$\nu^{\mathrm{app},(\mu)}\left(\underline{\mathbf{U}}^{\mathrm{app}}\right)^2 = \frac{\sum_{t_n \in \mathcal{T}^h} \|\underline{\mathbf{U}}^{\mathrm{app}}(t_n,\mu) - \underline{\mathbf{U}}^{\mathrm{ex}}(t_n,\mu)\|_2^2}{\sum_{t_n \in \mathcal{T}^h} \|\underline{\mathbf{U}}^{\mathrm{ex}}(t_n,\mu)\|_2^2}$$

40^o

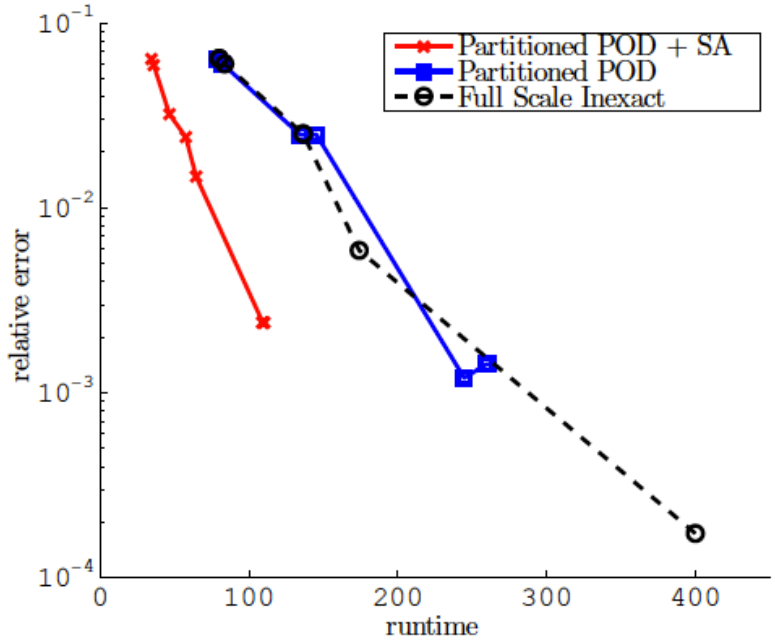

(c) Relative error for the different models using 441 nodes per subdomain

27^o

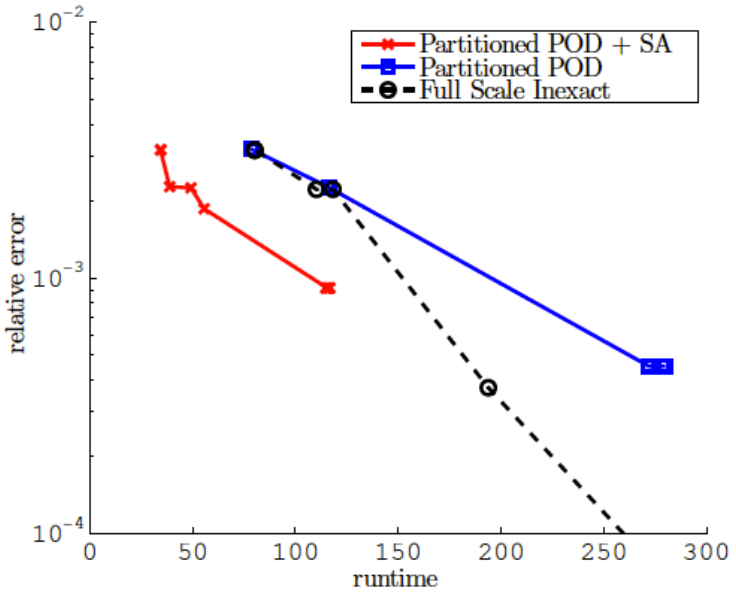

(c) Relative error for the different models using 441 nodes per subdomain

Performance: load angle 40 | 27 - 961 nodes

Relative error

- Relative error

$$\nu^{\mathrm{app},(\mu)}\left(\underline{\mathbf{U}}^{\mathrm{app}}\right)^2 = \frac{\sum_{t_n \in \mathcal{T}^h} \|\underline{\mathbf{U}}^{\mathrm{app}}(t_n,\mu) - \underline{\mathbf{U}}^{\mathrm{ex}}(t_n,\mu)\|_2^2}{\sum_{t_n \in \mathcal{T}^h} \|\underline{\mathbf{U}}^{\mathrm{ex}}(t_n,\mu)\|_2^2}$$

40^o

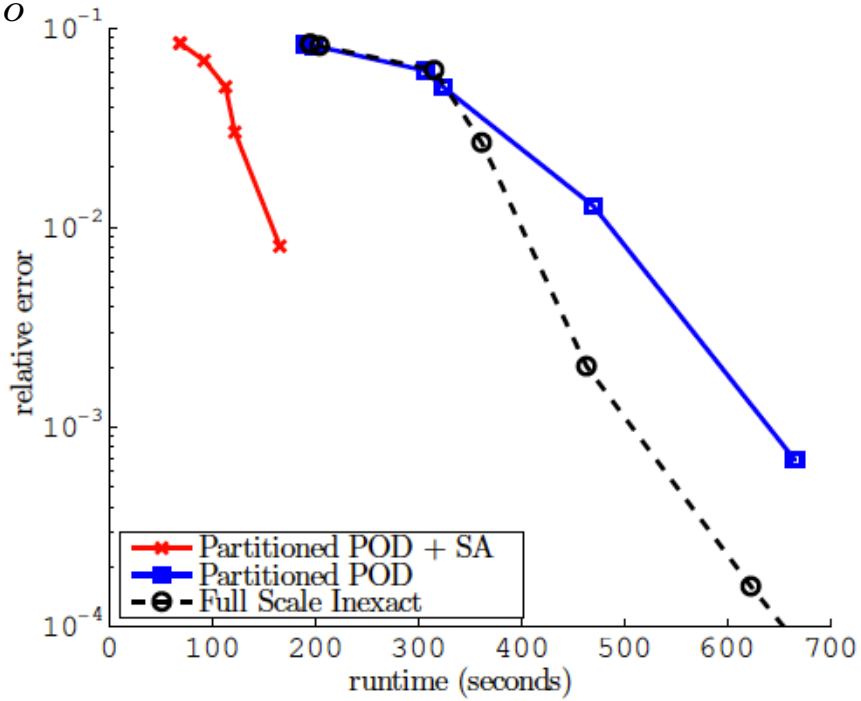

(d) Relative error for the different models using 961 nodes per subdomain

27^o

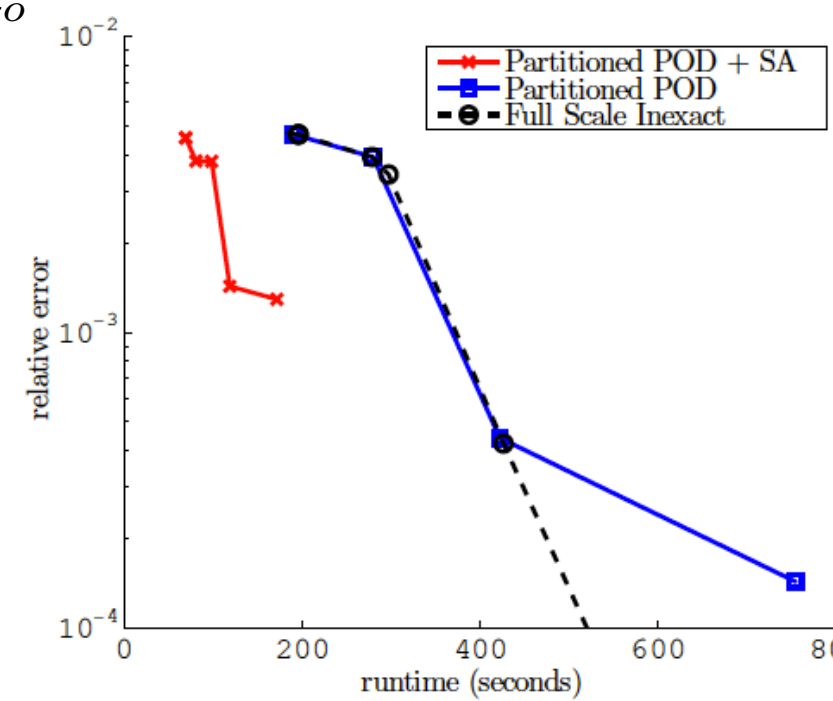

(d) Relative error for the different models using 961 per subdomain

Conclusions and perspectives

- Domain coupling using the primal Schur-complement domain decomposition method.
- Local subproblems have been reduced by projection in low-dimensional subspaces obtained by the snapshot POD.
- This approach permits to flexibly reduce the computational cost associated with highly nonlinear problems. In particular:
  - the **local reduced spaces are generated independently**, and have independent dimensions, which allows us to focus the numerical effort where it is most needed.
  - subdomains that are close to highly damaged zones need a richer model to account for the effect of topological changes. The local **POD transforms automatically generate local reduced spaces of larger dimension in these zones**.
  - the domain decomposition framework enables us to **switch from reduced local solvers to full local solvers** in a transparent manner. This is particularly useful for the subdomains that contain process zones, as a solution obtained by projection would be more expensive than a direct solution for a desirable accuracy.
  - the transition between ``offline'' and ``online'' computations becomes flexible. The **reduced models can be used in the zones where the local reduced spaces converge quickly** when enriching the snapshot space, while still computing snapshots and refining the reduced models via a direct local solver in the remaining subdomains.

Perspectives

- Further work related to domain decomposition
  - **load balancing** mismatch would occur when using such a strategy in parallel. CPUs which support domains that are not reduced, or domains for which the corresponding subproblems need to be projected in a space of relatively high dimension, would require to perform more operations. The domain partitioning itself should be performed jointly with the model reduction in order to distribute the load evenly.
  - **the interface problem itself was not reduced** here, to guarantee the interface kinematic compatibility.
    - ➡ Suboptimal reduced order model. Would generate expensive communications in parallel
    - ➡ A reduction of the interface problem using the POD can be done but is neither elegant nor easy
    - ➡ Dual Schur-complement domain decomposition method would allow the kinematic approximation of the subproblems to include the interface. However, this would only deflect the difficulty to the necessary reduction of the interface Lagrange multiplier space. This issue is our current direction of research.

Worst load combination

Scales of interest

Crack growth rate

INFORMATION

Inspection interval

Mission ?

DIGITAL TWIN OF THE SYSTEM

GEOMETRICAL MODEL

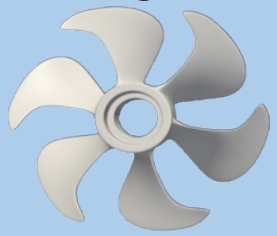

DISCRETISATION

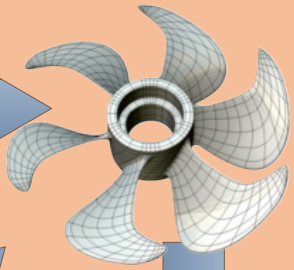

A POSTERIORI

LEARN MATERIAL MODELS

which scales?
what models?
what parameters?
what scale transition?
what data is missing?

NUMERICAL SOLUTION

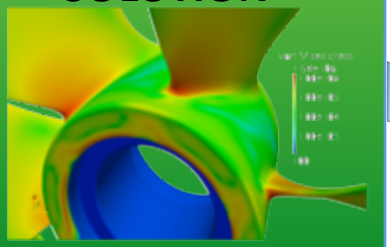

REAL SYSTEM

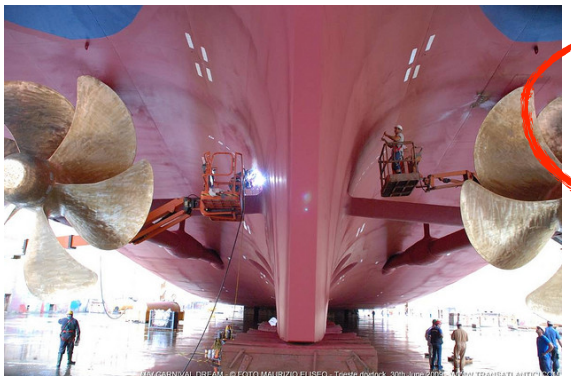

DATA

Strain

Environment Conditions

Structural Health

Cracks

Reducing the mesh burden in computational fracture mechanics

Part 0. Enrichment of the finite element method

Skip

Enrichment

- When the standard finite element method is unable to efficiently reproduce certain features of the sought solution:

1.	Discontinuities	-	cracks, *material interfaces*
2.	Large gradients	-	*yield lines, shock waves*
3.	Singularities	-	*notches, cracks, corners*
4.	Boundary layers	-	*fluid-fluid, fluid-solid*
5.	Oscillatory behavior	-	*vibrations, impact*

- The approximation space can be extended by introducing of an *a priori* knowledge about the sought solution, and thereby:

1. Rendering the mesh independent of any phenomena
2. reducing error of the approximation locally and globally
3. improving convergence rates

Classification of discontinuities

Strong discontinuities

- The primal field of the solution is discontinuous, e.g. cracks lead to strong discontinuities in the displacement field.

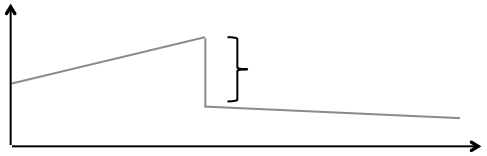

Weak discontinuities

- The first derivative of the solution is discontinuous, e.g. discontinuities in the strain field through a material interface.

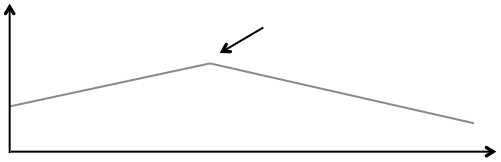

Classification of enrichments

Global enrichment

- The enrichment is employed on the global level, over the **entire domain**.
- Useful for problems that can be considered as **globally non-smooth** e.g. high-frequency solutions (Helmholtz equation)

Local enrichment

- This enrichment scheme is adopted locally, over a **local subdomain**.
- Useful for problems that only involve **locally non-smooth** phenomena, e.g. solutions with discontinuities.

Classification of enrichments

Extrinsic enrichment

- Associated with additional degrees of freedom and additional shape functions to augment the standard approximation basis.

1.	Extended finite element method (XFEM)	- Moës et al.	(1999)
2.	Generalised finite element method (GFEM)	- Strouboulis et al.	(2000a)
3.	Enriched element free Galerkin	- Ventura et al.	(2002)
4.	*hp* – clouds (Meshless/Hybrid)	- Duarte and Oden	(1996)

Intrinsic enrichment

- Not accompanied by additional degrees of freedom. Instead, some standard functions are replaced with special (problem specific) functions.

1.	Enriched moving least squares (Meshless)	- Fleming et al.	(1997)
2.	Enriched weight function (Meshless)	- Duflot et al.	(2004b)
3.	Intrinsic partition of unity methods	- Fries, Belytschko	(2006)
4.	Elements with embedded discontinuities		

Singular elements (Barsoum, 1974)

For simulating the crack tip singular field in LEFM

- A simple way how to introduce a singularity of $1/\sqrt{r}$ in isoperimetric finite elements is by displacing the mid-side nodes of two adjacent edges to one quarter of the element edge length from the node where the singularity is desired.

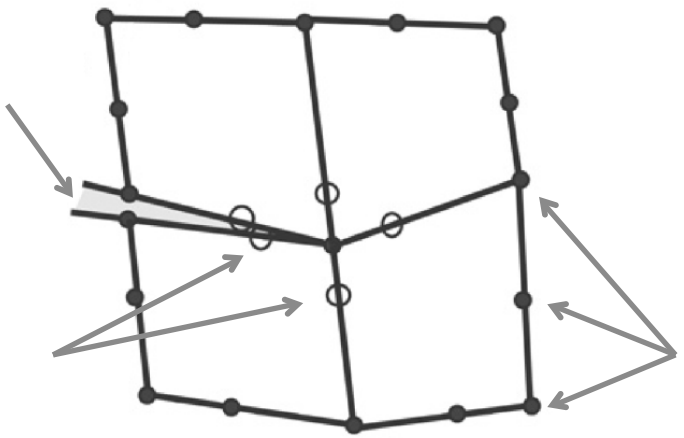

Partition of unity finite element method (PUFEM)

Partition of unity (PU)

- A set of functions ϕ_i whose sum at any point $\boldsymbol{x}$ inside a domain Ω is equal to unity:

$$\forall \mathbf{x} \in \Omega, \mathbf{x} : \sum_{I=1} \phi_I(\mathbf{x}) = 1$$

- Example PU functions are the finite element "hat" functions:

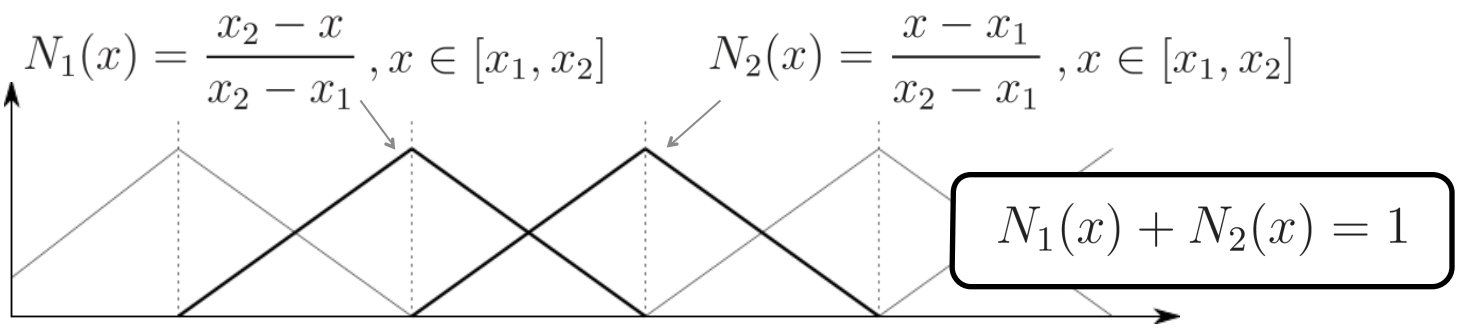

Partition of unity finite element method (PUFEM)

Reproducibility of PU

- Any function $\boldsymbol{p(x)}$ can be reproduced by a product of that function and the partition of unity functions:

$$\sum_{I=1} \phi_I(\mathbf{x}) p(\mathbf{x}) = p(\mathbf{x})$$

- The function can be adjusted if the sum is modified by introducing parameters $\boldsymbol{q_I}$:

$$\sum_{I=1} \phi_I(\mathbf{x}) p(\mathbf{x}) q_I = \bar{p}(\mathbf{x})$$

- Reproducibility of $\boldsymbol{p(x)}$ can be controlled and localised to arbitrary regions where $\boldsymbol{q_I \neq 0}$

Partition of unity finite element method (PUFEM)

Formulation of PUFEM (example)

- Find the solution to the following 1D boundary value problem (BVP):

$$\forall x \in [0, l] : \frac{\mathrm{d}^2 u}{\mathrm{d}x^2} + f = 0$$

$$\text{with BC} : u(0) = 0,\ u(l) = u_l$$

- If we define two bilinear forms:

$$a(w, u) = \int_0^l \frac{\mathrm{d}w}{\mathrm{d}x} \frac{\mathrm{d}u}{\mathrm{d}x}\, \mathrm{d}x \qquad (w, f) = \int_0^l wf\, \mathrm{d}x$$

- The discrete variational problem can be stated as:

find $u^h \in U^h$ satisfying the BC such that for all $w^h \in W^h$:

$$a(w^h, u^h) = (w^h, f)$$

Partition of unity finite element method (PUFEM)

Formulation of PUFEM (example)

- The approximation/trial function in PUFEM:

$$u^h(x) = \underbrace{\sum_{I=1} N_I(x) u_I}_{\text{standard FE}} + \underbrace{\sum_{J=1} \phi_J(x)\psi(x) q_J}_{\text{PU enriched}}$$

- By choosing $w^h = \delta u^h$, leads to the discrete system of equations:

$$a(\delta u^h, u^h) = (\delta u^h, f)$$

$$\Downarrow$$

$$\begin{bmatrix} \mathbf{K^{ss}} & \mathbf{K^{se}} \\ \mathbf{K^{es}} & \mathbf{K^{ee}} \end{bmatrix} \begin{Bmatrix} \mathbf{u}^s \\ \mathbf{q}^e \end{Bmatrix} = \begin{Bmatrix} \mathbf{f}^s \\ \mathbf{f}^e \end{Bmatrix}$$

$$\mathbf{K}_{ij}^{se} = \int_0^l \frac{\mathrm{d}N_i}{\mathrm{d}x} \frac{\mathrm{d}(\phi_j\psi)}{\mathrm{d}x}\,\mathrm{d}x \qquad \mathbf{K}_{ij}^{ss} = \int_0^l \frac{\mathrm{d}N_i}{\mathrm{d}x} \frac{\mathrm{d}N_j}{\mathrm{d}x}\,\mathrm{d}x$$

$$\mathbf{K}_{ij}^{es} = \int_0^l \frac{\mathrm{d}(\phi_i\psi)}{\mathrm{d}x} \frac{\mathrm{d}N_j}{\mathrm{d}x}\,\mathrm{d}x \qquad \mathbf{K}_{ij}^{ee} = \int_0^l \frac{\mathrm{d}(\phi_i\psi)}{\mathrm{d}x} \frac{\mathrm{d}(\phi_j\psi)}{\mathrm{d}x}\,\mathrm{d}x$$

$$f_i^s = \int_0^l N_i f_x\,\mathrm{d}x \qquad f_i^e = \int_0^l (\phi_i\psi) f_x\,\mathrm{d}x$$

Partition of unity finite element method (PUFEM)

Remarks

- Allows to introduce an arbitrary function $\boldsymbol{\psi}(\boldsymbol{x})$ in the approximation space by splitting the approximation into a **standard** and **enriched** parts.

- Enrichment can be **localised** to a small region around the features of interest – computationally advantageous.

- Provides a systematic means of introducing multiple enrichments.

References:

- Melenk and Babuska (1996)
- Duarte and Oden (1996)

The Generalised Finite Element Method (GFEM)

GFEM

- Originally associated with global PU enrichment
- Shape functions in the enriched part are usually different from the shape functions in the standard part i.e. $\phi_I(x) \neq N_I(x)$
- Introduced numerically generated enrichment functions, e.g. a solution in the vicinity of a bifurcated crack as enrichment

References:

- Melenk (1995)
- Melenk and Babuška (1996)
- Strouboulis et al. (2000)

The Extended Finite Element Method (XFEM)

XFEM

- Associated with local discontinuous PU enrichment e.g.:

  a. propagation of cracks
  b. evolution of dislocations
  c. phase boundaries

- Both GFEM and XFEM are essentially identical in their application, i.e. extrinsic PU enrichment

References:

- Belytschko and Black (1999)
- Moës et. al. (1999)
- Dolbow (1999)

Formulation for crack growth:

$$\mathbf{u}^h(\mathbf{x}) = \underbrace{\sum_{I\in\mathcal{N}_I} N_I(\mathbf{x})\mathbf{u}^I}_{\text{standard part}} + \underbrace{\sum_{J\in\mathcal{N}_J} N_J(\mathbf{x})H(\mathbf{x})\mathbf{a}^J}_{\text{discontinuous enrichment}} + \underbrace{\sum_{K\in\mathcal{N}_K} N_K(\mathbf{x})\sum_{\alpha=1}^{4} f_\alpha(\mathbf{x})\mathbf{b}^{K\alpha}}_{\text{singular tip enrichment}}$$

$$H(\mathbf{x}) = \begin{cases} +1 & \text{if } \mathbf{x} \text{ above crack} \\ -1 & \text{if } \mathbf{x} \text{ below crack} \end{cases}$$

$$\{f_\alpha(r,\theta), \alpha = 1,4\} = \left\{\sqrt{r}\sin\frac{\theta}{2}, \sqrt{r}\cos\frac{\theta}{2}, \sqrt{r}\sin\frac{\theta}{2}\sin\theta, \sqrt{r}\cos\frac{\theta}{2}\sin\theta\right\}$$

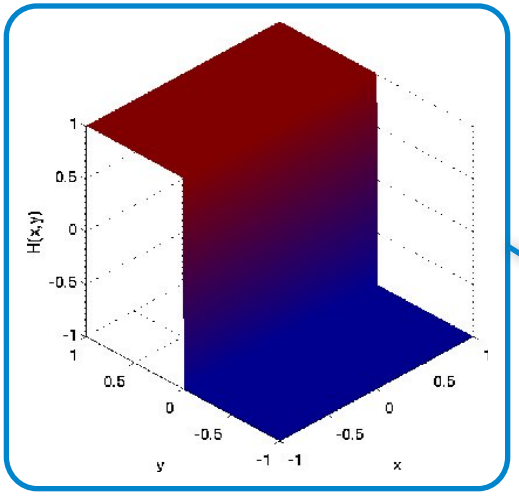

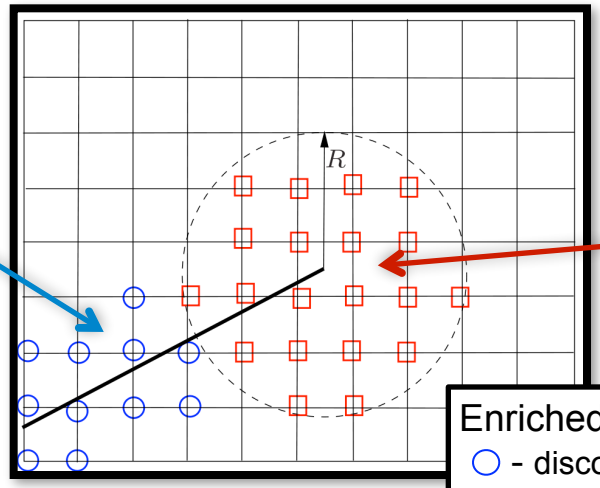

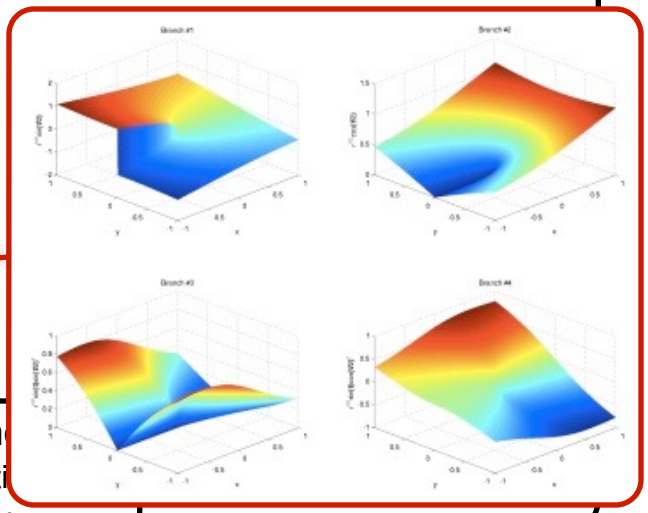

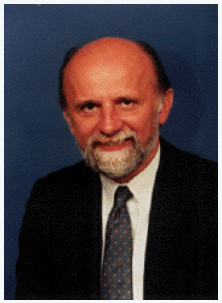

$$u_i^h(\mathrm{x}) = \sum_{\substack{I \\ n_I \subset \mathrm{N}}} N_I(\mathrm{x}) u_{iI} + \sum_{\substack{J \\ n_J \subset \mathrm{N}^c}} N_J(\mathrm{x}) a_{iJ} H(\mathrm{x}) + \sum_{\substack{K \\ n_K \subset \mathrm{N}^f}} \phi_K(\mathrm{x}) b_{iK} \Psi(\mathrm{x})$$

classical — **enriched**

$$H(\mathbf{x}) = \begin{cases} +1 & if\ \mathbf{x}\ above \\ -1 & if\ \mathbf{x}\ below \end{cases}$$

Heaviside function

Asymptotic fields

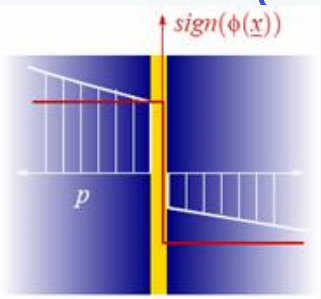

$$\psi(r,\theta) = \sqrt{r}\cos\frac{\theta}{2}, \sqrt{r}\sin\frac{\theta}{2}, \sqrt{r}\sin\theta\sin\frac{\theta}{2}, \sqrt{r}\sin\theta\cos\frac{\theta}{2}$$

Selection of enriched nodes

$$u_i^h(\mathrm{x}) = \sum_{\substack{I \\ n_I \subset \mathrm{N}}} N_I(\mathrm{x}) u_{iI} + \sum_{\substack{J \\ n_J \subset \mathrm{N}^c}} N_J(\mathrm{x}) a_{iJ} H(\mathrm{x}) + \sum_{\substack{K \\ n_K \subset \mathrm{N}^f}} \phi_K(\mathrm{x}) b_{iK} \Psi(\mathrm{x})$$

enriched

Heaviside function

Asymptotic fields

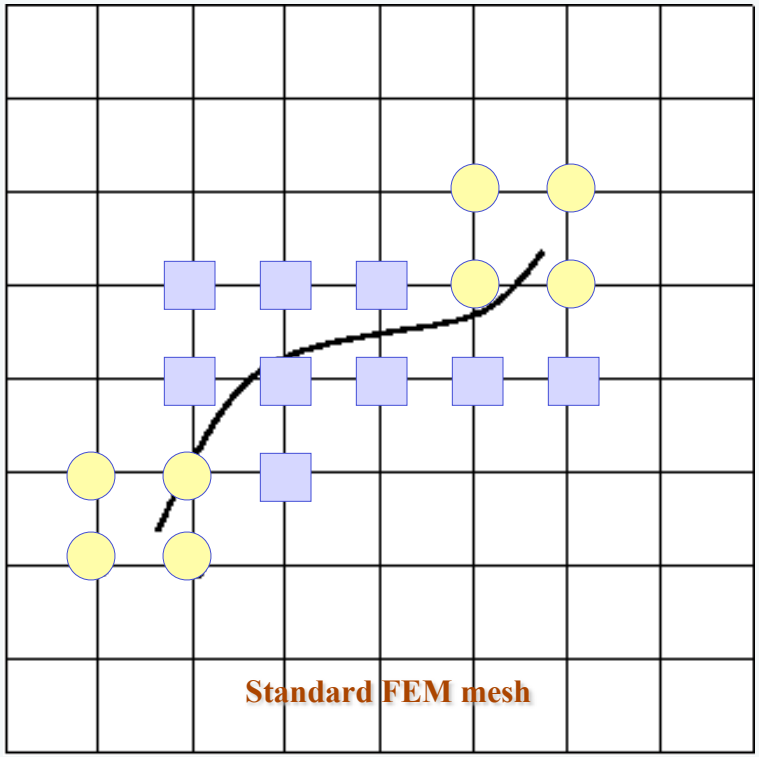

ENRICHED NODES

Tip

Interior

CARDIFF UNIVERSITY
PRIFYSGOL CAERDYDD

Part I. Streamlining the CAD-analysis transition

Part II. Some advances in enriched FEM

Part III. Application to H cutting of Si wafers

Part IV. Application to interactive cutting sim.

erc

IMAM
Institute of Mechanics & Advanced Materials

Worst load combination

Scales of interest

Crack growth rate

INFORMATION

Inspection interval

Mission ?

DIGITAL TWIN OF THE SYSTEM

GEOMETRICAL MODEL

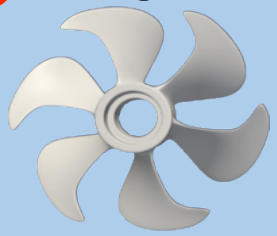

DISCRETISATION

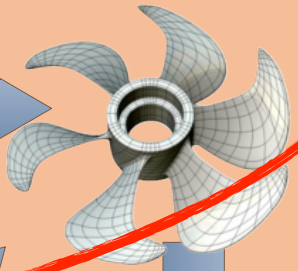

A POSTERIORI

LEARN MATERIAL MODELS

which scales?
what models?
what parameters?
what scale transition?
what data is missing?

NUMERICAL SOLUTION

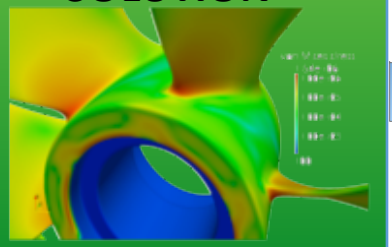

REAL SYSTEM

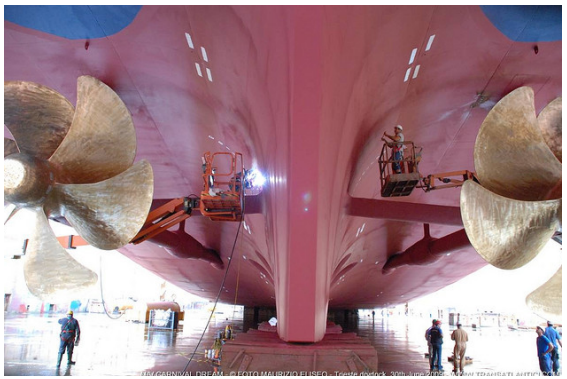

DATA

Strain

Environment Conditions

Cracks

Structural Health

Motivation: free boundary problems - mesh burden

FEM

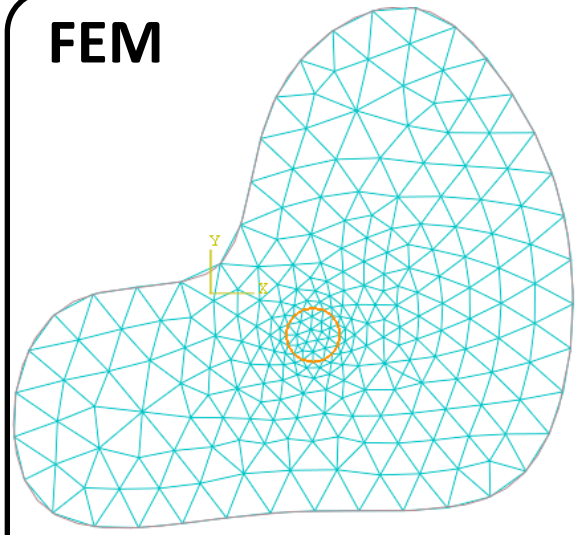

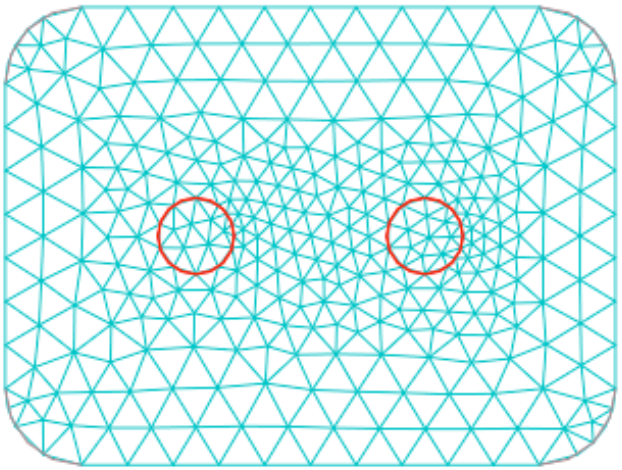

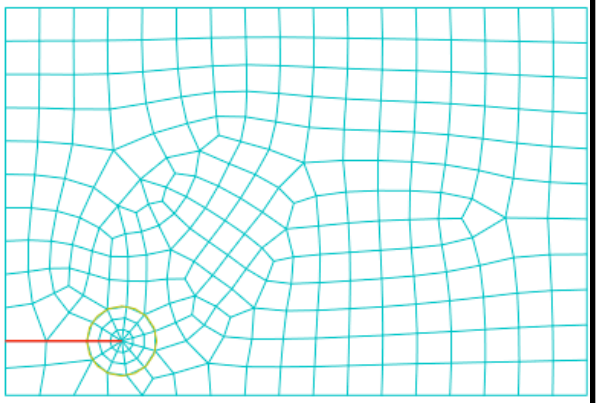

XFEM

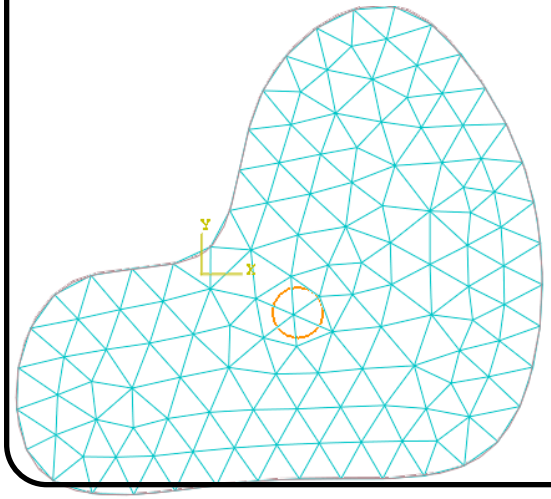

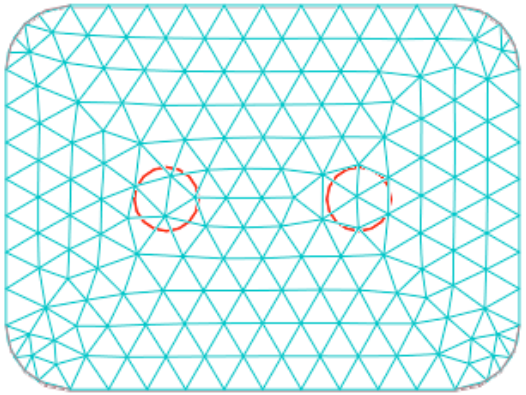

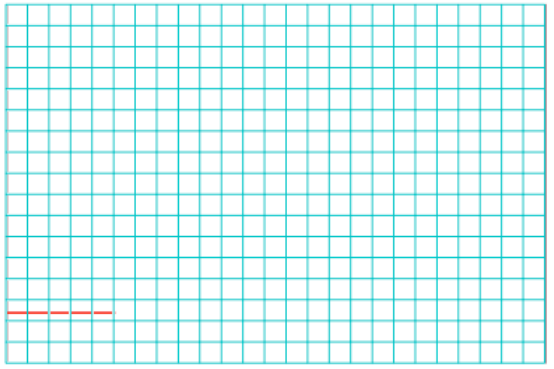

CARDIFF UNIVERSITY
PRIFYSGOL CAERDYDD

ITN INSIST

Part I. Streamlining the CAD-analysis transition

Coupling, or decoupling?

IMAM Institute of Mechanics & Advanced Materials

Reduce the mesh burden

Decouple geometry and analysis

- Meshfree methods (Monaghan, 1977, Belytschko, *et al.* 1994)
- PU enrichment (Melenk & Babuška, 1996; Belytschko, *et al.* 1999)
- Immersed boundary method (Mittal, *et al.* 2005)

Improve element formulations (use simplex elements)

- Smoothed FEM (Liu, *et al.* 2006), smoothed XFEM (Bordas,...)
- Polygonal FEM (Alwood, *et al.* 1969)

Boundary discretisation

- Boundary element method (Rizzo, 1967)
- Scaled boundary FEM (Song, *et al.* 1997)

Couple geometry and analysis: Isogeometric analysis (Hughes, 2005), Isogeometric BEM (Simpson, *et al.* 2012)

CARDIFF UNIVERSITY
PRIFYSGOL CAERDYDD

ITN INSIST

Part I.a. *Decoupling CAD and Analysis.*

IMAM
Institute of Mechanics & Advanced Materials

Separate field and boundary discretisation

- Immersed boundary method (Mittal, *et al.* 2005)
- Fictitious domain (Glowinski, *et al.* 1994)
- Embedded boundary method (Johansen, *et al.* 1998)
- Virtual boundary method (Saiki, *et al.* 1996)
- Cartesian grid method (Ye, *et al.* 1999, Nadal, 2013)

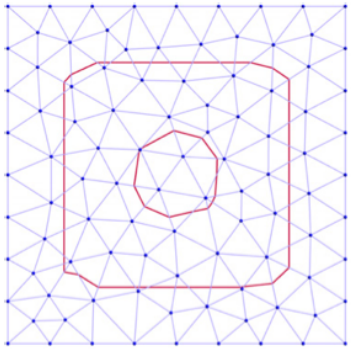

✓ Easy adaptive refinement + error estimation (Nadal, 2013)

✓ Flexibility of choosing basis functions

- Accuracy for complicated geometries? BCs on implicit surfaces?

➡ An accurate and implicitly-defined geometry from arbitrary parametric surfaces including corners and sharp edges (Moumnassi, *et al.* 2011)

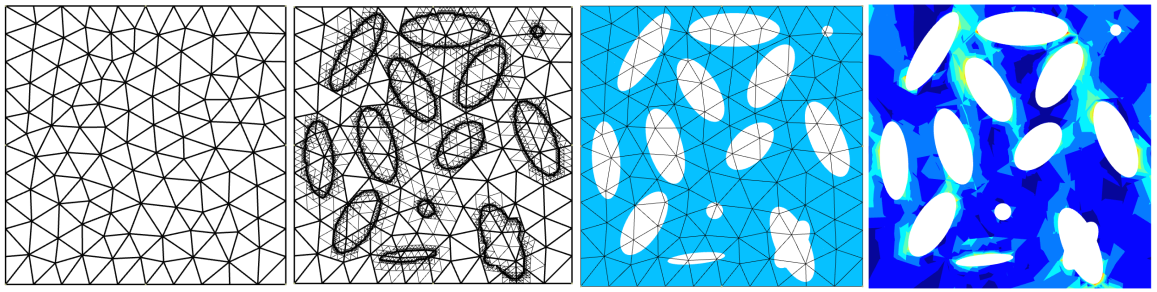

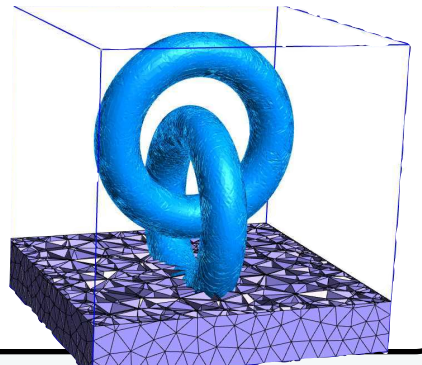

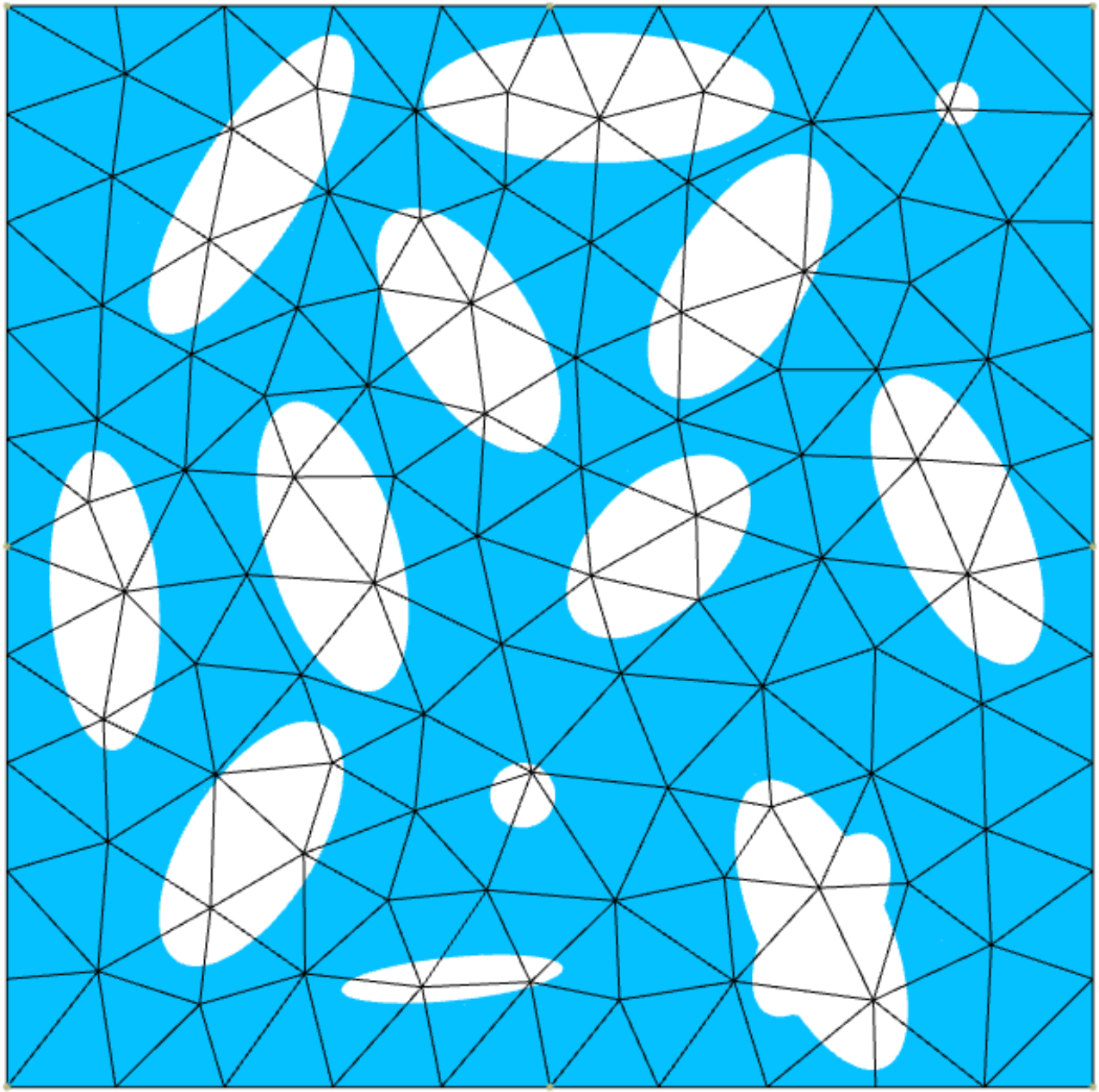

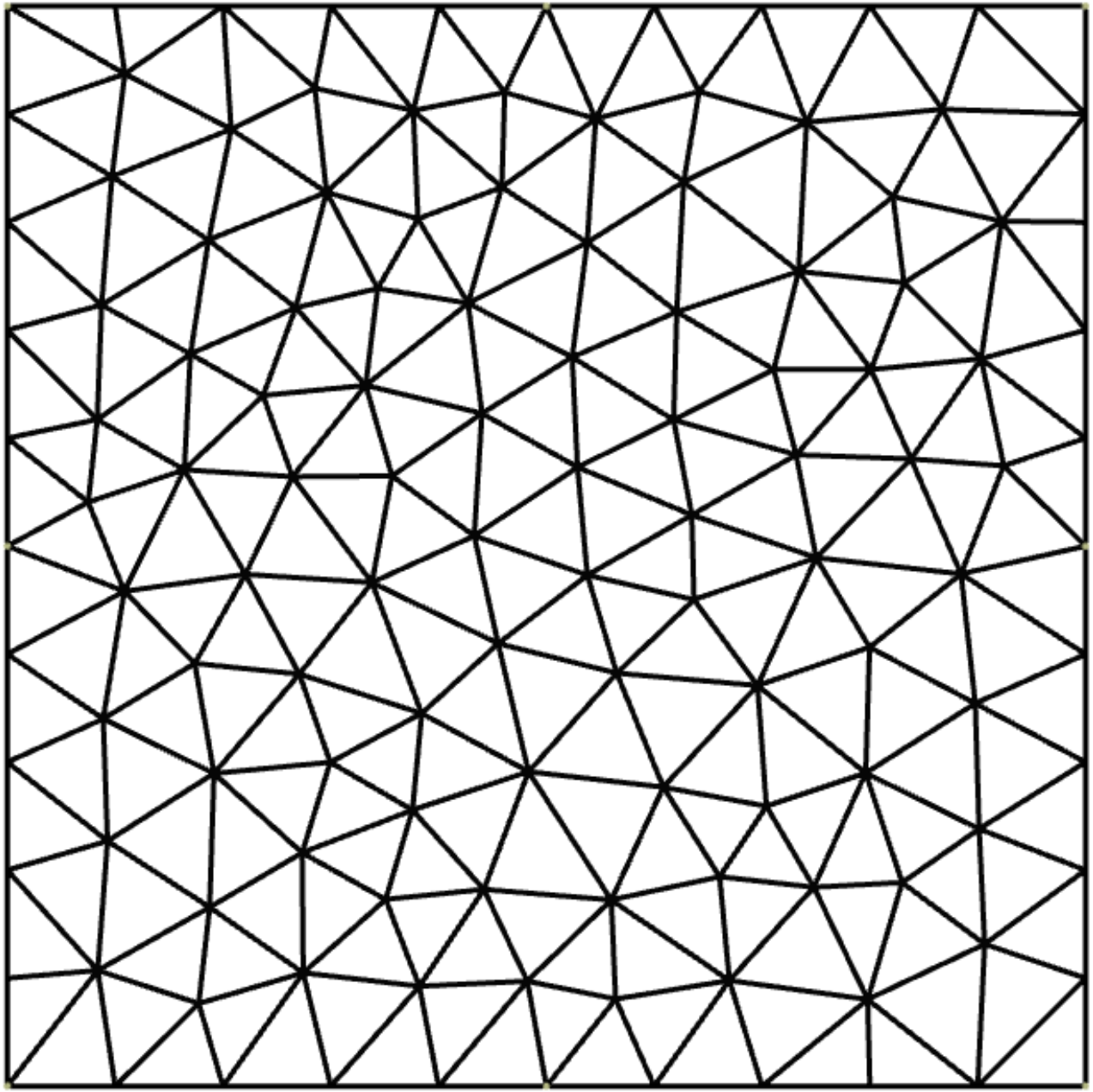

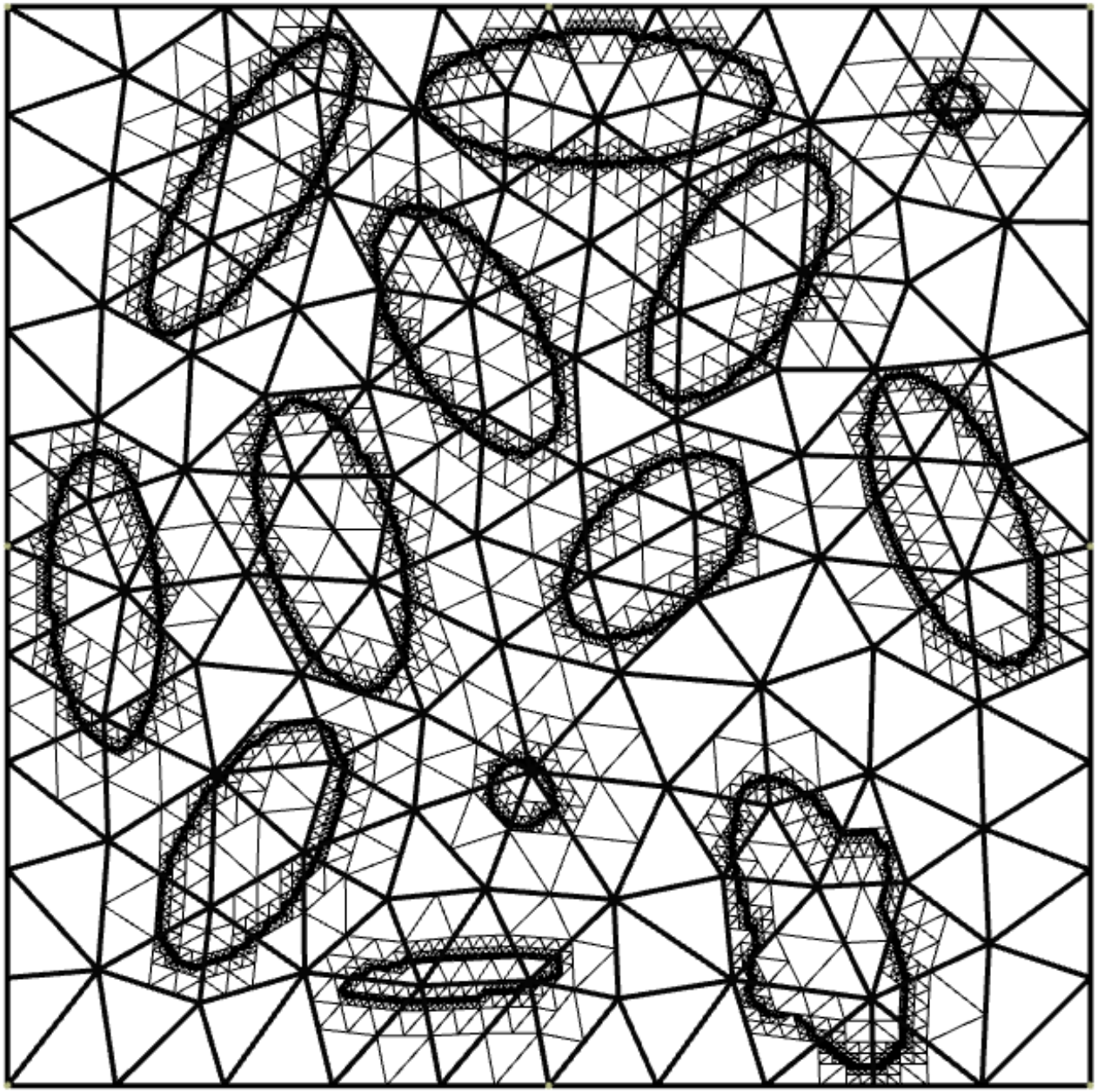

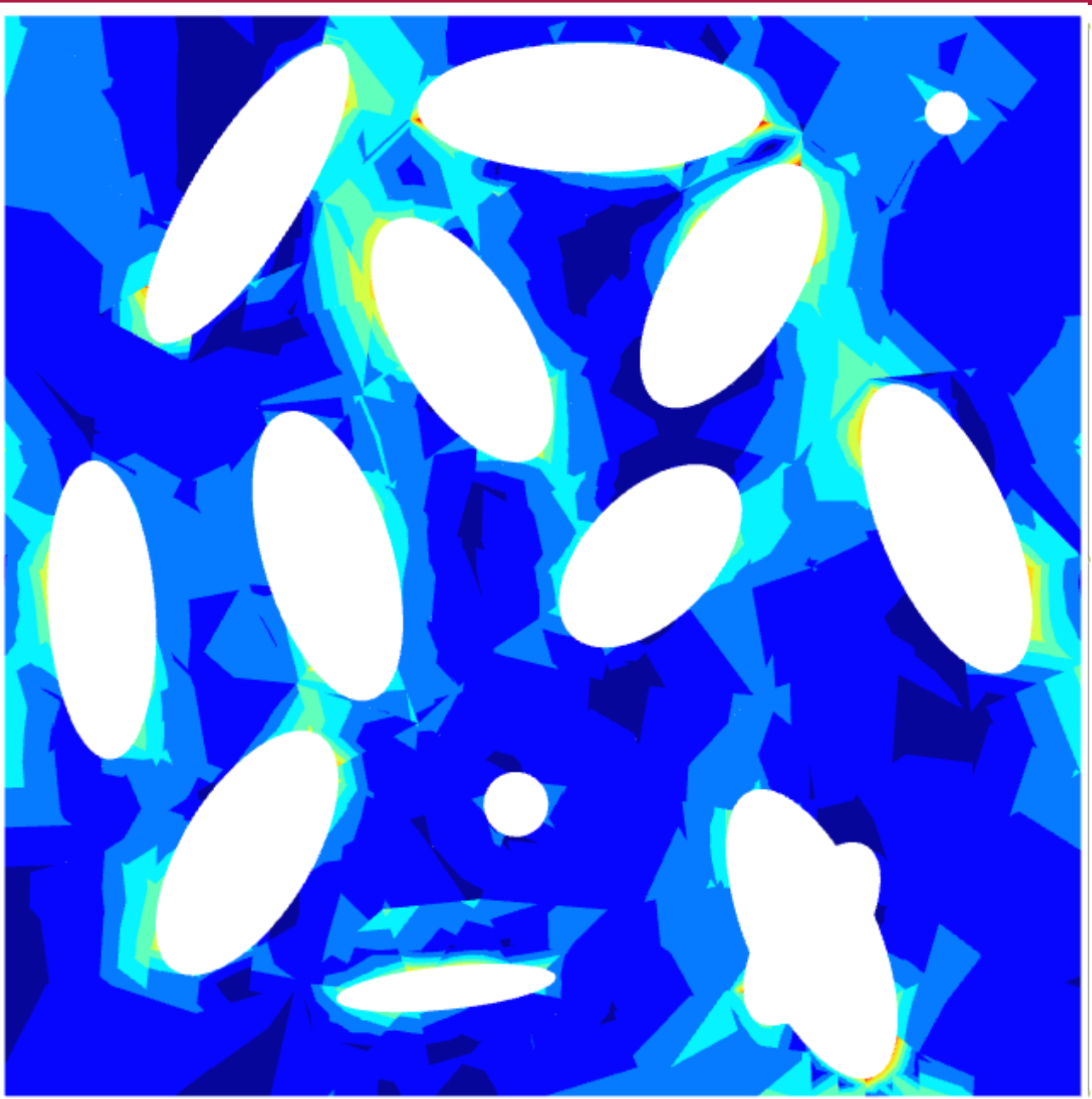

Moumnassi et al, CMAME DOI:10.1016/j.cma.2010.10.002

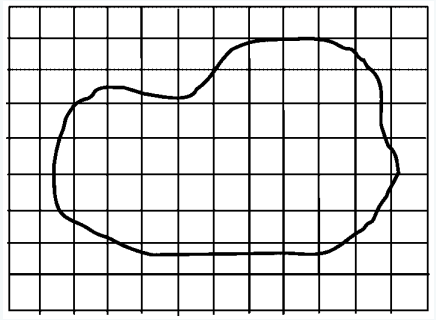

- Objectives
  - insert surfaces in a structured mesh
    - without meshing the surfaces (boundary, cracks, holes, inclusions, etc.)
    - directly from the underlying CAD model
    - model arbitrary solids, including sharp edges and vertices
  - keep as much as possible of the mesh as the CAD model evolves, i.e. reduce mesh dependence of the implicit boundary representation
  - maintain the convergence rates and implementation simplicity of the FEM

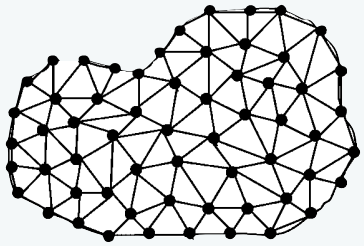

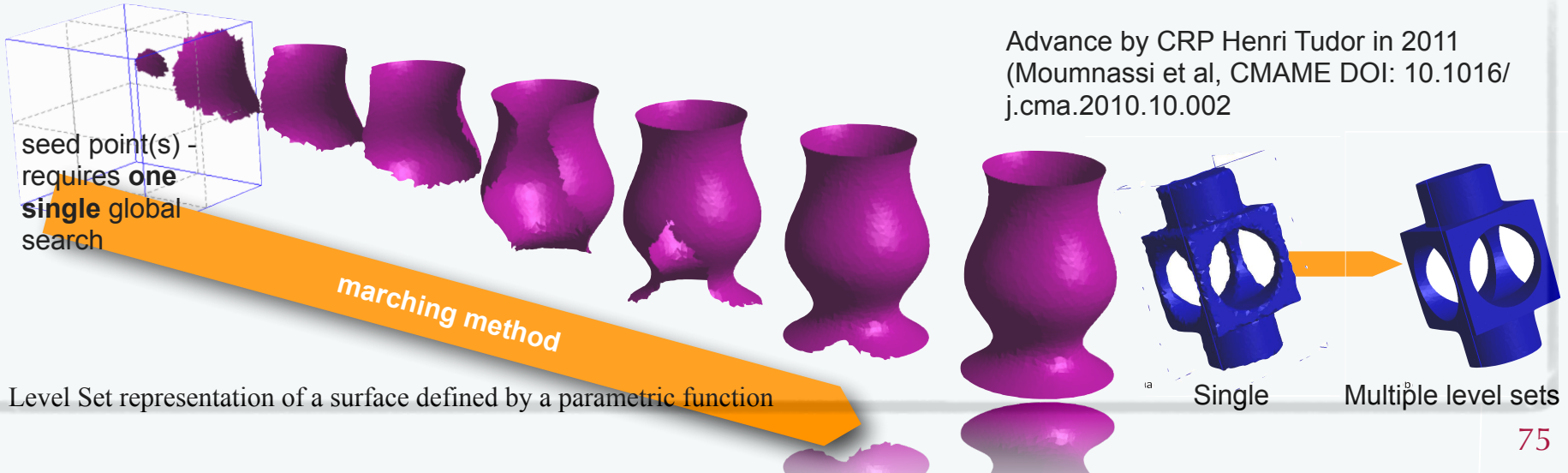

Level Set representation of a surface defined by a parametric function

Examples

- multiple level sets

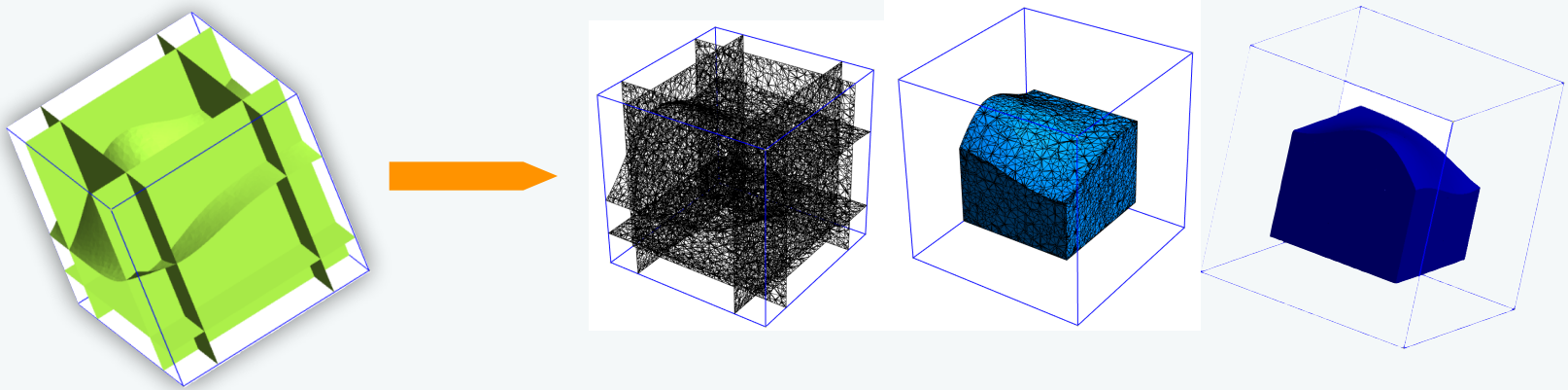

- single (left) versus multiple (right)

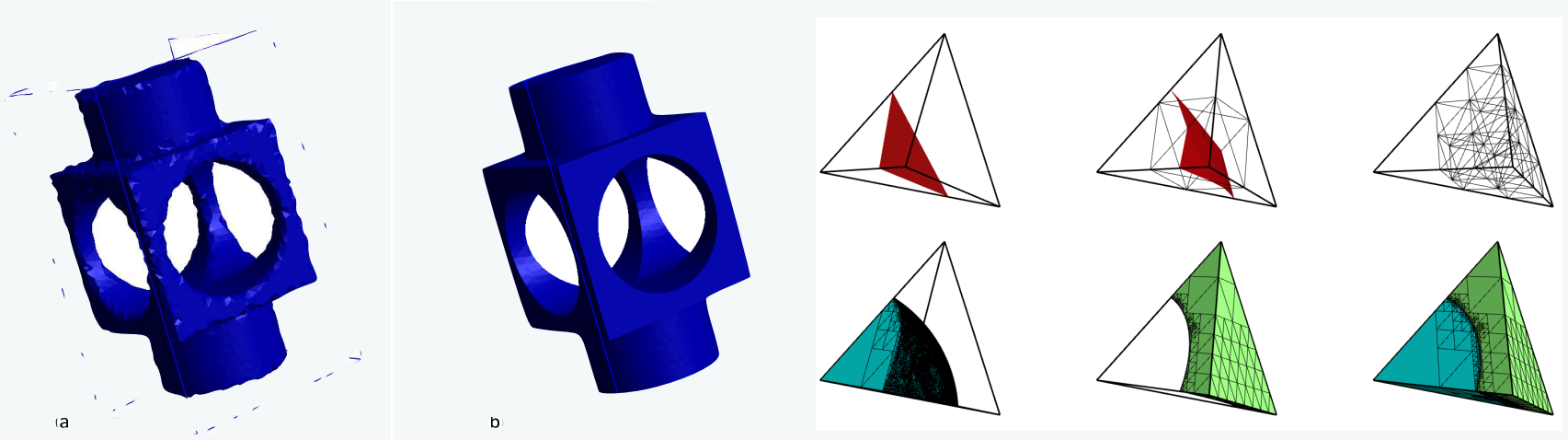

Three-dimensional model problem

- Laplace equation on a cube
- convergence rates
  - optimal
  - requires proper Lagrange multiplier space to eradicate spurious oscillations

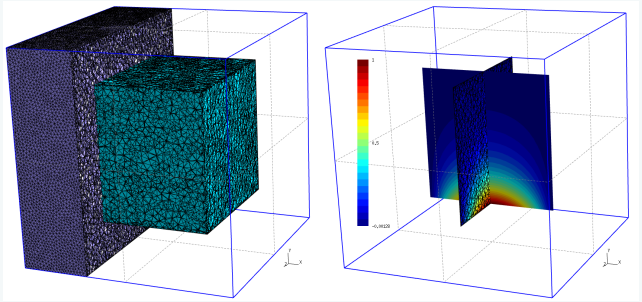

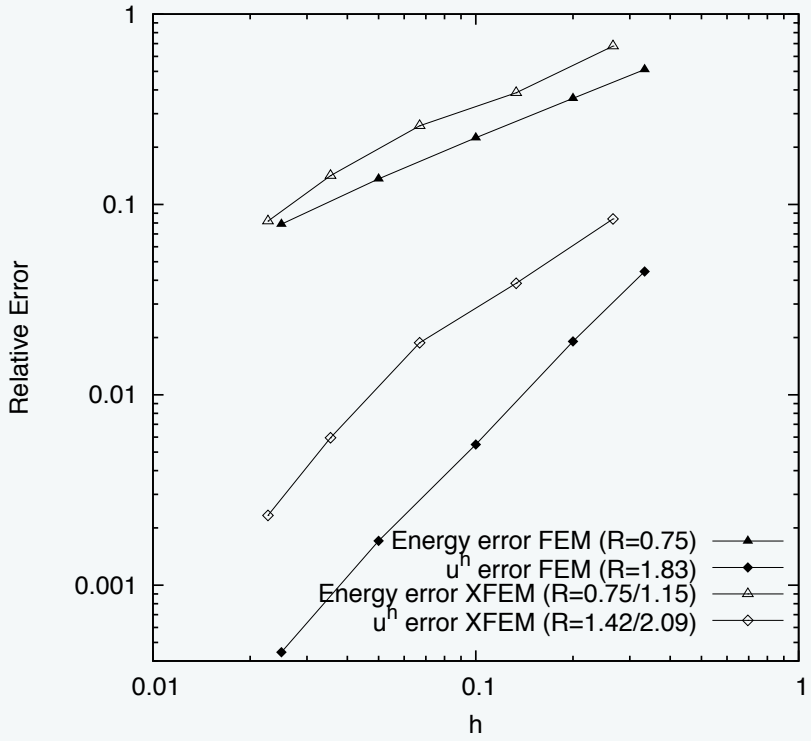

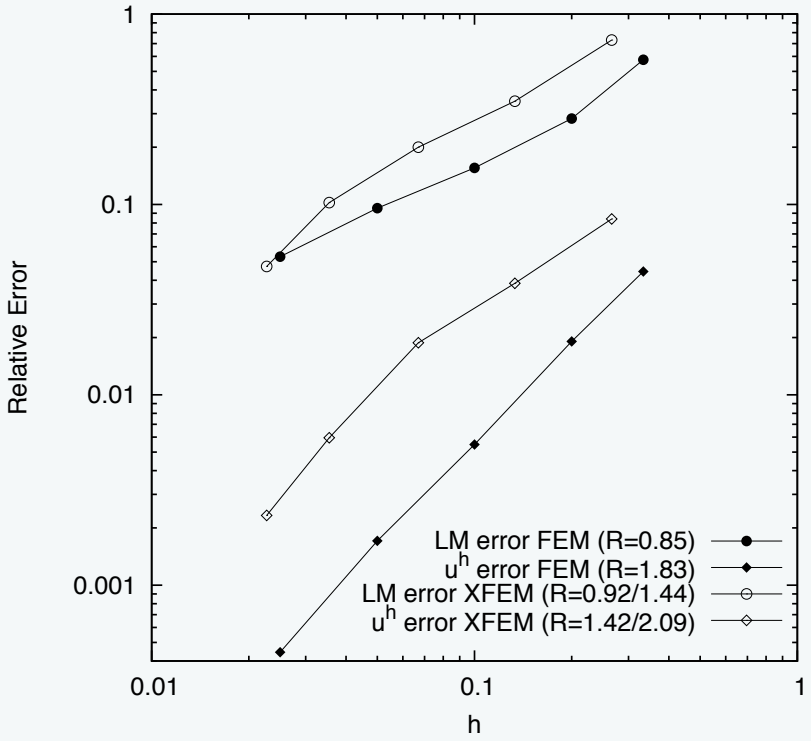

Pixel/Voxel-based FEA on Cartesian grids (Valencia)

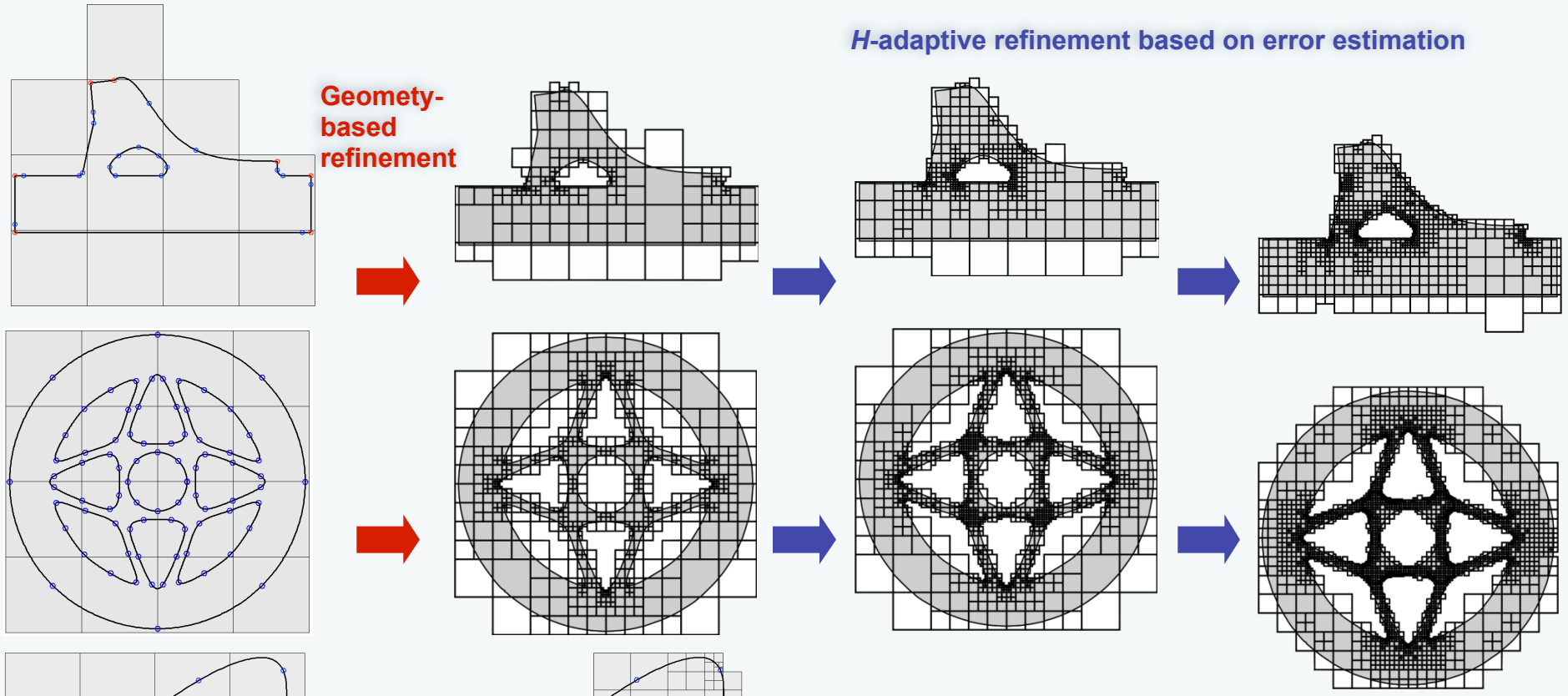

Pixel/Voxel-based FEA on Cartesian grids (Valencia)

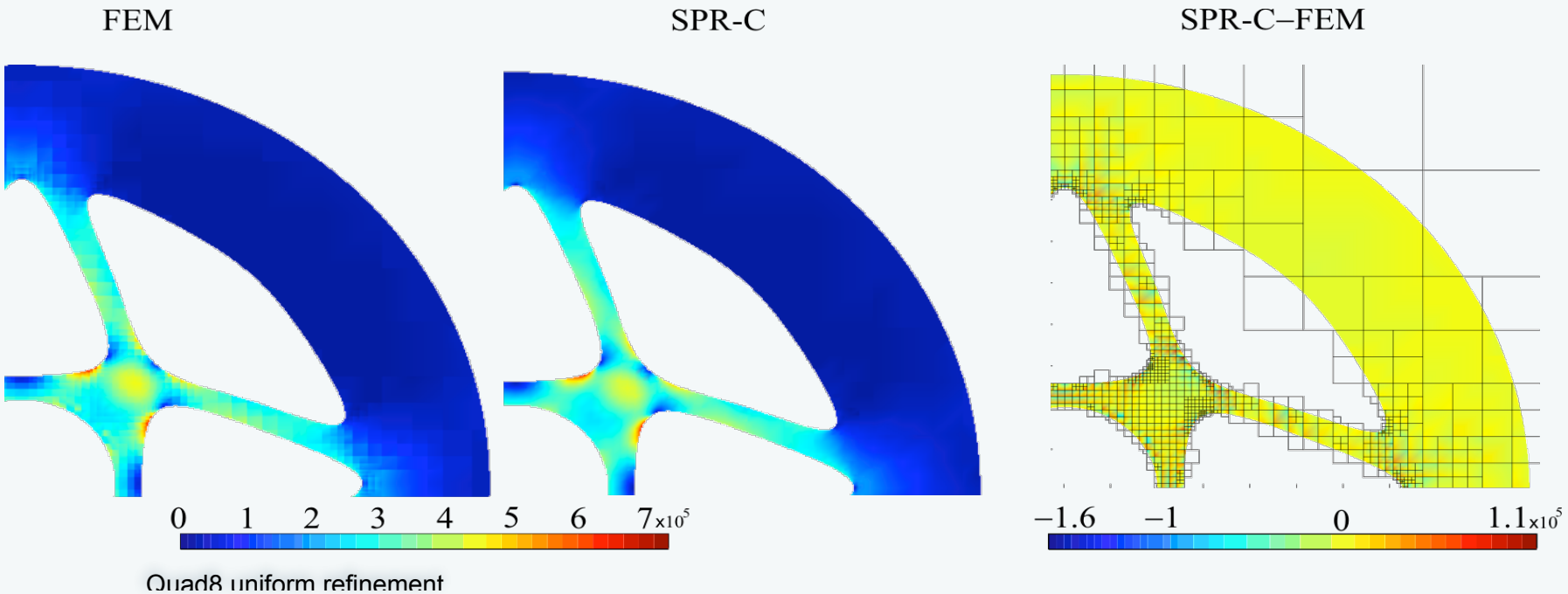

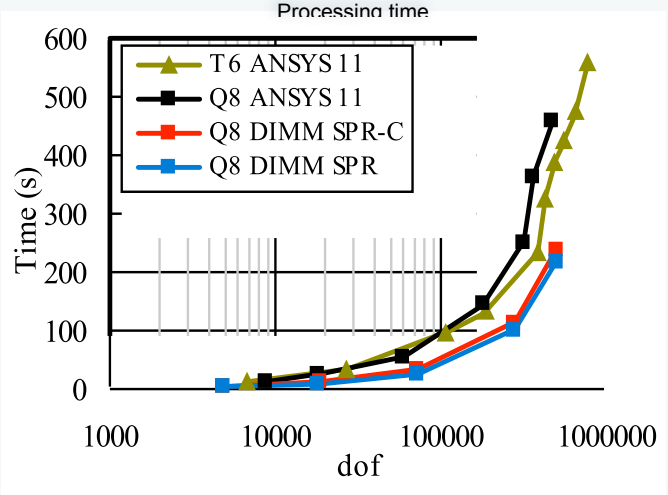

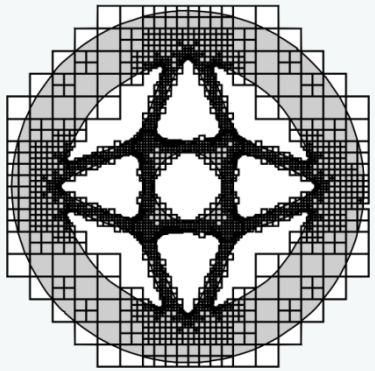

CARDIFF UNIVERSITY
PRIFYSGOL CAERDYDD

ITN INSIST

Part I.b. *Coupling CAD and Analysis.*

IMAM
Institute of Mechanics & Advanced Materials

Isogeometric analysis

- P. Kagan, A. Fischer, and P. Z. Bar-Yoseph. New B-Spline Finite Element approach for geometrical design and mechanical analysis. IJNME, 41(3):435–458, 1998.
- F. Cirak, M. Ortiz, and P. Schröder. Subdivision surfaces: a new paradigm for thin-shell finite-element analysis. IJNME, 47(12): 2039–2072, 2000.
- Constructive solid analysis: a hierarchical, geometry-based meshless analysis procedure for integrated design and analysis. D. Natekar, S. Zhang,and G. Subbarayan. CAD, 36(5): 473--486, 2004.
- T.J.R. Hughes, J.A. Cottrell, and Y. Bazilevs. Isogeometric analysis: CAD, finite elements, NURBS, exact geometry and mesh refinement. CMAME, 194(39-41):4135–4195, 2005.
- J. A. Cottrell, T. J.R. Hughes, and Y. Bazilevs. Isogeometric Analysis: Toward Integration of CAD and FEA. Wiley, 2009.

Isogeometric analysis

- P. Kagan, A. Fischer, and P. Z. Bar-Yoseph. New B-Spline Finite Element approach for geometrical design and mechanical analysis. IJNME, 41(3):435–458, 1998.
- F. Cirak, M. Ortiz, and P. Schröder. Subdivision surfaces: a new paradigm for thin-shell finite-element analysis. IJNME, 47(12): 2039–2072, 2000.
- **Constructive solid analysis: a hierarchical, geometry-based meshless analysis procedure for integrated design and analysis. D. Natekar, S. Zhang,and G. Subbarayan. CAD, 36(5): 473--486, 2004.**
- **T.J.R. Hughes, J.A. Cottrell, and Y. Bazilevs. Isogeometric analysis: CAD, finite elements, NURBS, exact geometry and mesh refinement. CMAME, 194(39-41):4135–4195, 2005.**
- J. A. Cottrell, T. J.R. Hughes, and Y. Bazilevs. Isogeometric Analysis: Toward Integration of CAD and FEA. Wiley, 2009.

Non-uniform rational B-splines

Knot vector

a non-decreasing set of coordinates in the parametric space.

$$\Xi = \{\xi_1,\ \xi_2\ ,\ \cdots,\ \xi_{n+p+1}\}$$

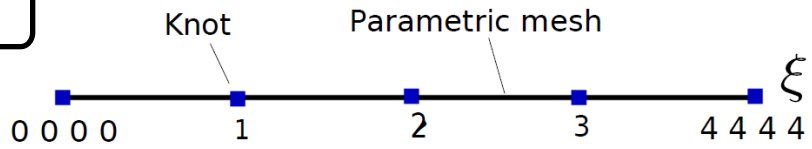

B-spline basis function

$$N_{a,0}(\xi) = \begin{cases} 1, & \text{if } \xi_a \le \xi < \xi_{a+1} \\ 0, & \text{otherwise.} \end{cases}$$

$$N_{a,p}(\xi) = \frac{\xi - \xi_a}{\xi_{a+p} - \xi_a} N_{a,p-1}(\xi) + \frac{\xi_{a+p+1} - \xi}{\xi_{a+p+1} - \xi_{a+1}} N_{a+1,p-1}(\xi).$$

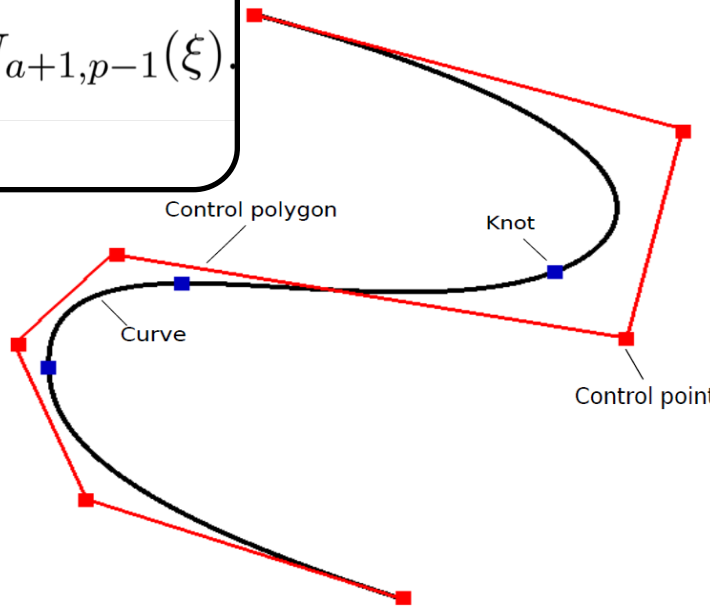

NURBS basis function

$$R_{a,p}(\xi) = \frac{N_{a,p}(\xi) w_a}{W(\xi)} = \frac{N_{a,p}(\xi) w_a}{\sum_{\hat{a}=1}^{n} N_{\hat{a},p} w_{\hat{a}}},$$

Properties of NURBS

- Partition of Unity

$$\sum_{i=1}^{n} R_{i,p}(\xi) = 1$$

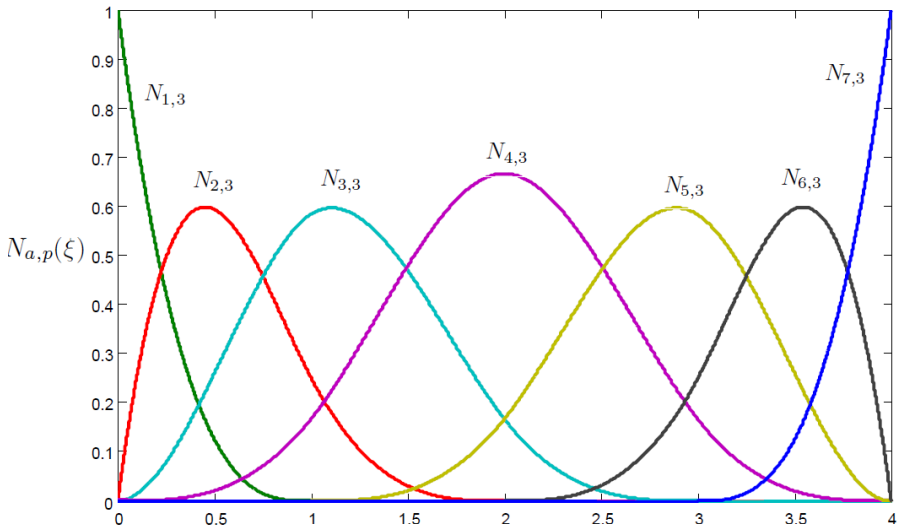

- Non-negative
- *p-1* continuous derivatives
- Tensor product property

$$\mathbf{S}(\xi,\eta) = \sum_{i=1}^{n}\sum_{j=1}^{m} R^{1}{}_{i,p}(\xi) R^{2}{}_{j,q}(\eta)\mathbf{B}_{i,j}$$

$$\sum_{i=1}^{n}\sum_{j=1}^{m} R^{1}{}_{i,p}(\xi) R^{2}{}_{j,q}(\eta) = \left(\sum_{i=1}^{n} R^{1}{}_{i,p}(\xi)\right)\left(\sum_{j=1}^{m} R^{2}{}_{j,q}(\eta)\right)$$

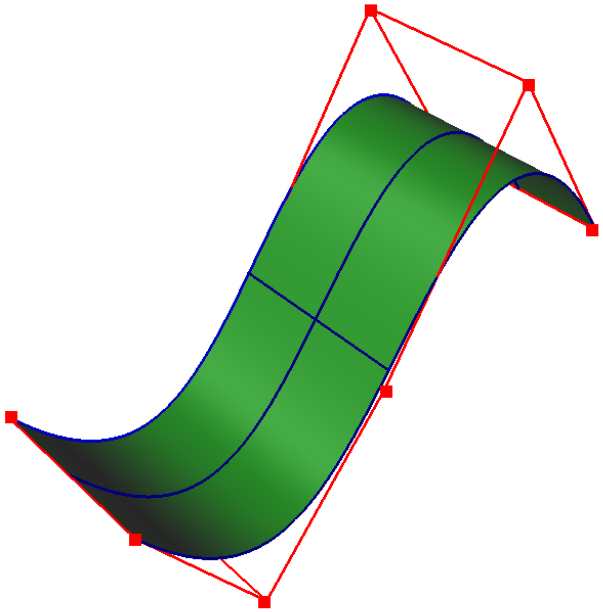

NURBS to T-splines

www.tsplines.com

(NURBS geometry)

www.tsplines.com

(T-splines geometry)

NURBS

- No watertight geometry
- No local refinement scheme

T-splines

- Local knot vector (as Point-based splines)
- Global topology

Y. Bazilevs, V.M. Calo, J.A. Cottrell, J.A. Evans, T.J.R. Hughes, S. Lipton, M.A. Scott, and T.W. Sederberg. Isogeometric analysis using T-splines. CMAME, 199(5-8):229–263, 2010.

Isogeometric Analysis with BEM

Boundary representation

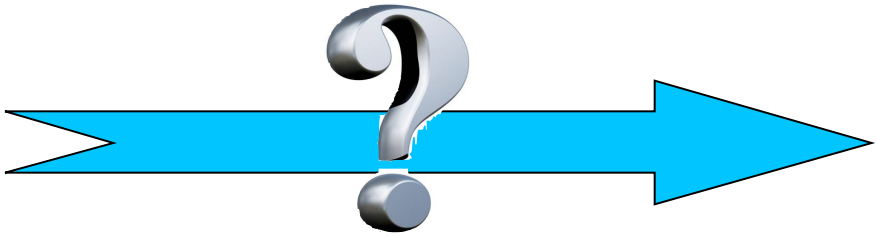

Domain representation

1. IGABEM with NURBS for 2D elastic problems (Simpson, *et al*. CMAME, 2011).

2. IGABEM with T-splines for 3D elastic problems (Scott, *et al.* CMAME, 2012).

3. IGABEM with T-splines for 3D acoustic problems (Simpson, *et al*. 2013 - MAFELAP2013 TH1515).

Difficulties in dealing with nonlinear problems and non-homogeneous materials.

IGABEM formulation

Regularised form of boundary integral equation for 2D linear elasticity

$$\int_\Gamma \mathbf{T}(\mathbf{s},\mathbf{x})[\mathbf{u}(\mathbf{x})-\mathbf{u}(\mathbf{s})]\,\mathrm{d}\Gamma(\mathbf{x}) = \int_\Gamma \mathbf{U}(\mathbf{s},\mathbf{x})\mathbf{t}(\mathbf{x})\,\mathrm{d}\Gamma(\mathbf{x})$$

where $\mathbf{x}$ and $\mathbf{s}$ are field point and source point respectively, $\mathbf{u}$ and $\mathbf{t}$ are displacement and traction around the boundary, $\mathbf{T}$ and $\mathbf{U}$ are fundamental solutions.

Discretise the geometry and solution field using NURBS

$$\mathbf{x} = \sum_{A=1}^{n_A} N_A(\xi)\mathbf{B}_A = N_A(\xi)\mathbf{B}_A$$

$$\mathbf{u} = \sum_{A=1}^{n_A} N_A(\xi)\mathbf{u}_A = N_A(\xi)\mathbf{u}_A$$

$$\mathbf{t} = \sum_{B=1}^{n_B} N_B(\xi)\mathbf{t}_B = N_B(\xi)\mathbf{t}_B$$

Approximate the unknown fields with the same basis functions (NURBS, T-splines …) as that used to generate the CAD model

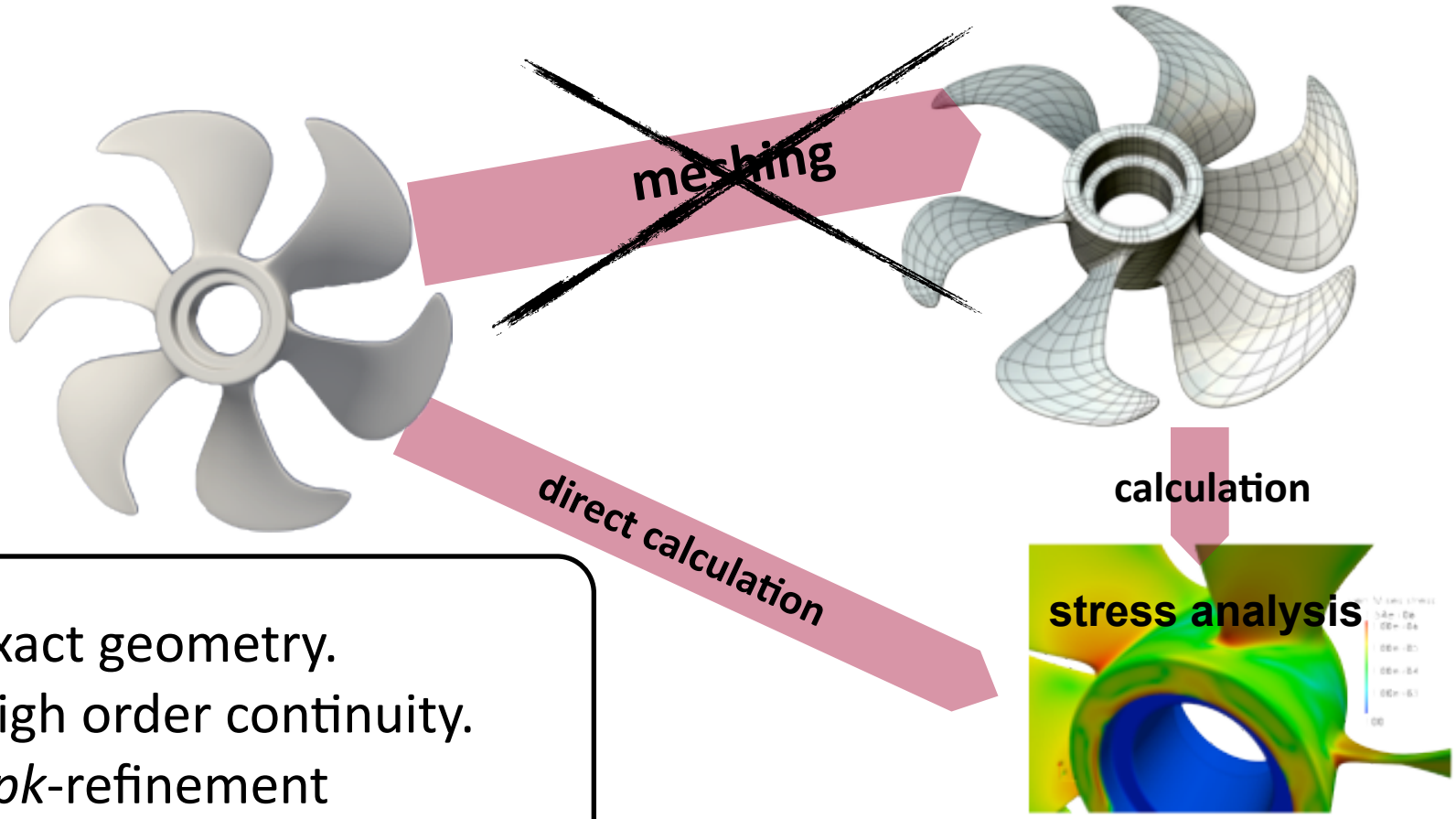

- Exact geometry.
- High order continuity.
- *hpk*-refinement

Nuclear reactor

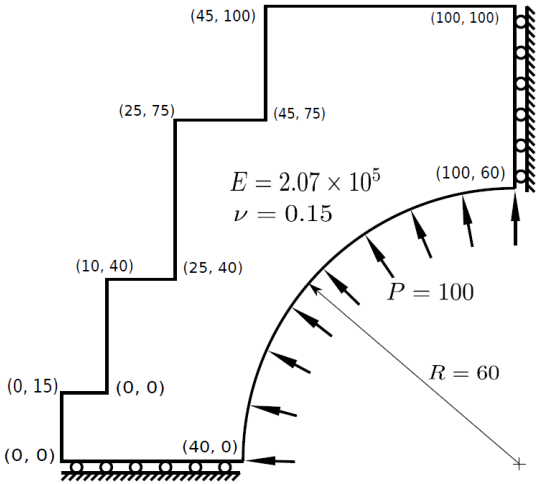

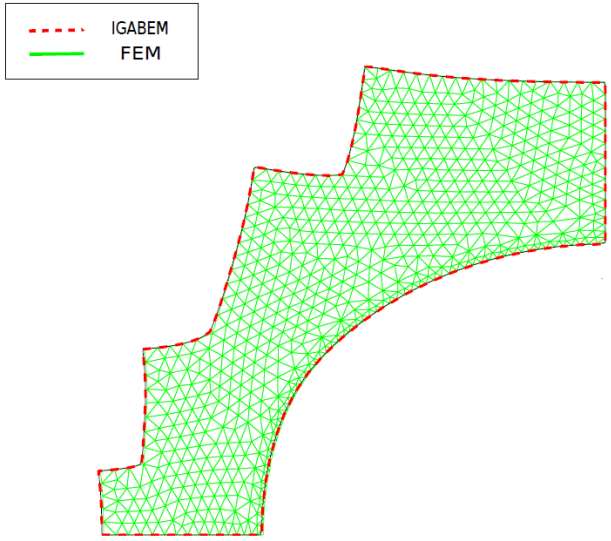

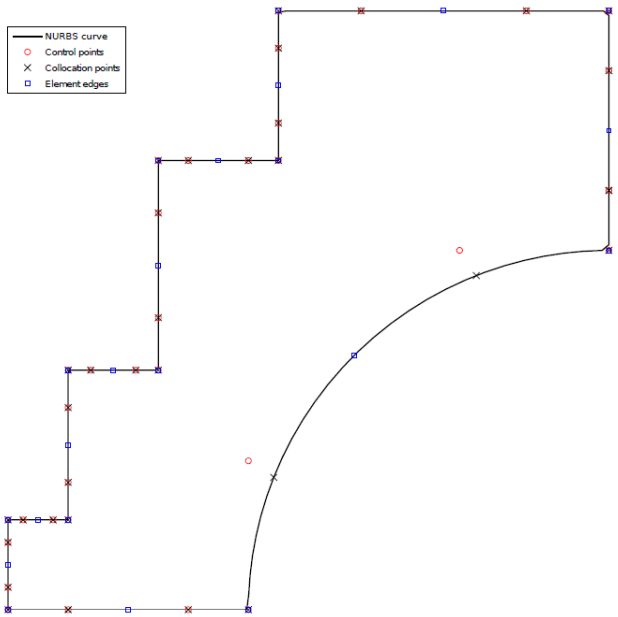

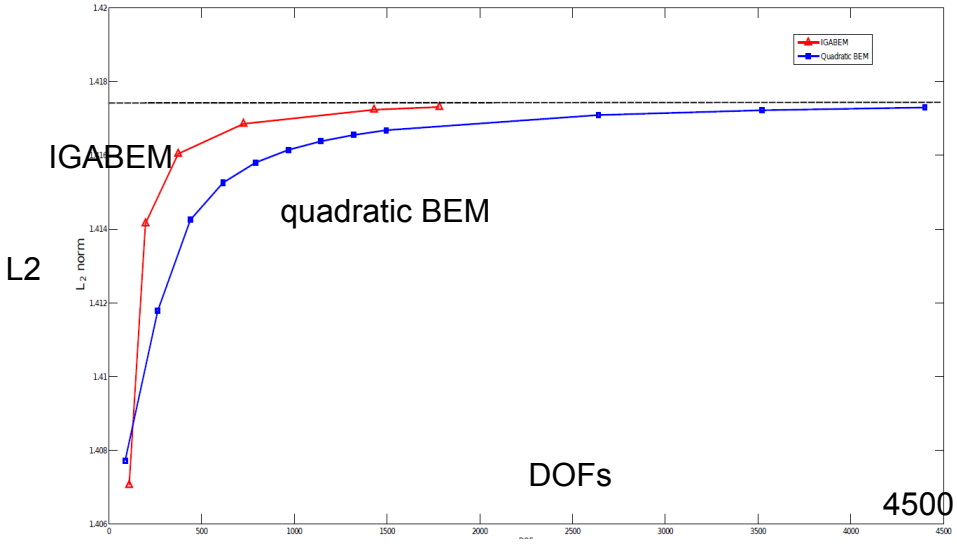

Dam

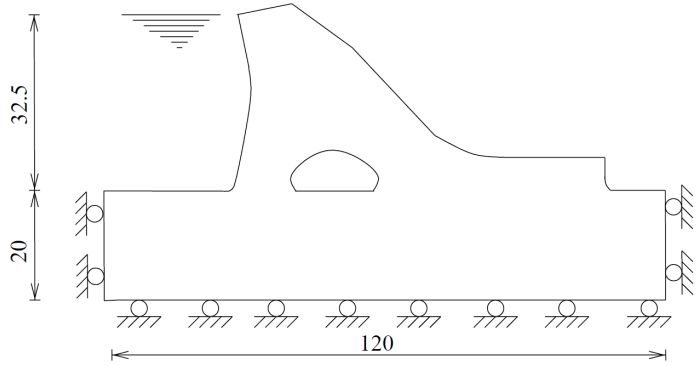

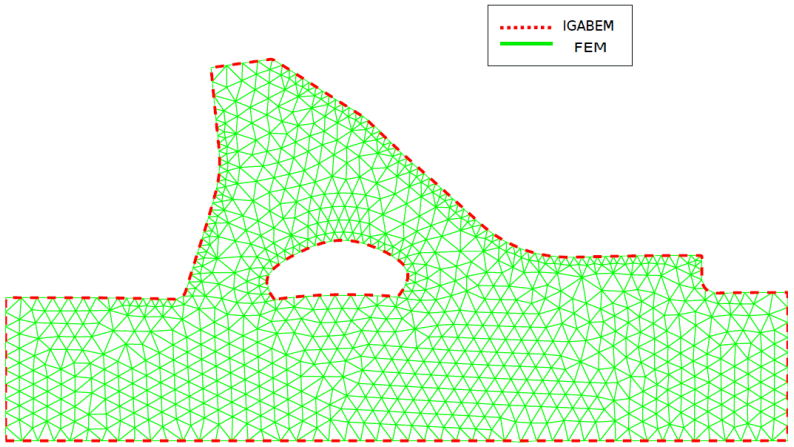

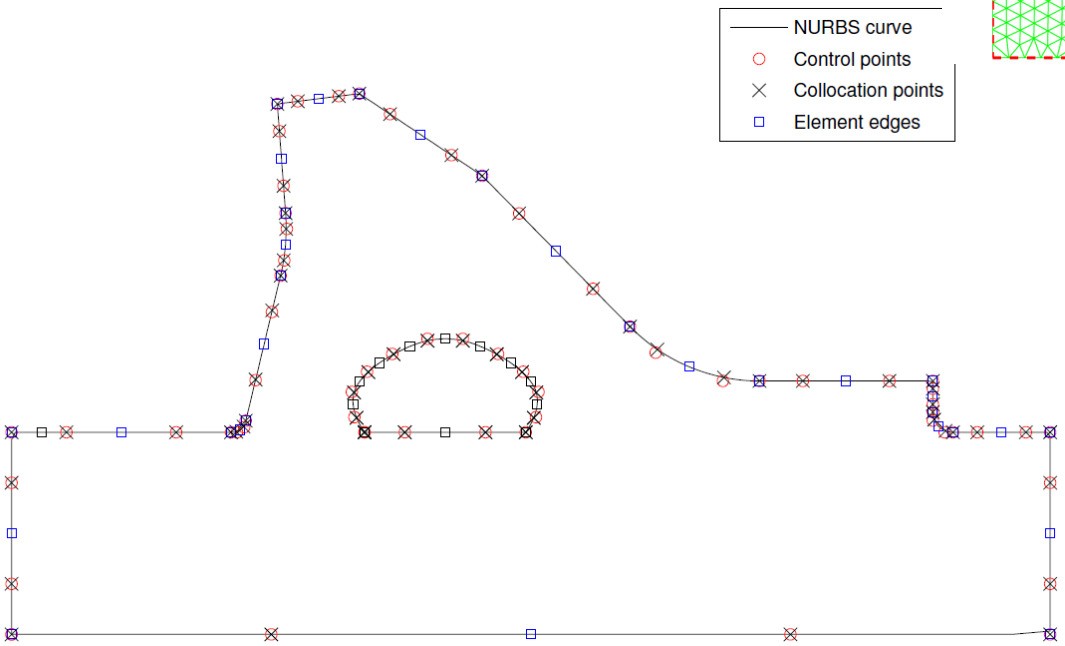

Stress analysis without meshing: isogeometric boundary-element method
ICE Proceeding, 2013, H Lian, RN Simpson, SPA Bordas

Propeller: NURBS would require several patches - single patch T-splines

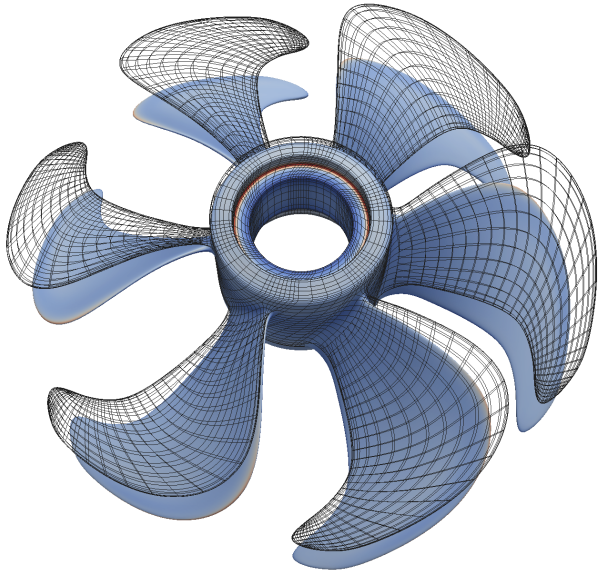

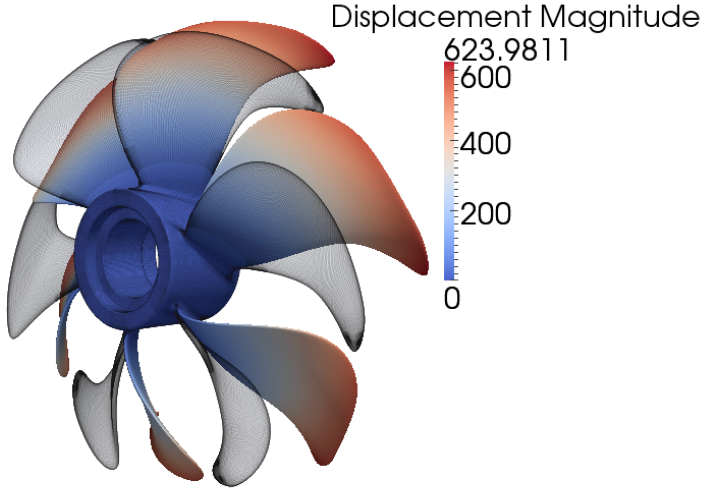

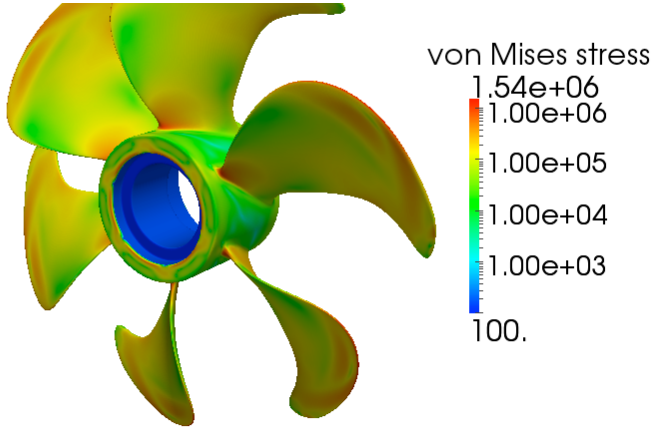

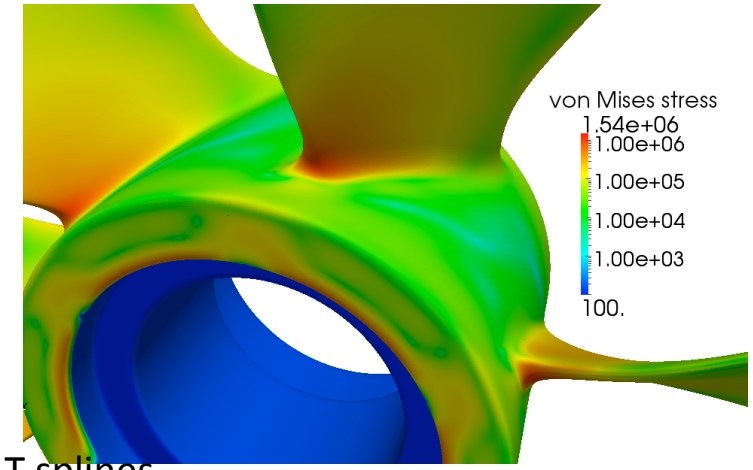

Isogeometric boundary element analysis using unstructured T-splines
MA Scott, RN Simpson, JA Evans, S Lipton, SPA Bordas, TJR Hughes, TW Sederberg
CMAME, 2013.

Part I.b.1

Shape optimisation directly from CAD

Stéphane P.A. Bordas, Pierre Kerfriden, Elena Atroshchenko, Xuan Peng, Haojie Lian

IGABEM sensitivity analysis formulation

Governing equations in parametric space, which can be viewed as material coordinate system

$$\int_\Gamma \mathbf{T}(\mathbf{s}(\zeta),\mathbf{x}(\xi))[\mathbf{u}(\mathbf{x}(\xi))-\mathbf{u}(\mathbf{s}(\zeta))]J(\xi)\mathrm{d}\xi = \int_\Gamma \mathbf{U}(\mathbf{s}(\zeta),\mathbf{x}(\xi))\mathbf{t}(\mathbf{x}(\xi))J(\xi)\mathrm{d}\xi$$

Differentiate the equation w.r.t. design variables (implicit differentiation)

$$\begin{aligned}&\int_\Gamma (\mathbf{T}_{,m}J+\mathbf{T}J_{,m})(\mathbf{u}-\mathbf{u}^s)\mathrm{d}\xi + \int_\Gamma (\mathbf{T}J)(\mathbf{u}_{,m}-\mathbf{u}^s_{,m})\mathrm{d}\xi \\ &= \int_\Gamma (\mathbf{U}_{,m}J+\mathbf{U}J_{,m})\mathbf{t}\mathrm{d}\xi + \int_\Gamma (\mathbf{U}J)\mathbf{t}_{,m}\mathrm{d}\xi\end{aligned}$$

Discretise the derivatives of displacement and traction using NURBS basis

$$\mathbf{u}_{,m} = \sum_{A=1}^{n_A} N_A(\xi)\mathbf{u}^A_{,m} = N_A(\xi)\mathbf{u}^A_{,m}$$

$$\mathbf{t}_{,m} = \sum_{B=1}^{n_B} N_B(\xi)\mathbf{t}^B_{,m} = N_B(\xi)\mathbf{t}^B_{,m}$$

Finally

$$\mathbf{H}_m\mathbf{u}+\mathbf{H}\mathbf{u}_m = \mathbf{G}_m\mathbf{t}+\mathbf{G}\mathbf{t}_m$$

Pressure cylinder problem

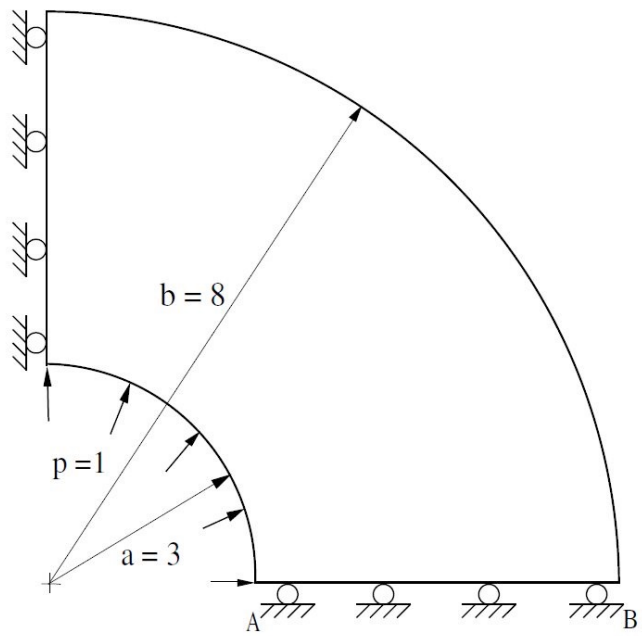

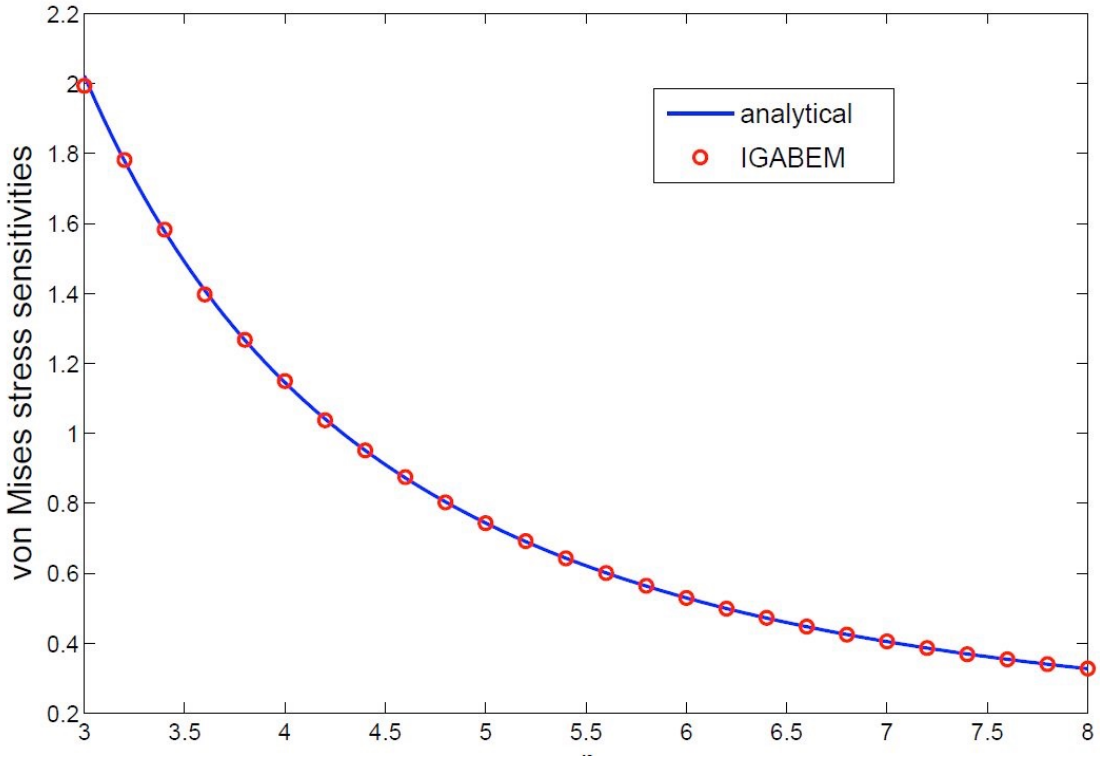

Design variable is outer circle radius *b*

Infinite plate with a hole

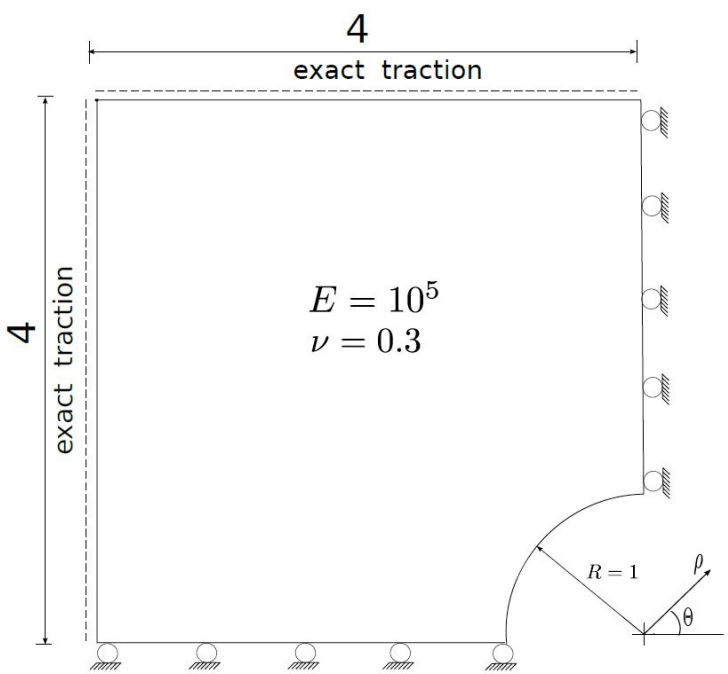

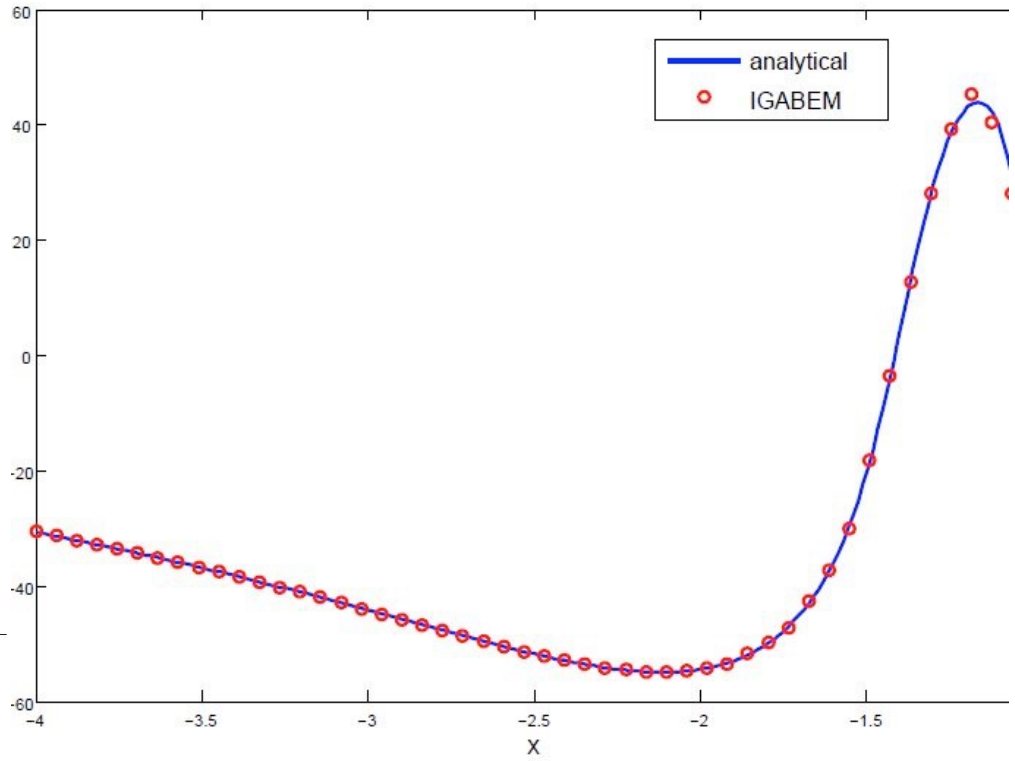

Design variable is radius *R*

3D Lamé problem

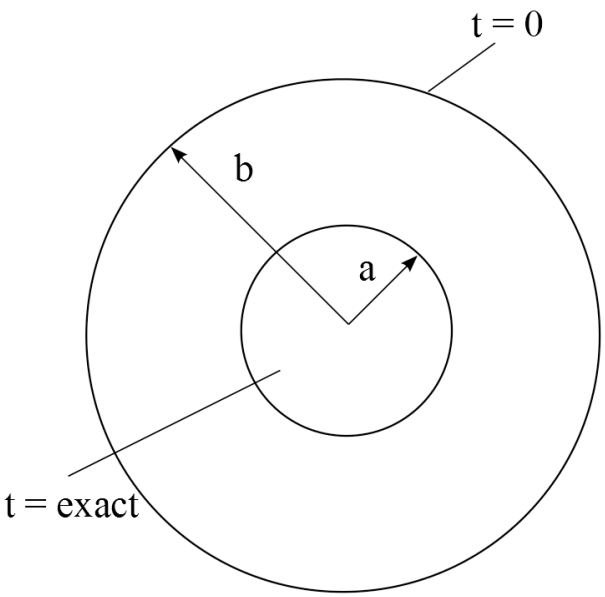

Design parameter: *b*

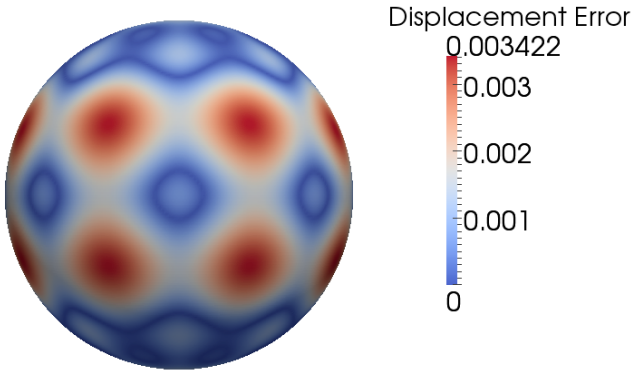

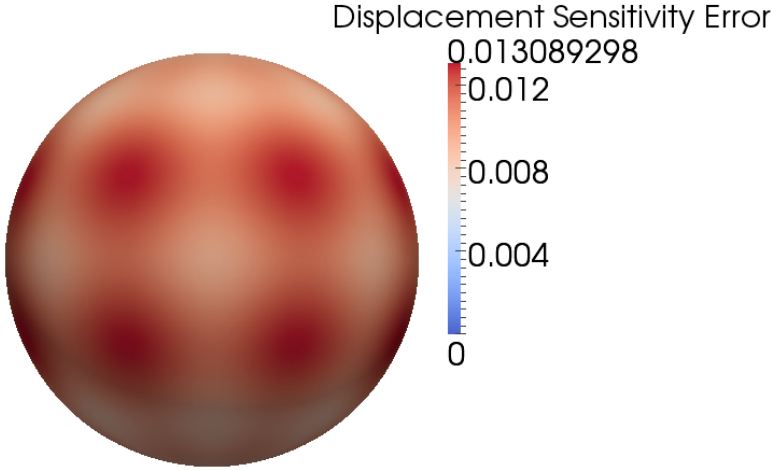

Fillet

Design curve is *ED*.

Minimise the area without violating von Mises stress criterion.

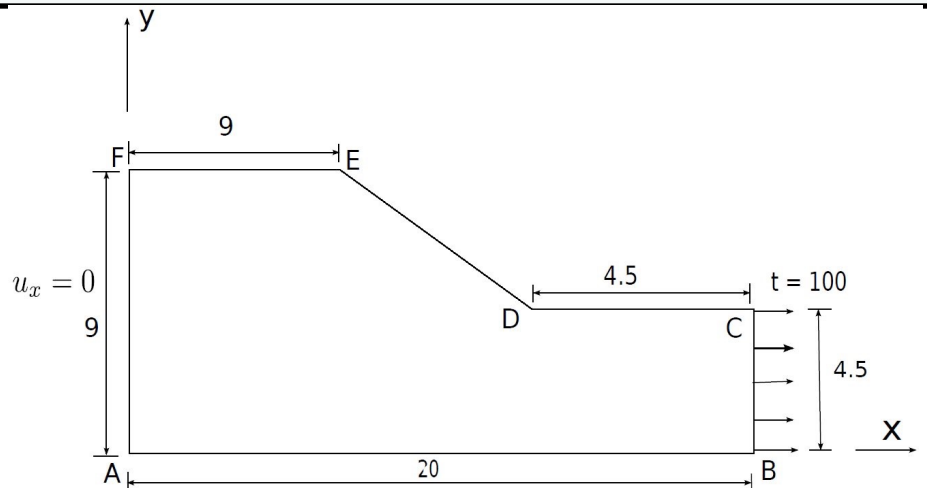

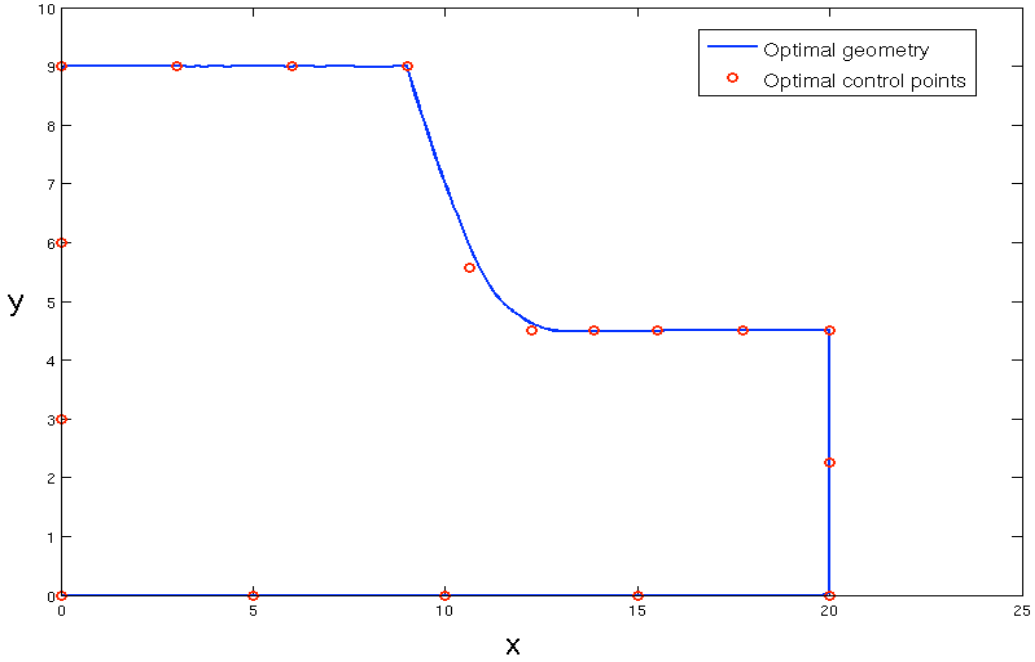

- IGA
- BEM
- T-splines
- Control points and weights as design variables
- Maximize stiffness, minimise volume

Shape optimisation directly from CAD

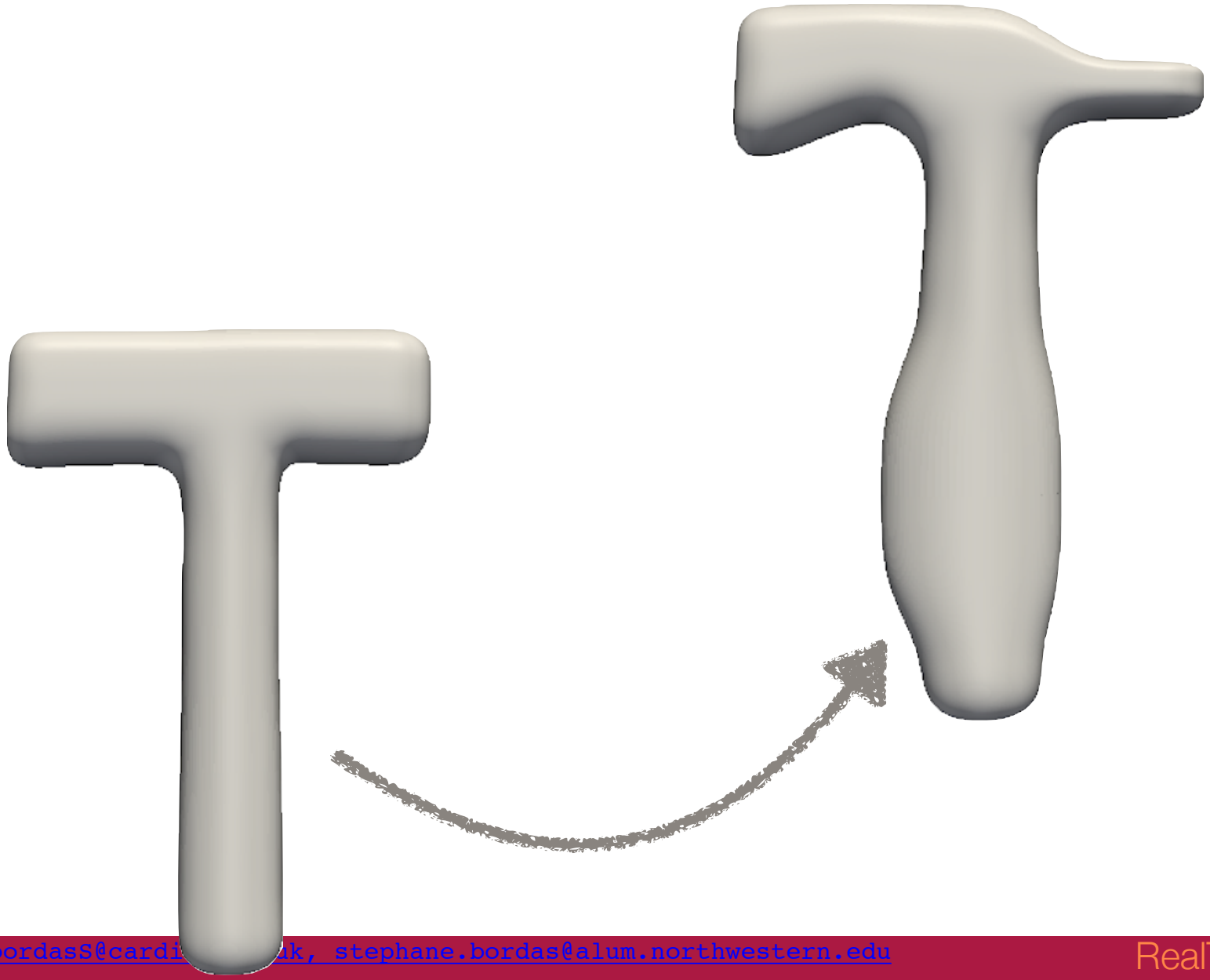

R. Alwood, G. Cornes, “A polygonal finite element for plate bending problems using the assumed stress approach”, International Journal for Numerical Methods in Engineering, 1(2): 135–149, 1969.

T. Belytschko, Y. Lu, L. Gu, “Element-free Galerkin methods”, International Journal for Numerical Methods in Engineering, 37: 229–256, 1994.

T. Belytschko, T. Black, “Elastic crack growth in finite elements with minimal remeshing”, International Journal for Numerical Methods in Engineering, 45: 601–620, 1999.

R. Mittal, G. Iaccarino, “Immersed boundary methods”, Annual Review of Fluid Mechanics, 37: 239–261, 2005.

G.R. Liu, K. Dai, T. Nguyen, “A smoothed finite element method for mechanics problems”, Computational Mechanics, 39: 859–877, 2007.

LB da Veiga, F Brezzi, LD Marini - Virtual Elements for linear elasticity problems SIAM Journal on Numerical Analysis, 2013.

F. Rizzo, “An integral equation approach to boundary value problems of classical elastostatics”, Quart. Appl. Math, 25(1): 83–95, 1967.

R. Glowinski, T. Pan, J. Periaux, “A fictitious domain method for Dirichlet problem and applications”, Computer Methods in Applied Mechanics and Engineering, 111(3-4): 283–303, 1994.

C. Song, J. Wolf, “The scaled boundary finite-element method–alias consistent infinitesimal finite-element cell method–for elastodynamics”, Computer Methods in Applied Mechanics and Engineering, 147(3): 329–355, 1997.

R. Simpson, S. Bordas, J. Trevelyan, T. Rabczuk, “A two-dimensional isogeometric boundary element method for elastostatic analysis”, Computer Methods in Applied Mechanics and Engineering, 209-212: 87–100, 2012.

Isogeometric boundary element analysis using unstructured T-splines MA Scott, RN Simpson, JA Evans, S Lipton, SPA Bordas, TJR Hughes, TW Sederberg Computer Methods in Applied Mechanics and Engineering, 2013.

E. Saiki, S. Biringen, “Numerical simulation of a cylinder in uniform flow: application of a virtual boundary method”, Journal of Computational Physics, 123(2): 450–465, 1996.

H. Johansen, P. Colella, “A Cartesian grid embedded boundary method for Poisson’s equation on irregular domains”, Journal of Computational Physics, 147(1): 60–85, 1998.

T. Ye, R. Mittal, H. Udaykumar, W. Shyy, “An accurate Cartesian grid method for viscous incompressible flows with complex immersed boundaries”, Journal of Computational Physics, 156(2): 209–240, 1999.

M. Moumnassi, S. Belouettar, E. Bechet, S. Bordas, D. Quoirin, M. Potier Ferry, “Finite element analysis on implicitly defined domains: An accurate representation based on arbitrary parametric surfaces”, Computer Methods in Applied Mechanics and Engineering, 200(5): 774–796, 2011.

Part I.b.2 Isogeometric Boundary Element Method for Damage Tolerance Assessment directly from CAD

CARDIFF UNIVERSITY
PRIFYSGOL CAERDYDD

IMAM
Institute of Mechanics & Advanced Materials

➢Fatigue Fracture Failure of Structure

- Initiation: micro defects
- Loading : cyclic stress state (temperature, corrosion)

➢Numerical methods for crack growth

- Volume methods:
  FEM, XFEM/GFEM, Meshfree
- Boundary methods: BEM

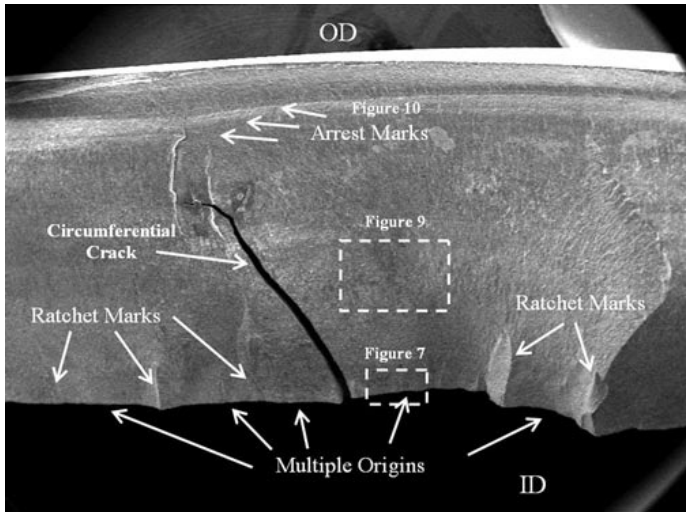

Fatigue cracking of nozzle sleeve
http://met-tech.com/

Bordas & Moran, 2006

XFEM+LEVEL SET

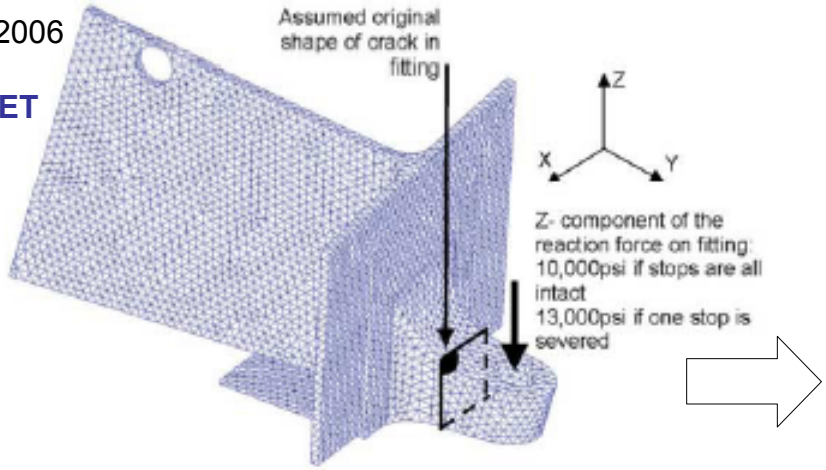

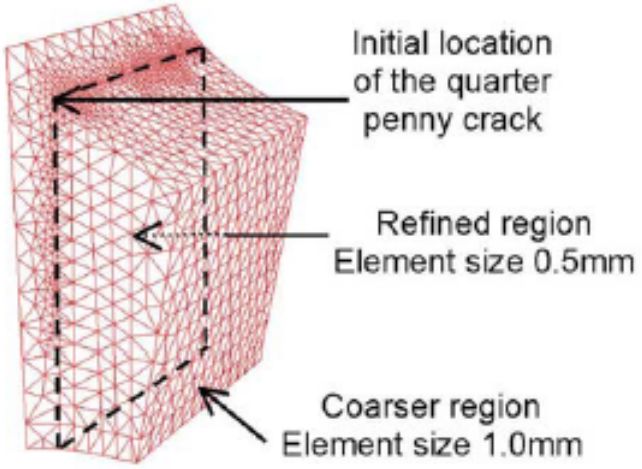

➢ Challenges in volume-based methods

- Remeshing (FEM)
- Local mesh refinement

Efficiency & Accuracy

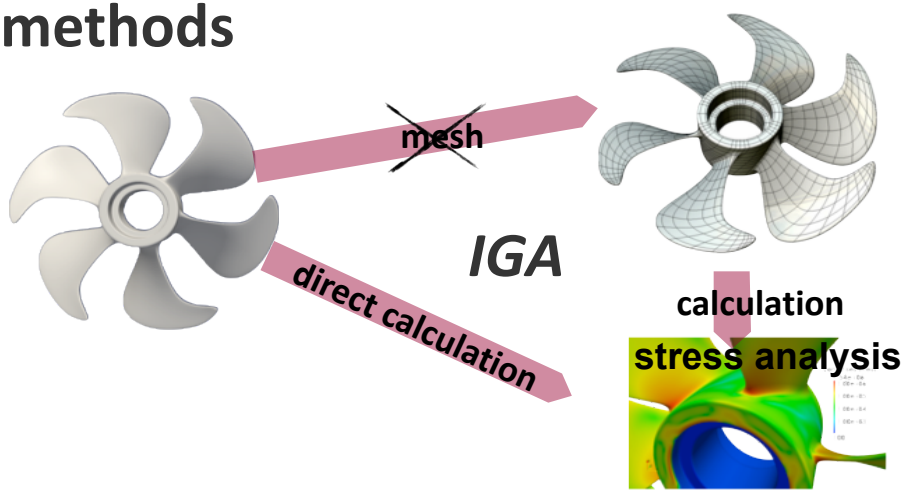

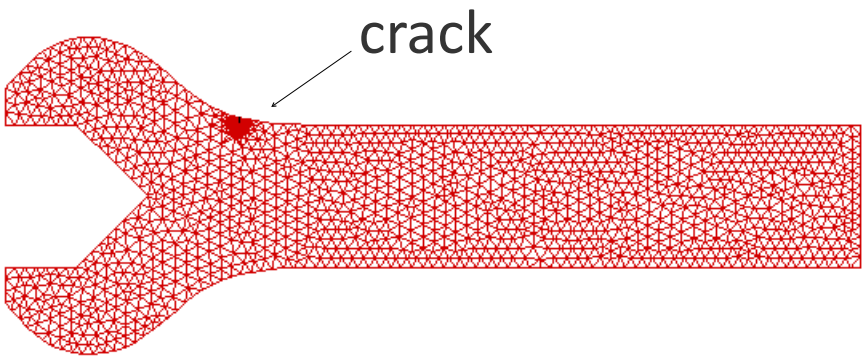

XFEM
adaptive refinement

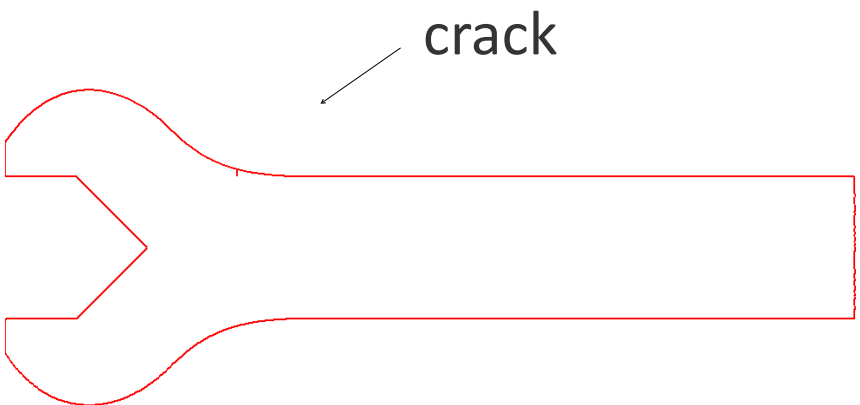

IGABEM
Direct CAD used

Weighted residual method, collocation

Linear elasticity problem:

$$\mathscr{L}(\mathbf{u}) = \nabla \cdot (\mathbf{C}\nabla^s \mathbf{u}) = \mathbf{f}, \quad \text{in } \Omega$$

$$\mathbf{u} = \bar{\mathbf{u}}, \quad \text{on } \Gamma_u$$

$$\mathbf{t} = (\mathbf{C}\nabla^s \mathbf{u}) \cdot \mathbf{n} = \bar{\mathbf{t}}, \quad \text{on } \Gamma_t$$

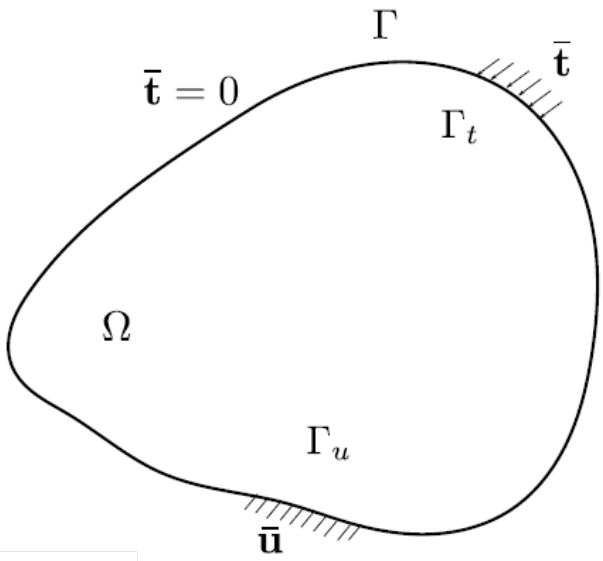

Approximation of $\mathbf{u}$:

$$\mathbf{u}^h = \bar{\mathbf{u}} + \sum_{I=1}^{n} N_I(\mathbf{x})\mathbf{u}^I$$

Weighted residual form:

$$\int_\Omega (\nabla \cdot (\mathbf{C}\nabla^s \mathbf{u}) - \mathbf{f}) \cdot \mathbf{v} \mathrm{d}\Omega + \int_{\Gamma_t} (\mathbf{t} - \bar{\mathbf{t}}) \cdot \mathbf{v} \mathrm{d}\Gamma = 0$$

Collocation method: $\mathbf{v}(\mathbf{z}) = \sum_{I=1}^{k} \mathbf{v}^I \delta(\mathbf{s}_I, \mathbf{z})$

sifting property: $\int_\Omega g(\mathbf{z})\delta(\mathbf{s}, \mathbf{z}) \mathrm{d}\Omega = g(\mathbf{s})$

Galerkin method (variational principle): $\mathbf{v}(\mathbf{z}) = \sum_{I=1}^{k} N_I(\mathbf{z})\mathbf{v}^I$

$$\int_\Omega (\nabla \mathbf{v} : \mathbf{C}\nabla^s \mathbf{u} - \mathbf{f} \cdot \mathbf{v}) \mathrm{d}\Omega + \int_{\Gamma_t} \mathbf{t} \cdot \mathbf{v} \mathrm{d}\Gamma = 0$$

Kelvin fundamental solution

Navier equation: $\mu\nabla^2\mathbf{u} + (\mu+\lambda)\nabla(\nabla\cdot\mathbf{u}) = \mathbf{f}$

Kelvin solution: assuming a unit concentrated force applied on a point $\mathbf{s}$ in the infinite domain $\mathbf{f}(\mathbf{z}) = \mathbf{e}\delta(\mathbf{s},\mathbf{z})$, we seek $\mathbf{u}(\mathbf{z})$ and $\mathbf{t}(\mathbf{z})$ for any point $\mathbf{z}$

$$u_i^* = U_{ij}e_j \qquad t_i^* = T_{ij}e_j$$

for 3D problems, the expressions are:

$$U_{ij}(\mathbf{s},\mathbf{z}) = \frac{1}{16\pi\mu(1-\nu)r}[(3-4\nu)\delta_{ij} + r_{,i}r_{,j}]$$

$$T_{ij}(\mathbf{s},\mathbf{z}) = -\frac{1}{8\pi(1-\nu)}\left[\frac{\partial r}{\partial n}((1-2\nu)\delta_{ij} + 3r_{,i}r_{,j}) - (1-2\nu)(n_j r_{,i} - n_i r_{,j})\right]$$

Boundary integral equations (BIEs) and IGABEM crack modeling

- **Displacement BIE** $$c_{ij}(\mathbf{s})u_j(\mathbf{s}) + \int_\Gamma T_{ij}(\mathbf{s},\mathbf{x})u_j(\mathbf{x})\mathrm{d}\Gamma(\mathbf{x}) = \int_\Gamma U_{ij}(\mathbf{s},\mathbf{x})t_j(\mathbf{x})\mathrm{d}\Gamma(\mathbf{x})$$
- **Traction BIE** $$c_{ij}(\mathbf{s})t_j(\mathbf{s}) + \int_\Gamma S_{ij}(\mathbf{s},\mathbf{x})u_j(\mathbf{x})\mathrm{d}\Gamma(\mathbf{x}) = \int_\Gamma K_{ij}(\mathbf{s},\mathbf{x})t_j(\mathbf{x})\mathrm{d}\Gamma(\mathbf{x})$$
- **NURBS approximation**

$$u_i(\xi) = \sum_{A=1}^{n} R_{A,p}(\xi)d_i^A$$

$$t_i(\xi) = \sum_{A=1}^{n} R_{A,p}(\xi)q_i^A$$

displacement BIE for $\mathbf{s}^+$

Γ_{c^+} $\mathbf{s}^+$

Γ_{c^-} $\mathbf{n}^+$ $\mathbf{s}^-$

traction BIE for $\mathbf{s}^-$

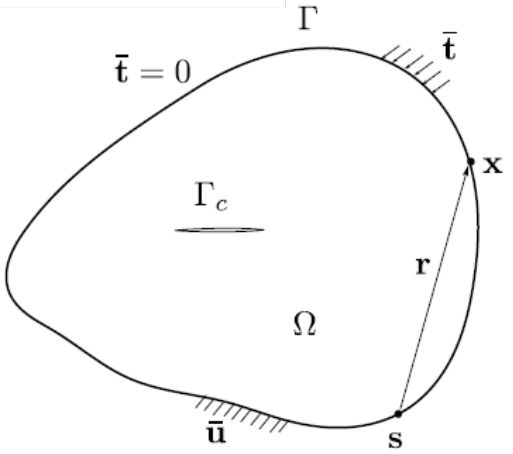

- **Collocation: Greville Abscissae**

$$\xi_s = \frac{\xi_{i+1} + \ldots + \xi_{i+p}}{p}$$

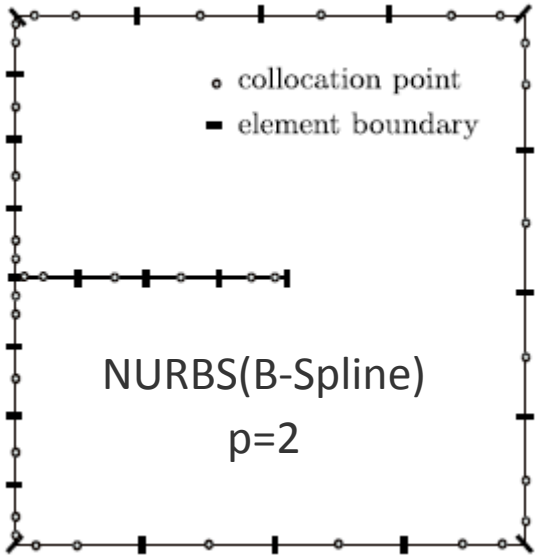

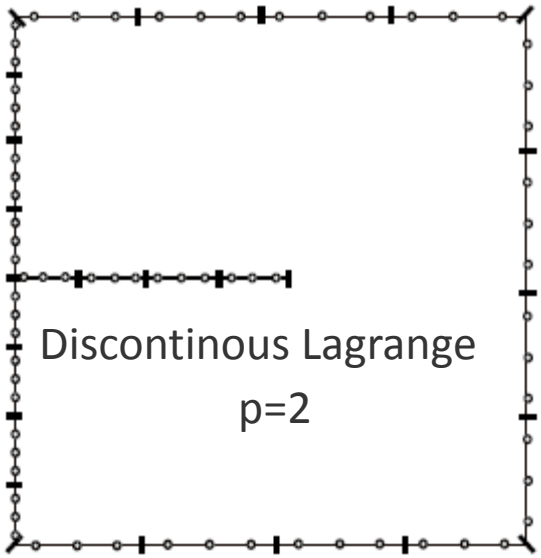

Treatment of crack tip singularity

- Partition of unity enrichment (2D)

$$u_i(\mathbf{x}) = \sum_{I \in \mathcal{N}_I} N_I(\mathbf{x}) d_i^I + \sum_{J \in \mathcal{N}_J} N_J(\mathbf{x}) \phi(\mathbf{x}) a_i^J \qquad \phi = \sqrt{r}$$

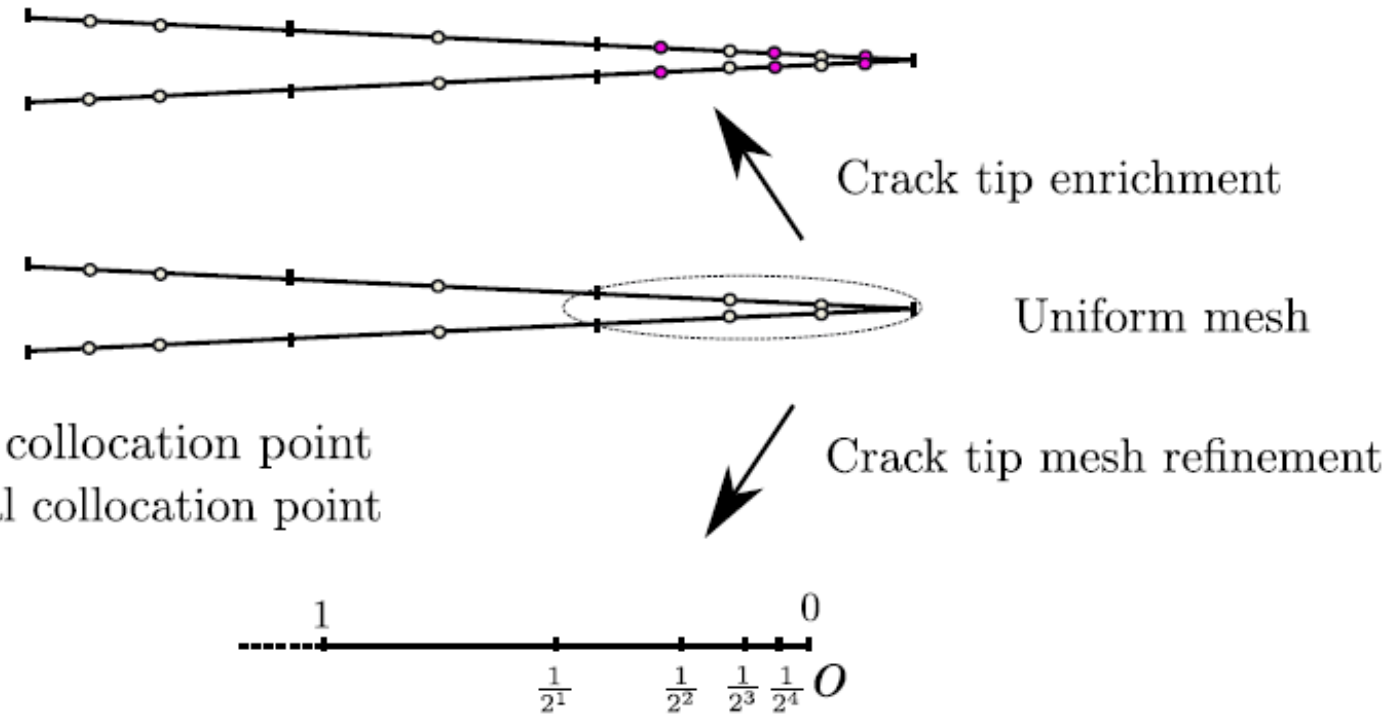

- Consecutive knot insertion at crack tip (2D) or along crack front (3D)

Crack tip refinement VS enrichment

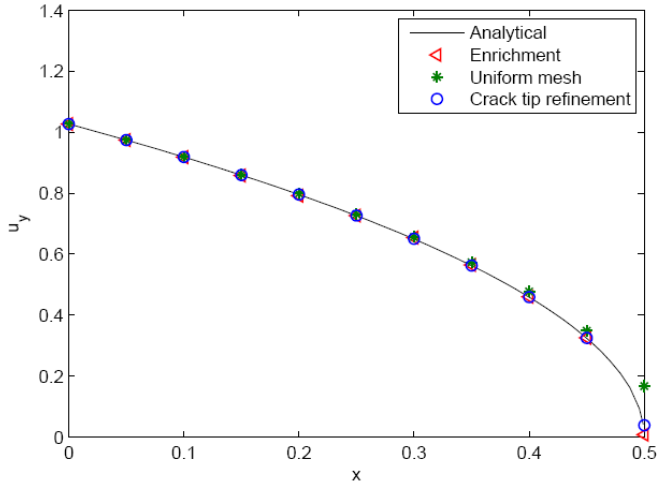

Crack opening displacement

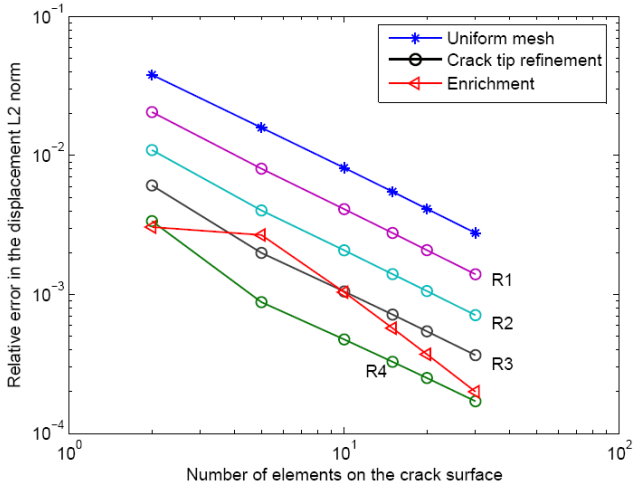

Error in displacement L2 norm

NURBS VS Lagrange: convergence in SIFs, no crack tip treatment

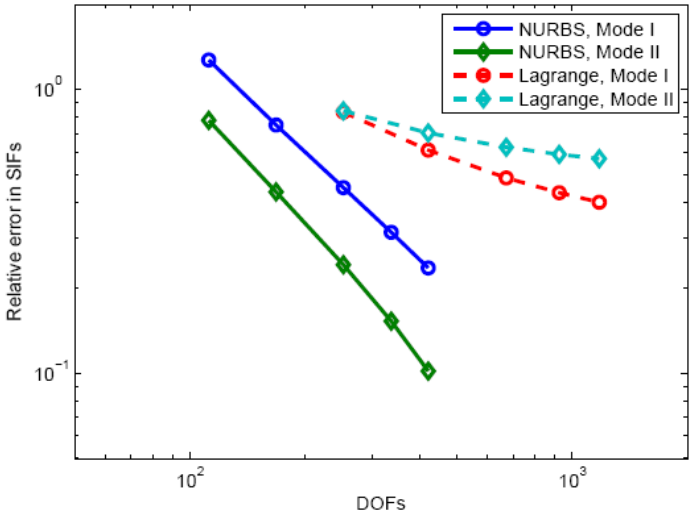

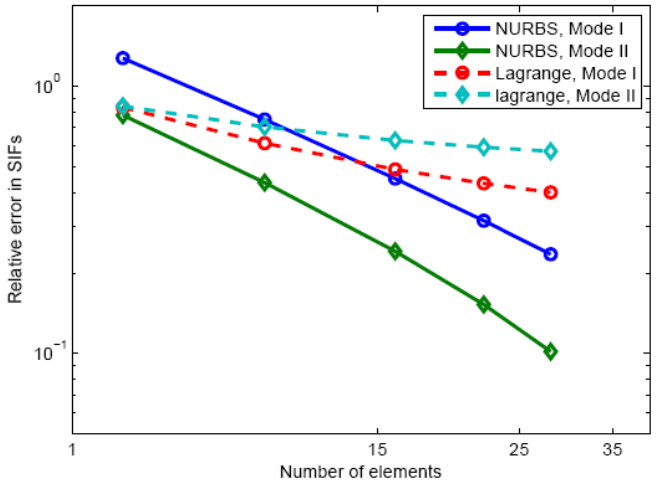

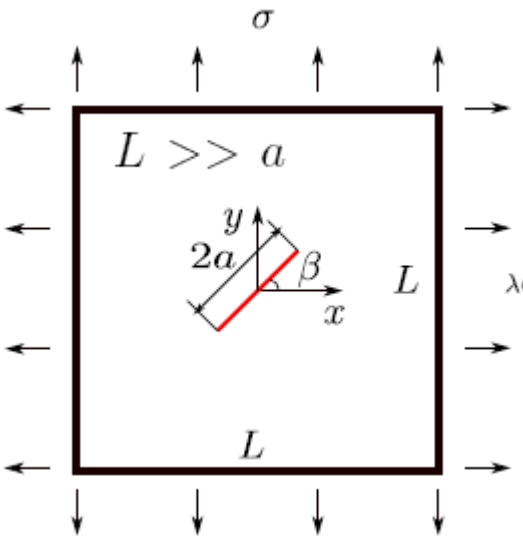

$$K_I = \sigma\sqrt{\pi a}(\cos^2\beta + \lambda\sin^2\beta)$$

$$K_{II} = \sigma\sqrt{\pi a}(1-\lambda)\cos\beta\sin\beta$$

$$\beta = \pi/6, \quad \sigma = 1, \quad \lambda = 0.5$$

- IGABEM(r) :Uniform mesh (refined tip element)
- LBEM: discontinuous Lagrange BEM
- SGBEM: symmetric Galerkin BEM, Sutrahar&Paulino (2004)

m: number of elements in uniform mesh along the crack surface

	K_I/K_I^{exact}			
m	SGBEM	LBEM	IGABEM	IGABEM(r)
3	0.9913	1.00451	1.00982	1.00120
4	1.0002	1.00333	1.00769	1.00105
5	1.0001	1.00268	1.00633	1.00090
6	1.0002	1.00230	1.00539	1.00080
7	1.0003	1.00206	1.00474	1.00074
8	1.0003	1.00190	1.00426	1.00070
9	1.0003	1.00177	1.00389	1.00066
10	1.0003	1.00167	1.00359	1.00064
11	1.0003	1.00159	1.00336	1.00062
12	1.0003	1.00152	1.00316	1.00060
14	1.0003	1.00142	1.00285	1.00058

	K_{II}/K_{II}^{exact}			
m	SGBEM	LBEM	IGABEM	IGABEM(r)
3	1.0075	1.00104	1.00647	1.00146
4	1.0009	1.00129	1.00656	1.00129
5	1.0010	1.00158	1.00607	1.00113
6	1.0009	1.00160	1.00550	1.00102
7	1.0014	1.00153	1.00500	1.00096
8	1.0005	1.00143	1.00458	1.00091
9	0.9997	1.00134	1.00424	1.00087
10	1.0009	1.00126	1.00396	1.00085
11	0.9992	1.00119	1.00373	1.00083
12	1.0013	1.00112	1.00353	1.00081
14	1.0004	1.00102	1.00322	1.00079

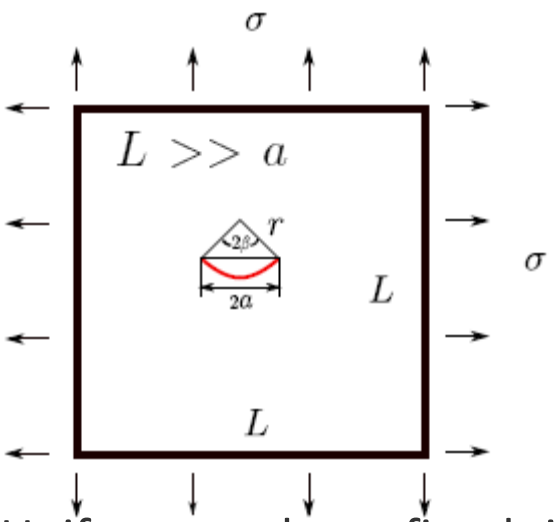

$$K_I = \sigma\sqrt{\pi a}\frac{\cos(\beta/2)}{1+\sin^2(\beta/2)}$$

$$K_{II} = \sigma\sqrt{\pi a}\frac{\sin(\beta/2)}{1+\sin^2(\beta/2)}$$

$$\sigma = 1, \quad \beta = \pi/4$$

- Uniform mesh + refined tip element
- Splitting parameter in **J** integral: $r_{split} = 0.03R_J, 0.04R_J, 0.05R_J, 0.06R_J, 0.07R_J$

m: number of elements in uniform mesh along the crack surface

	K_I/K_I^{exact}		K_{II}/K_{II}^{exact}	
m	M integral	J_k integral	M integral	J_k integral
10	1.00045	0.99972	0.97506	1.00309
14	1.00014	0.99979	0.98621	1.00248
17	1.00011	0.99982	0.98642	1.00217
20	1.00009	0.99985	0.98657	1.00195
23	1.00002	0.99987	0.99407	1.00176
26	1.00002	0.99989	0.99413	1.00163

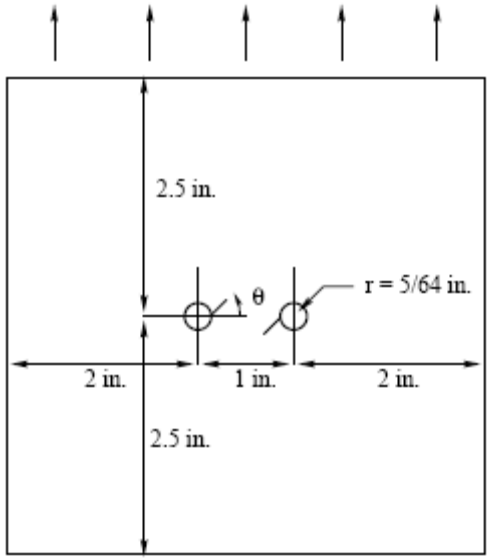

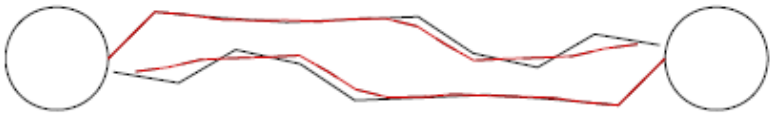

(a) XFEM by Möes et al (1999)

(b) IGABEM

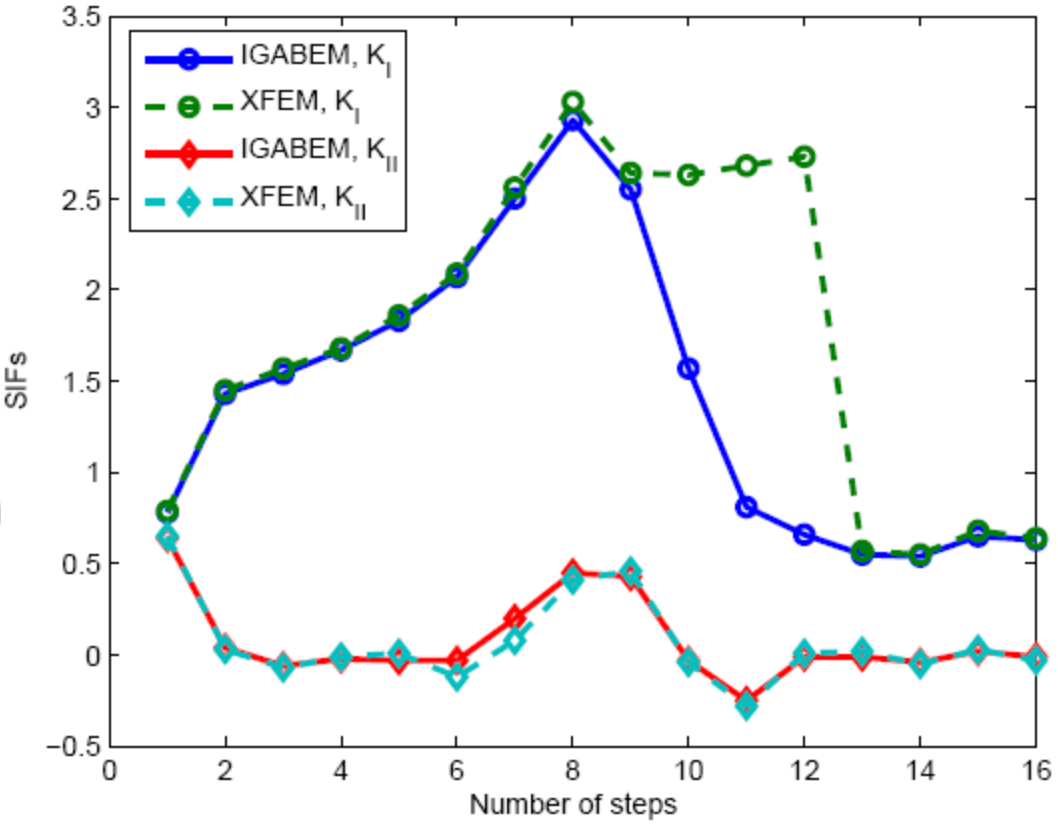

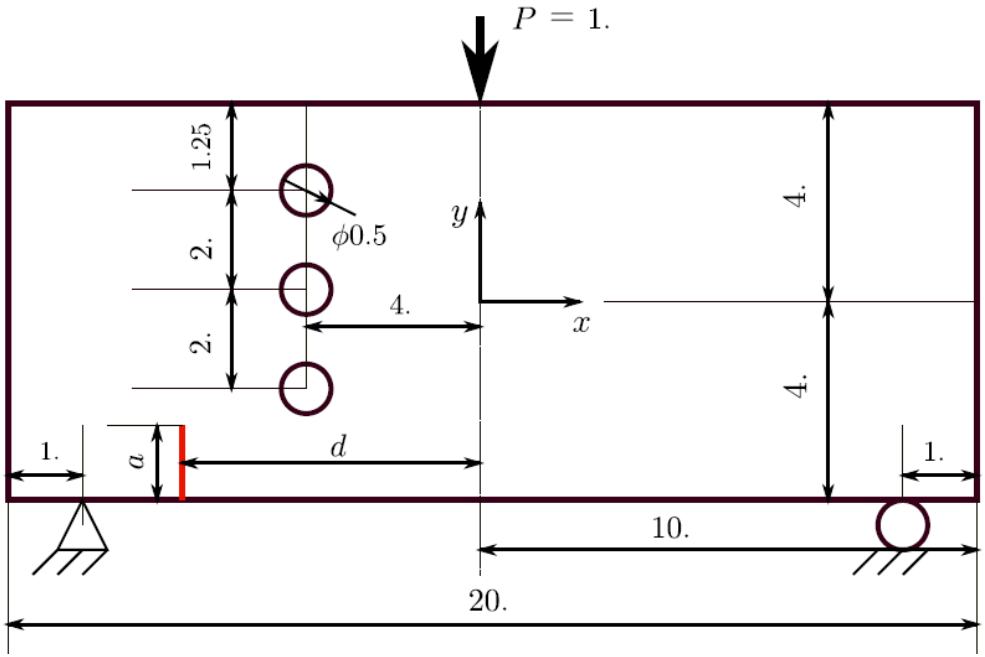
P = 1.
1.25
2.
2.
φ0.5
y
x
4.
4.
4.
1.
a
d
1.
10.
20.

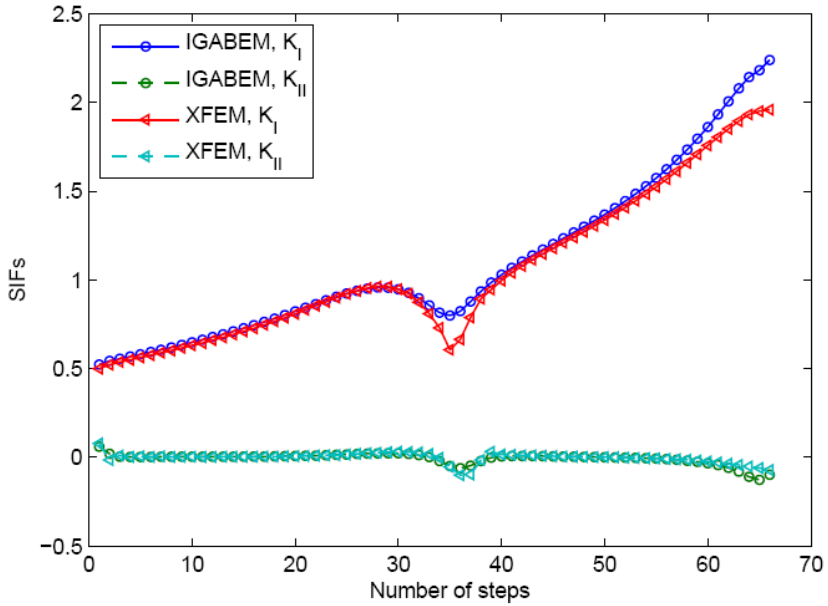
IGABEM, K_I
IGABEM, K_II
XFEM, K_I
XFEM, K_II
SIFs
Number of steps
2.5
2
1.5
1
0.5
0
−0.5
0
10
20
30
40
50
60
70

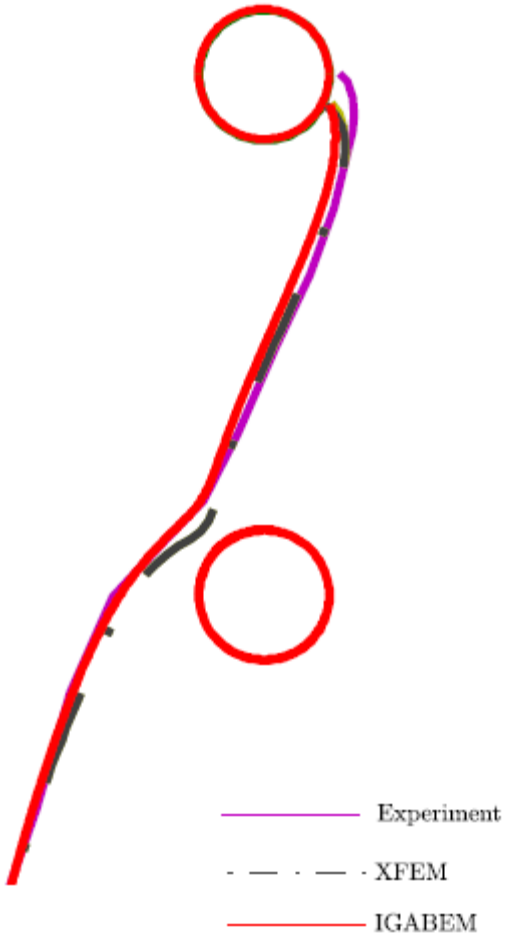
Experiment
XFEM
IGABEM

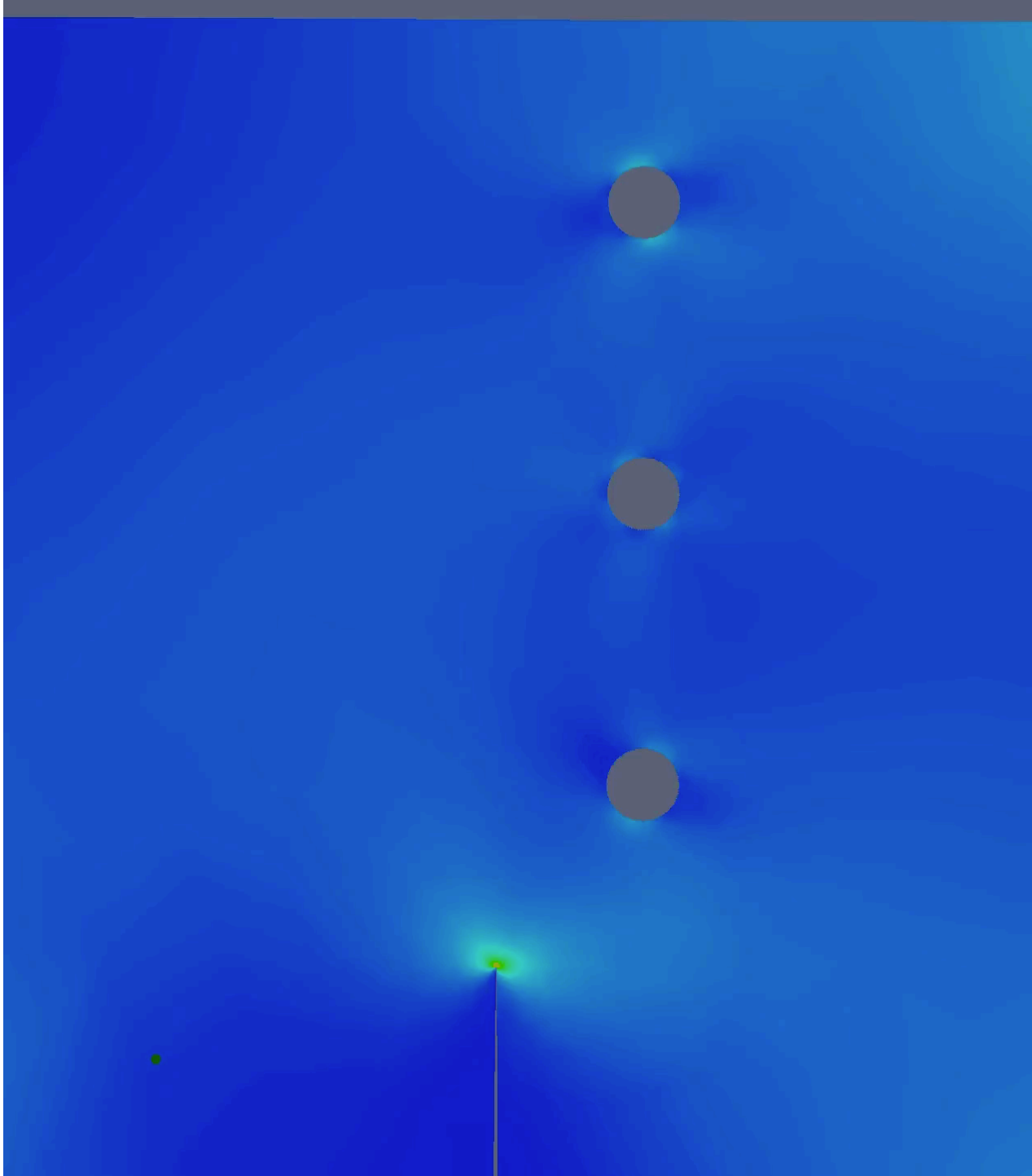

Penny-shaped crack under remote tension

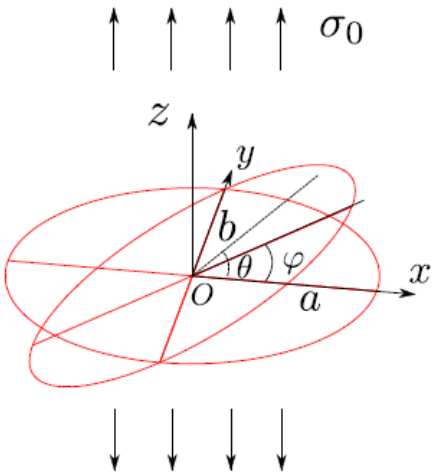

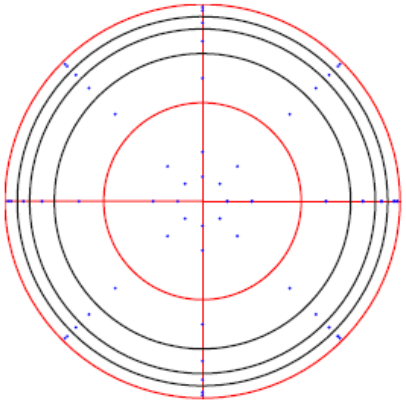

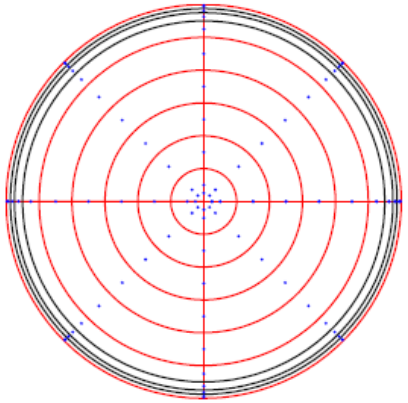

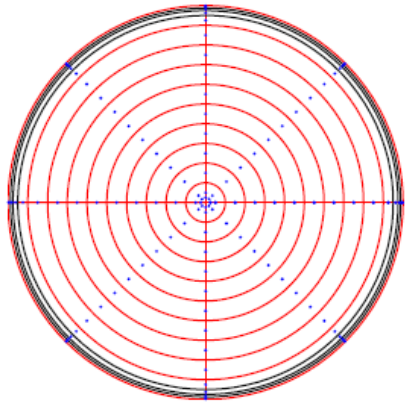

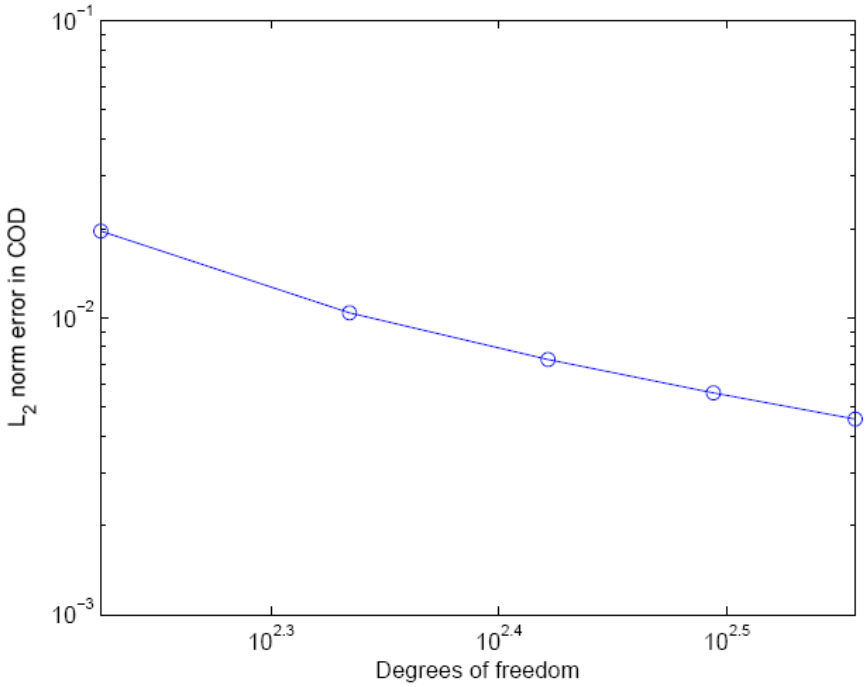

L_2 norm error of COD for penny-shaped crack

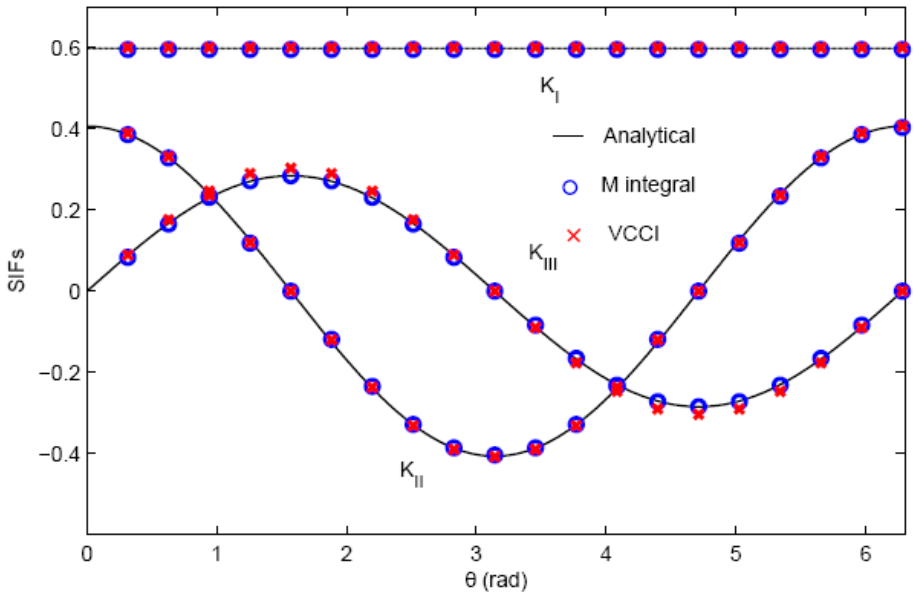

stress intensity factors for penny crack with $\varphi = \pi/6$

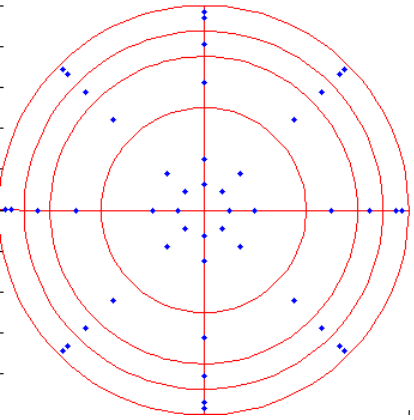

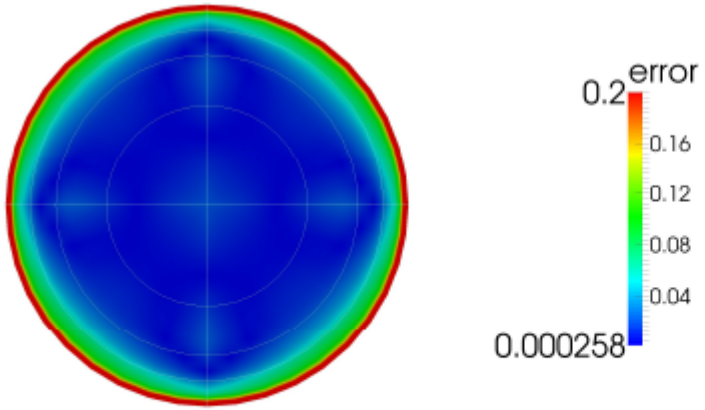

(a) original SST, ngp_s=30, e_{L_2} =3.344418e-2

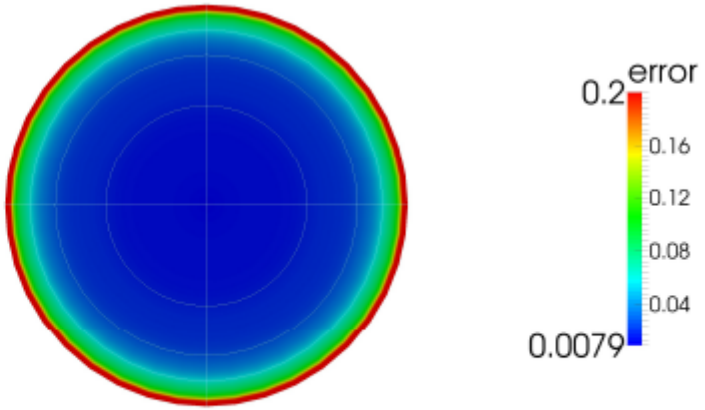

(b) improved SST, ngp_s=30, e_{L_2} =3.844282e-2

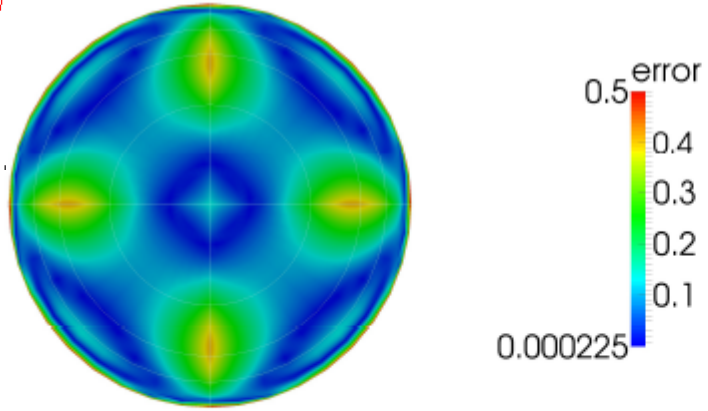

(c) original SST, ngp_s=18, e_{L_2} =1.467716e-1

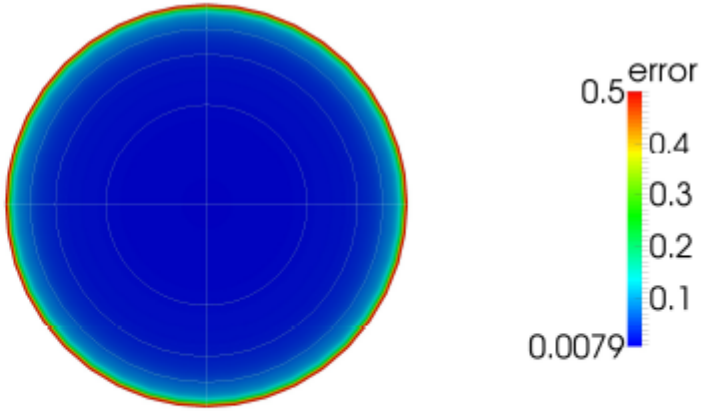

(d) improved SST, ngp_s=18, e_{L_2}=3.844282e-2

Figure 5: Error in crack opening displacement for penny crack

Penny crack under remote tension (embeded crack)

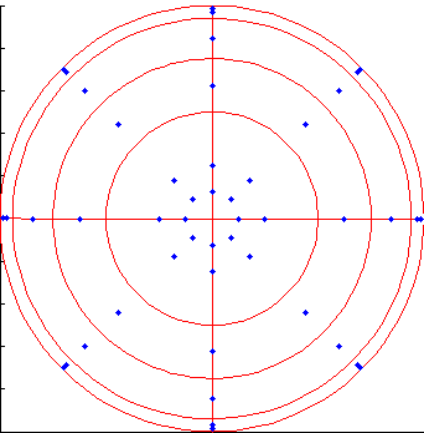

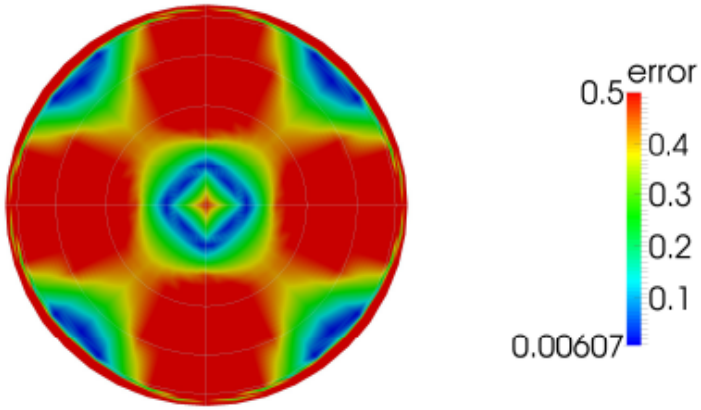

(a) original SST, ngp_s=30, e_{L_2}=8.138911e-1

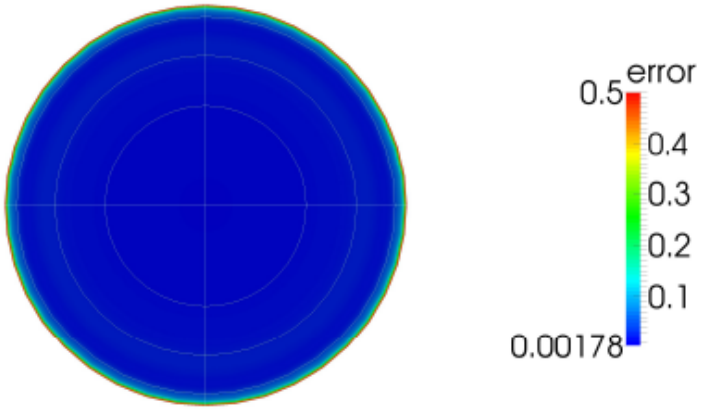

(b) improved SST, ngp_s=30, e_{L_2}=1.755681e-2

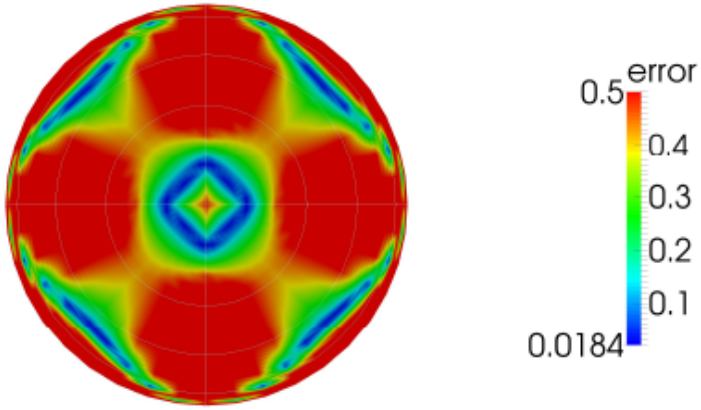

(c) original SST, ngp_s=18, e_{L_2}=7.110011e-1

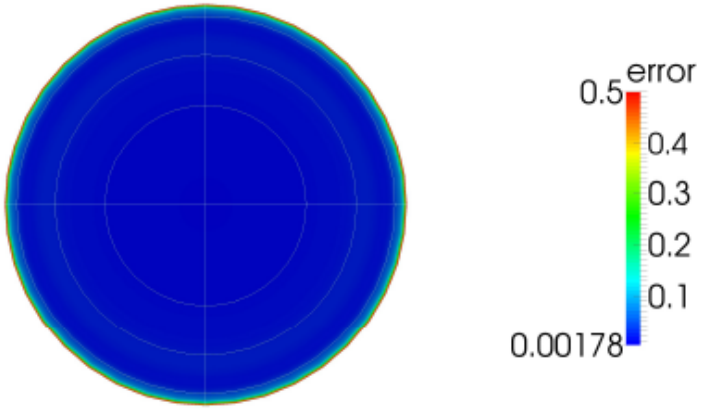

(d) improved SST, ngp_s=18, e_{L_2}=1.755679e-002

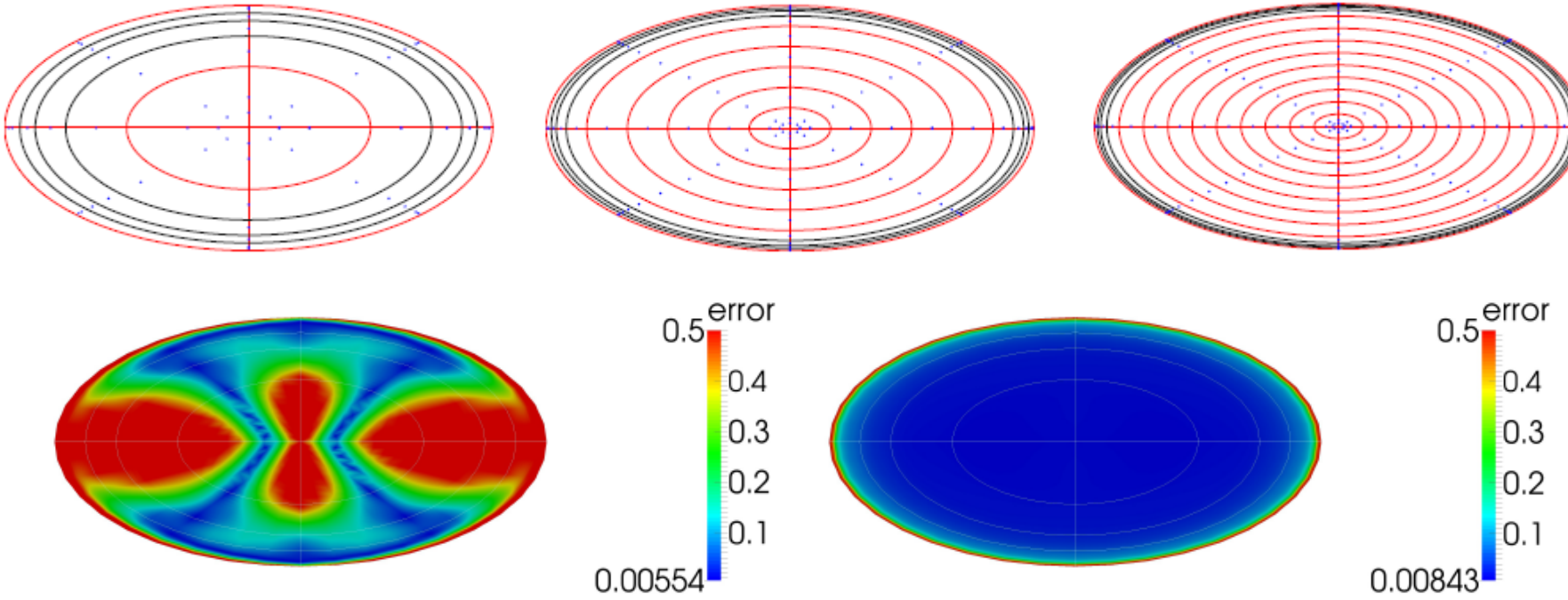

(a) original SST, ngp_s=18, e_{L_2}=4.603473e-1

(b) improved SST, ngp_s=18, e_{L_2}=3.798002e-2

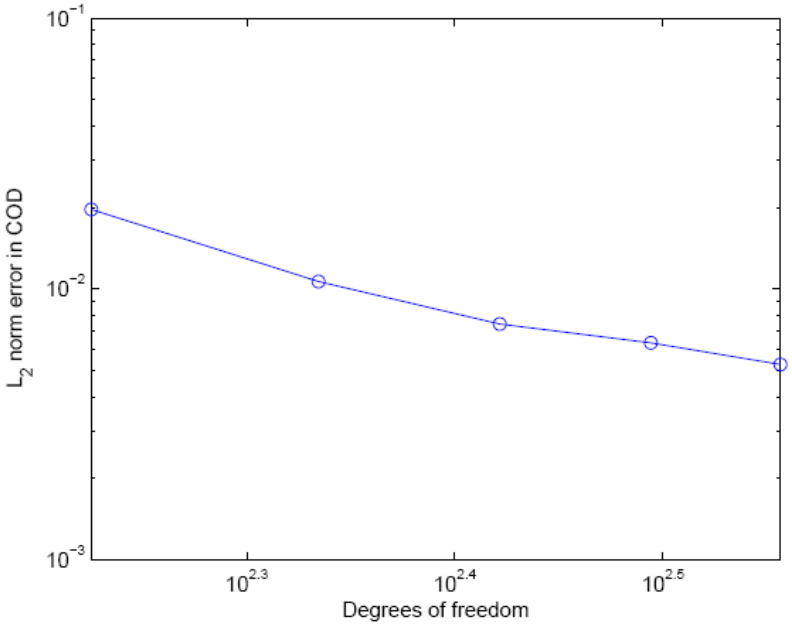

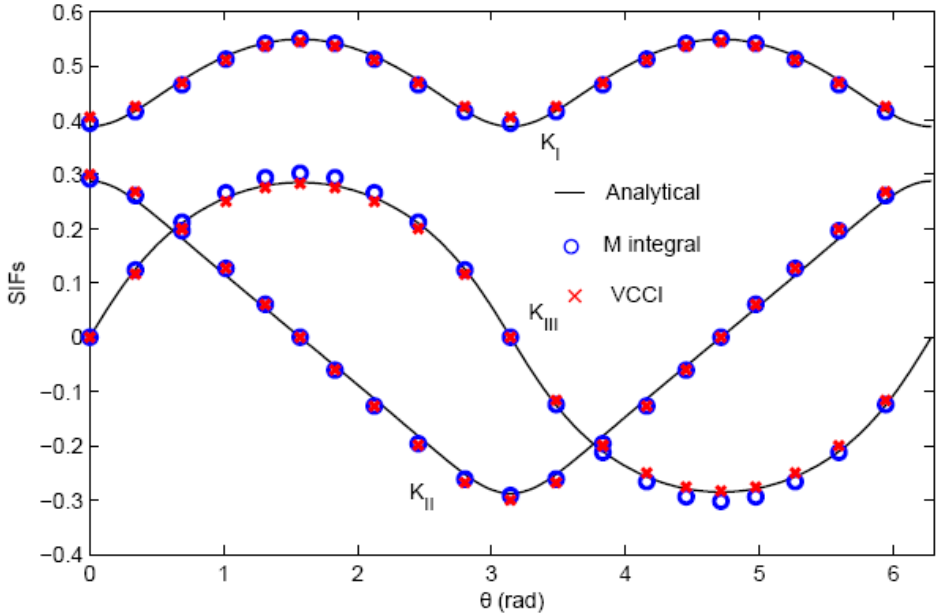

Difficulties in 3D application

➢How far are we from non-trivial 3D workpieces?

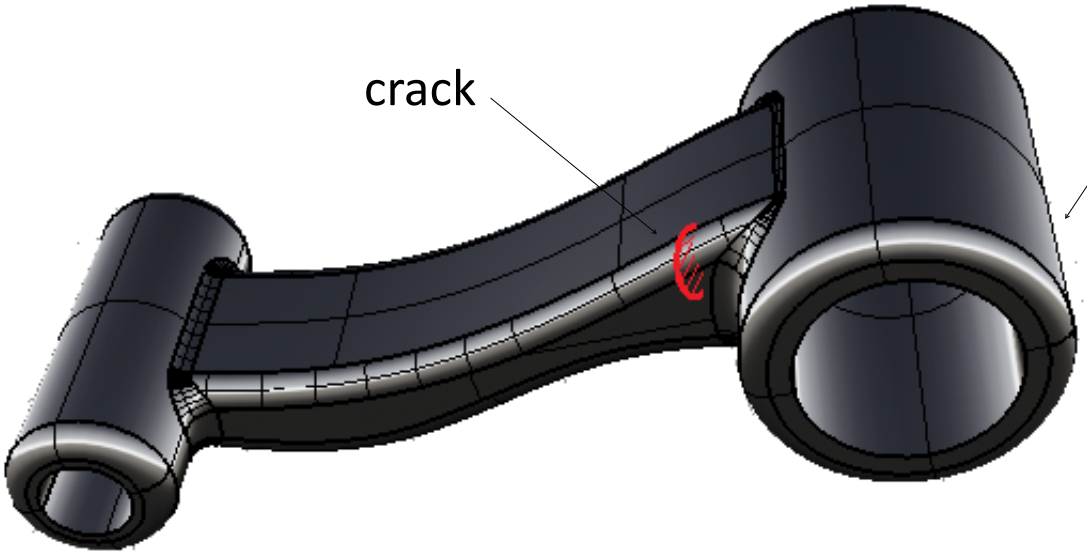

Input from Rhino, ProE, UG,…

CAD model (trimmed NURBS)

untrimmed multiple patches & T-Splines

Analysis-suitable Splines

Stress analysis

crack evolution description

fracture analysis

Conclusions

- Dual boundary integral equations combined with isogeometric analysis are used to model fracture (2D & 3D) and crack growth (2D)
- Partition of unity enrichment (2D) and graded mesh refinement (2D & 3D) are used to improve accuracy near the crack tip or crack front
- Stable quadrature scheme is proposed for singular integration in 3D. This makes the method non-sensitive to mesh distortion
- Different ways to extract stress intensity factors based on the framework of IGABEM

➡ **Questions**

- Geometry-independent field approximation (GIFT)
- Independent displacement and traction approximations
- Independent geometry and field approximations
- Contact (BETI)
- BEM Acceleration

Handling discontinuities in isogeometric formulations

with Nguyen Vinh Phu, Marie Curie Fellow

Discontinuities modeling

PUM enriched methods

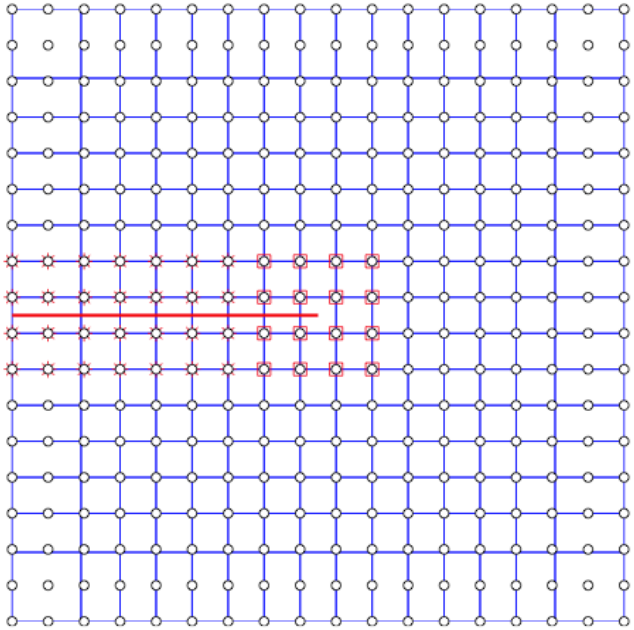

- IGA: link to CAD and accurate stress fields
- XFEM: no remeshing

Mesh conforming methods

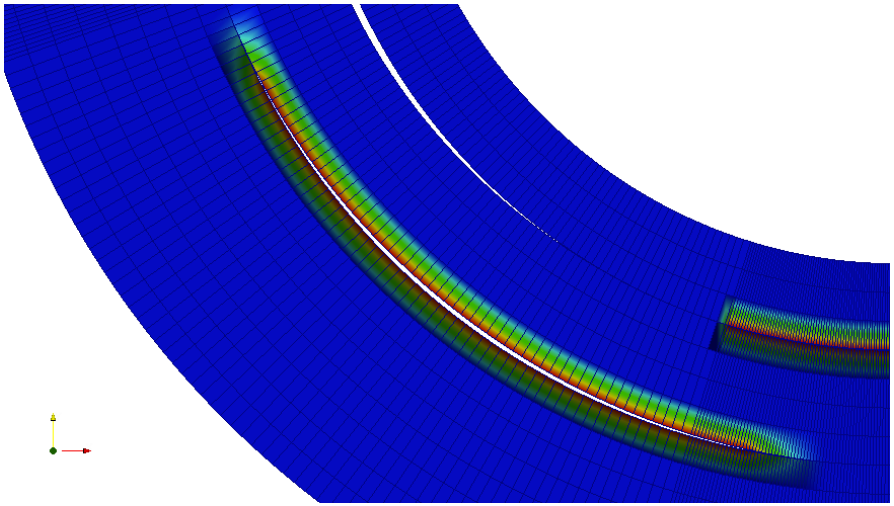

- IGA: link to CAD and accurate stress fields
- Apps: delamination

PUM enriched methods (XIGA)

$$\mathbf{u}^h(\mathbf{x}) = \sum_{I \in \mathcal{S}} R_I(\mathbf{x})\mathbf{u}_I + \sum_{J \in \mathcal{S}^c} R_J(\mathbf{x})\Phi(\mathbf{x})\mathbf{a}_J$$

NURBS basis functions

enrichment functions

1. E. De Luycker, D. J. Benson, T. Belytschko, Y. Bazilevs, and M. C. Hsu. X-FEM in isogeometric analysis for linear fracture mechanics. IJNME, 87(6):541–565, 2011.
2. S. S. Ghorashi, N. Valizadeh, and S. Mohammadi. Extended isogeometric analysis for simulation of stationary and propagating cracks. IJNME, 89(9): 1069–1101, 2012.
3. D. J. Benson, Y. Bazilevs, E. De Luycker, M.-C. Hsu, M. Scott, T. J. R. Hughes, and T. Belytschko. A generalized finite element formulation for arbitrary basis functions: From isogeometric analysis to XFEM. IJNME, 83(6):765–785, 2010.
4. A. Tambat and G. Subbarayan. Isogeometric enriched field approximations. CMAME, 245–246:1 – 21, 2012.

Delamination analysis with cohesive elements (standard approach)

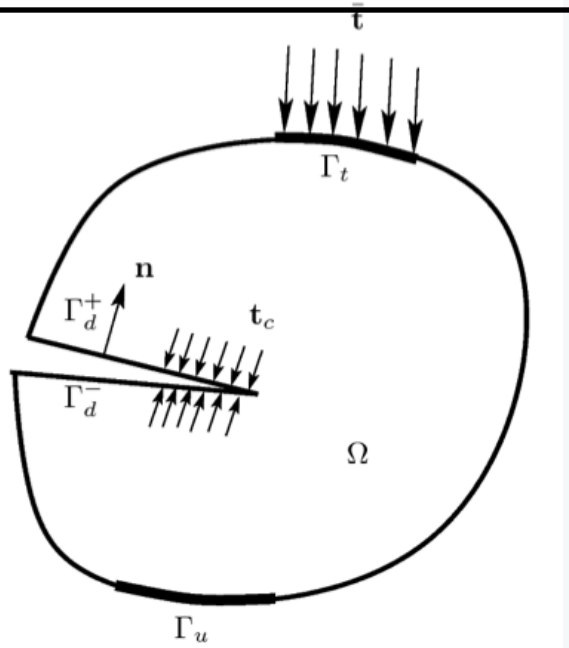

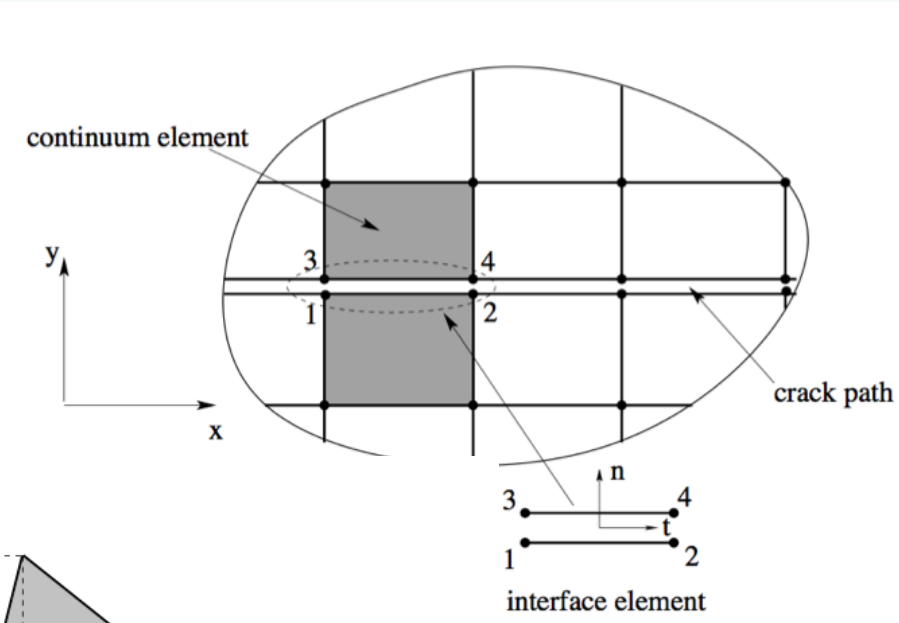

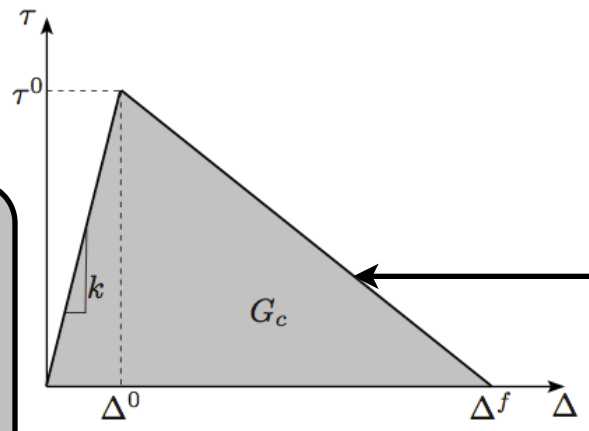

- No link to CAD
- Long preprocessing
- Refined meshes

$$\int_\Omega \delta\mathbf{u}\cdot\mathbf{b}\mathrm{d}\Omega + \int_{\Gamma_t} \delta\mathbf{u}\cdot\bar{\mathbf{t}}\mathrm{d}\Gamma_t = \int_\Omega \delta\boldsymbol{\epsilon}:\boldsymbol{\sigma}(\mathbf{u})\mathrm{d}\Omega + \int_{\Gamma_d} \delta[\![\mathbf{u}]\!]\cdot \mathrm{t}^{\mathrm{c}}([\![\mathbf{u}]\!])\mathrm{d}\Gamma_d$$

Isogeometric cohesive elements

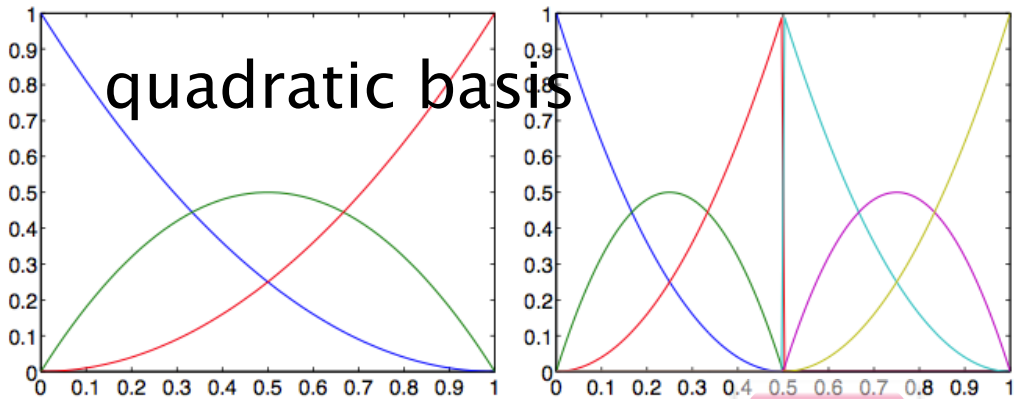

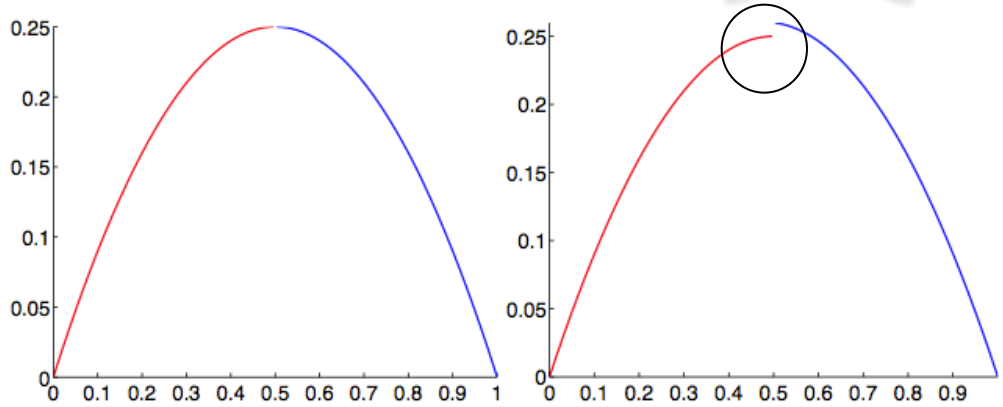

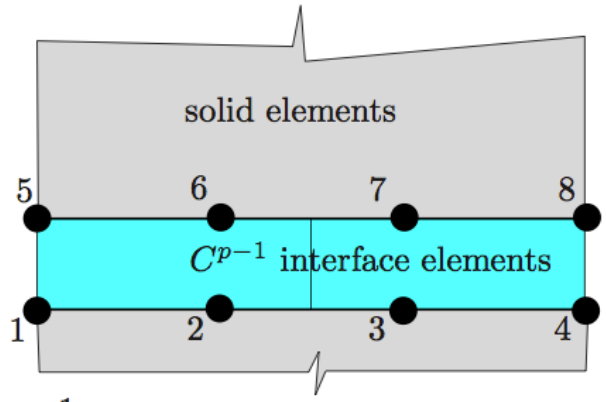

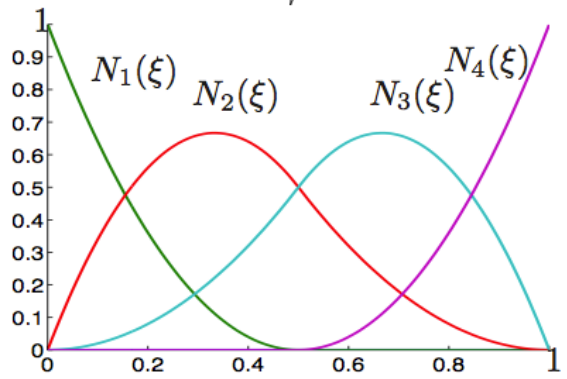

Knot insertion

1. C. V. Verhoosel, M. A. Scott, R. de Borst, and T. J. R. Hughes. An isogeometric approach to cohesive zone modeling. IJNME, 87(15):336–360, 2011.
2. V.P. Nguyen, P. Kerfriden, S. Bordas. Isogeometric cohesive elements for two and three dimensional composite delamination analysis, 2013, Arxiv.

Isogeometric cohesive elements: advantages

- Direct link to CAD
- Exact geometry
- Fast/straightforward generation of interface elements
- Accurate stress field
- Computationally cheaper

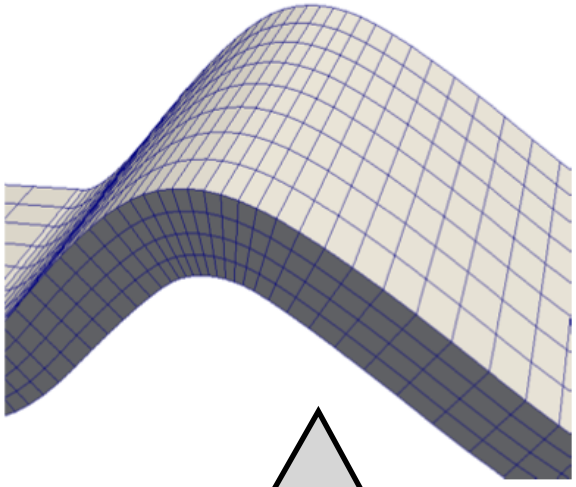

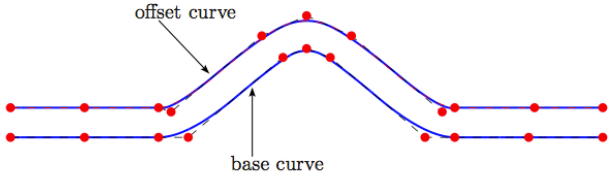

- 2D Mixed mode bending test (MMB)
- 2 x 70 quartic-linear B-spline elements
- Run time on a laptop 4GBi7: 6 s
- Energy arc-length control

V. P. Nguyen and H. Nguyen-Xuan. High-order B-splines based finite elements for delamination analysis of laminated composites. Composite Structures, 102:261–275, 2013.

Isogeometric cohesive elements: 2D example

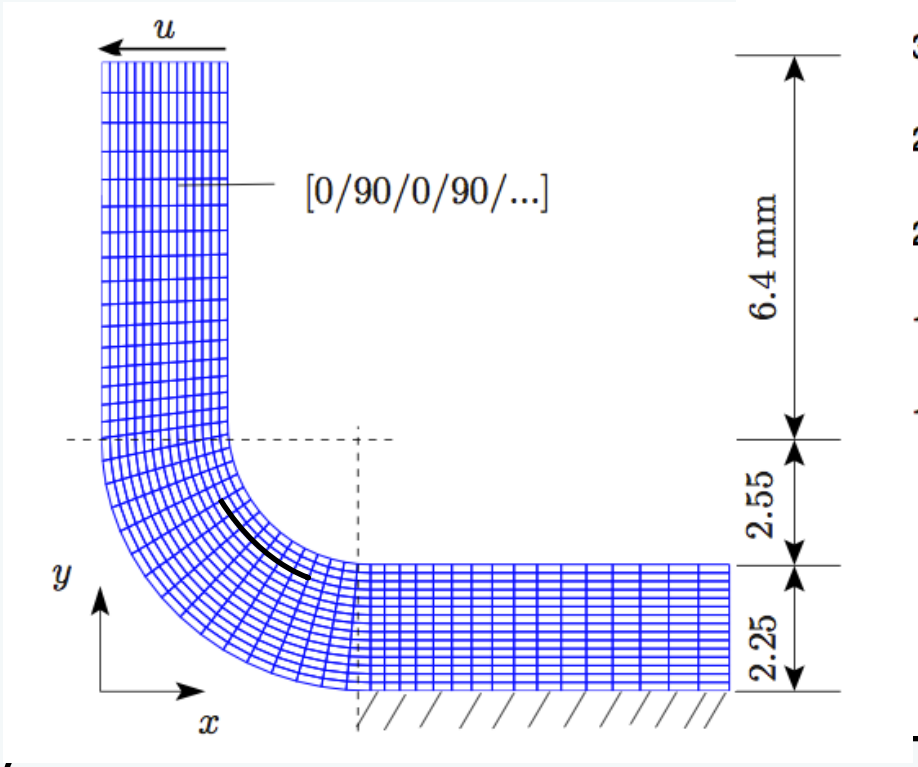

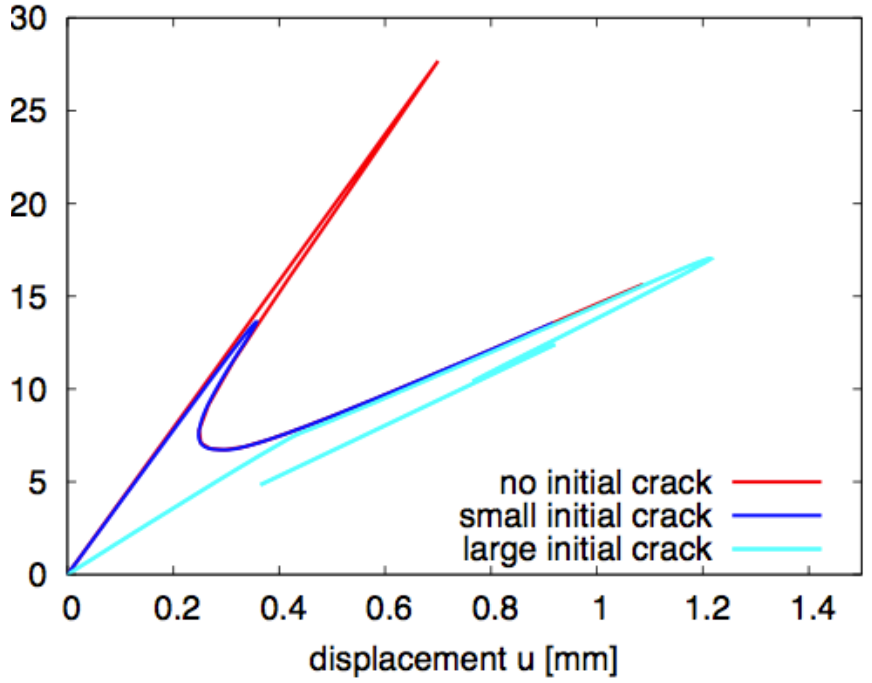

- Exact geometry by NURBS + direct link to CAD
- It is straightforward to vary
  (1) the number of plies and
  (2) # of interface elements:
- Suitable for parameter studies/design
- Solver: energy-based arc-length method (Gutierrez, 2007)

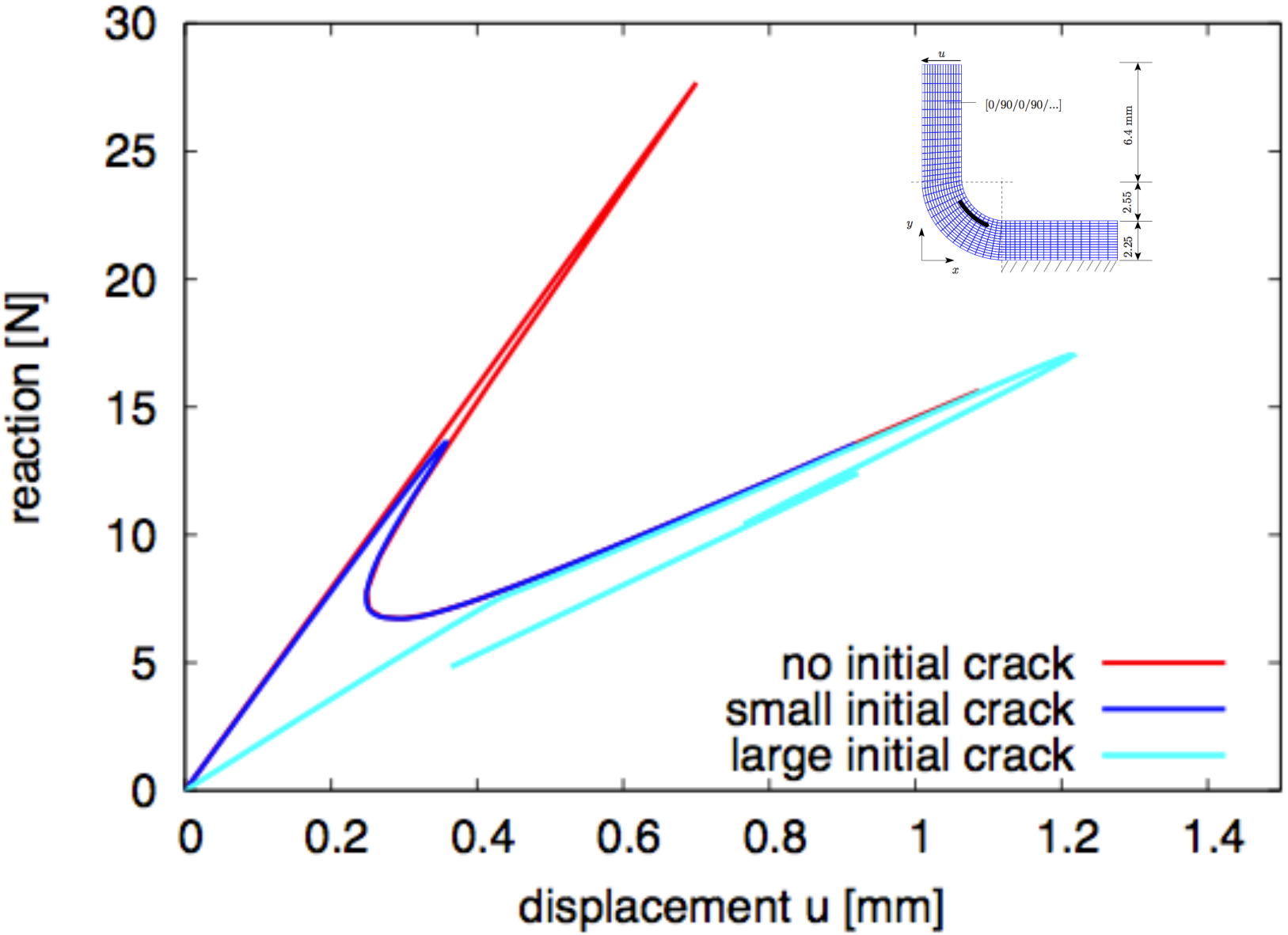
reaction [N]
displacement u [mm]
0
5
10
15
20
25
30
0
0.2
0.4
0.6
0.8
1
1.2
1.4
no initial crack
small initial crack
large initial crack
u
[0/90/0/90/...]
6.4 mm
2.55
2.25
y
x

Isogeometric cohesive elements: 2D example

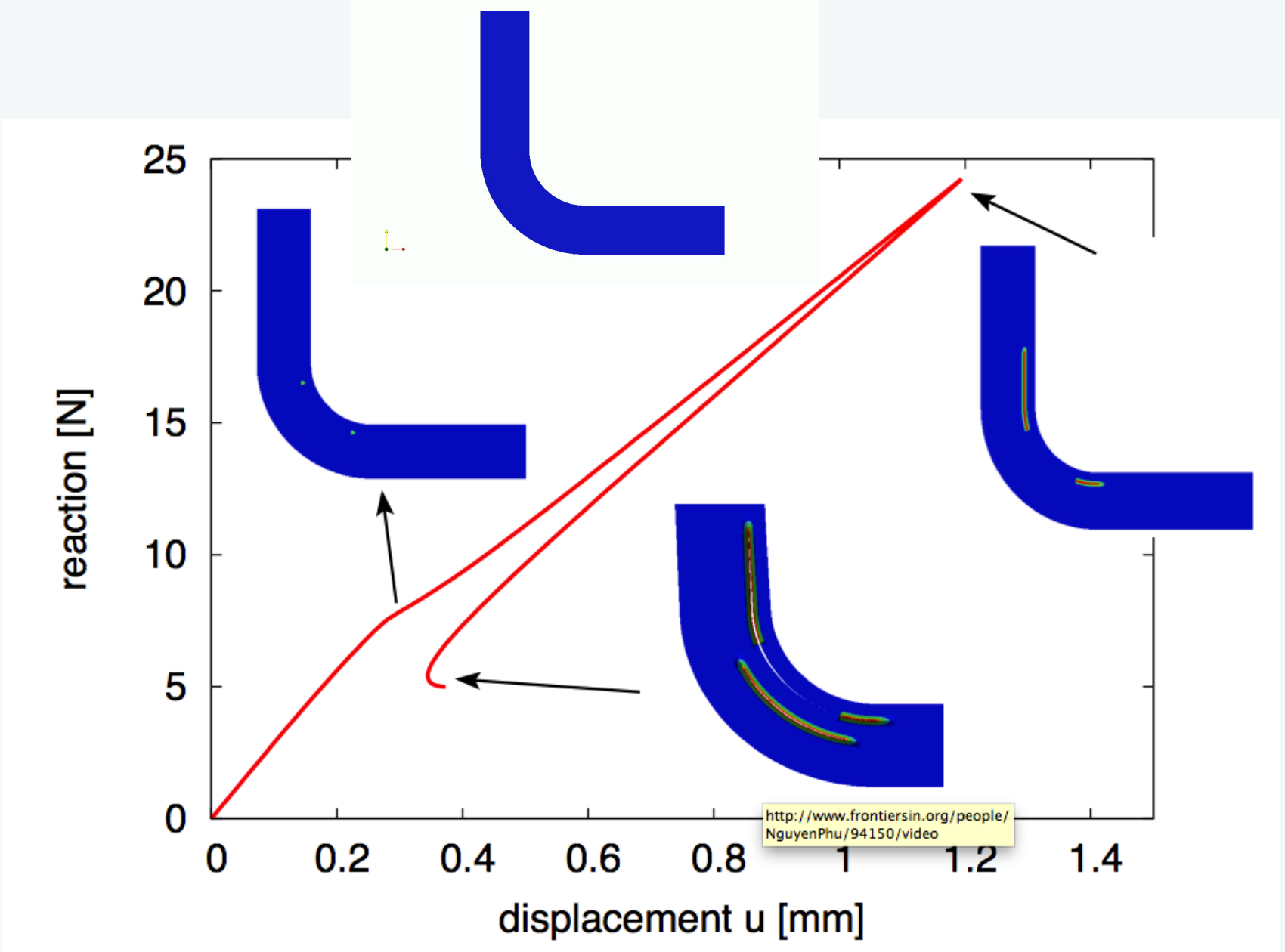

Isogeometric cohesive elements: 3D example with shells

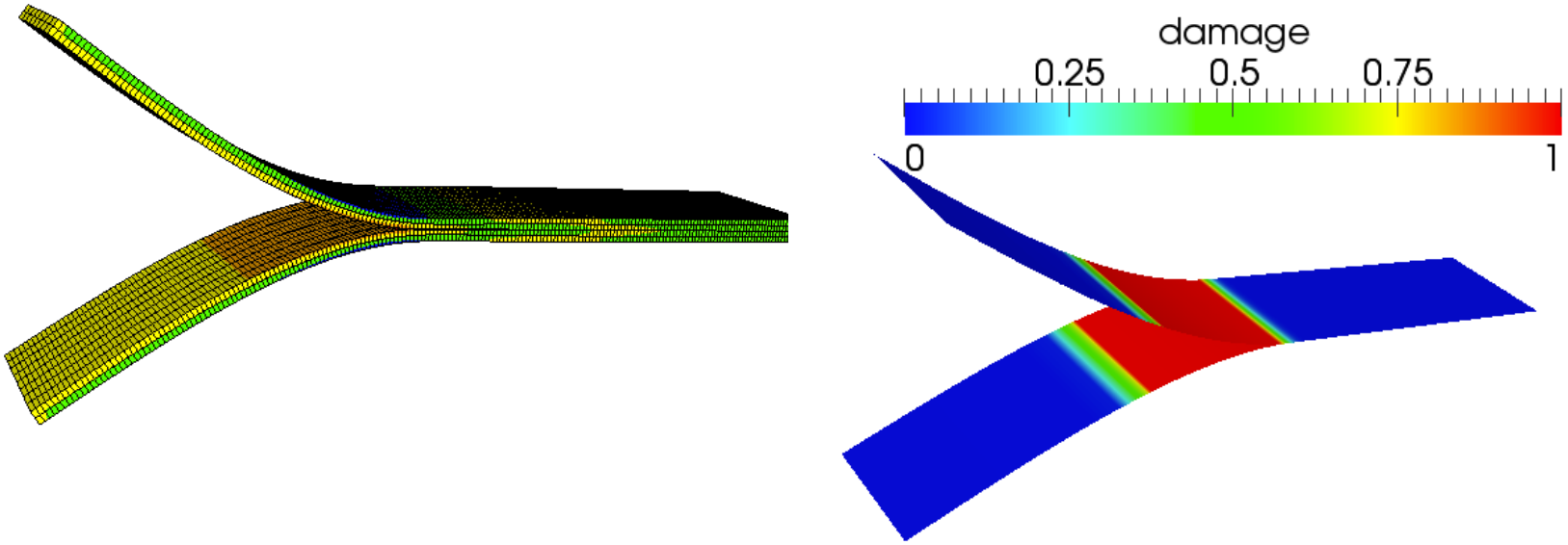

- Rotation free B-splines shell elements (Kiendl et al. CMAME)
- Two shells, one for each lamina
- Bivariate B-splines cohesive interface elements in between

Isogeometric cohesive elements: 3D examples

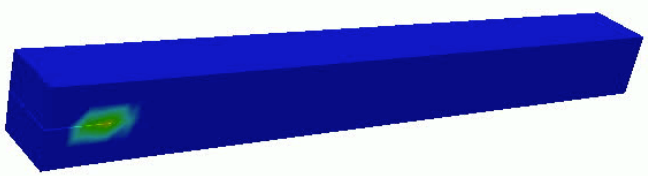

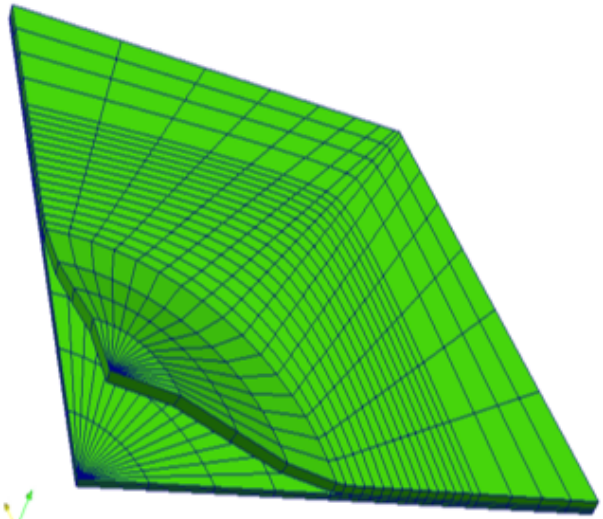

- cohesive elements for 3D meshes the same as 2D
- large deformations

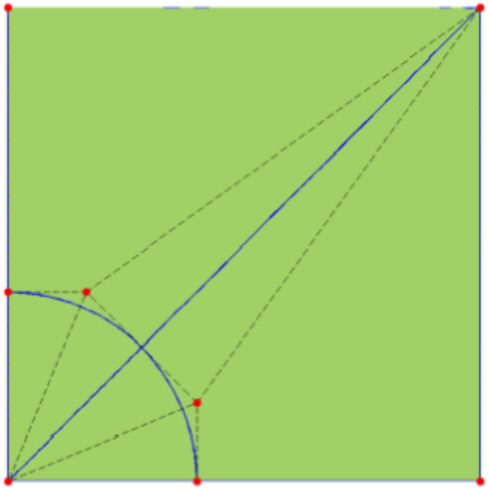

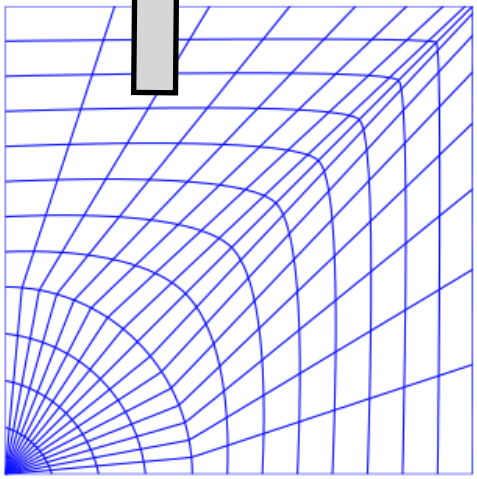

Isogeometric cohesive elements

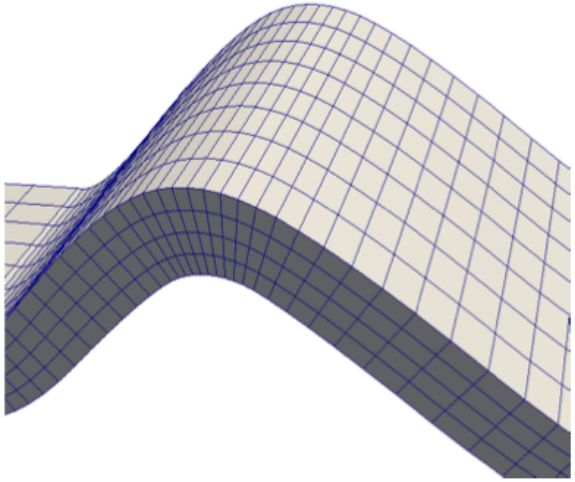

- singly curved thick-wall laminates
- geometry/displacements: NURBS
- trivariate NURBS from NURBS surface(*)
- cohesive surface interface elements

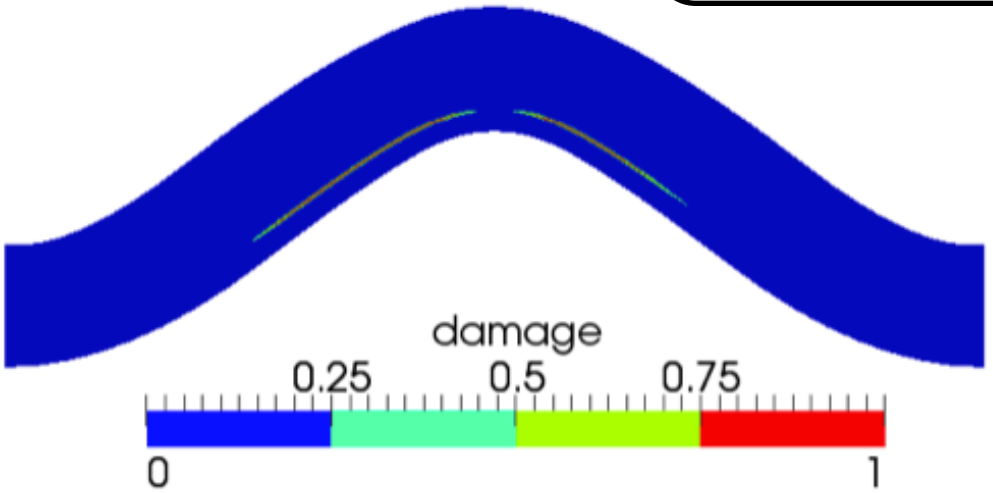

(*)V. P. Nguyen, P. Kerfriden, S.P.A. Bordas, and T. Rabczuk. An integrated design-analysis framework for three dimensional composite panels. Computer Aided Design, 2013. submitted.

Future work: model selection (continuum, plate, beam, shell?)

Model selection

- Model with shells
- Identify “hot spots” - dual
- Couple with continuum
- Coarse-grain

- Nitsche coupling - NURBS-NURBS

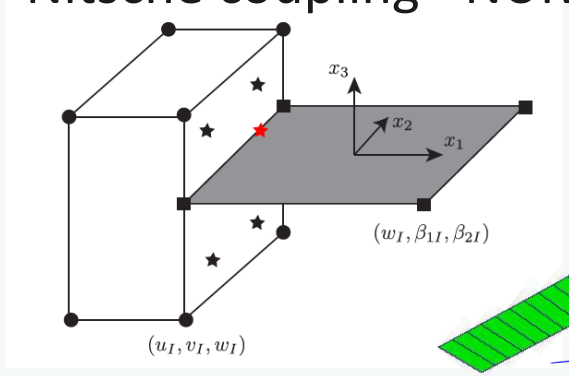

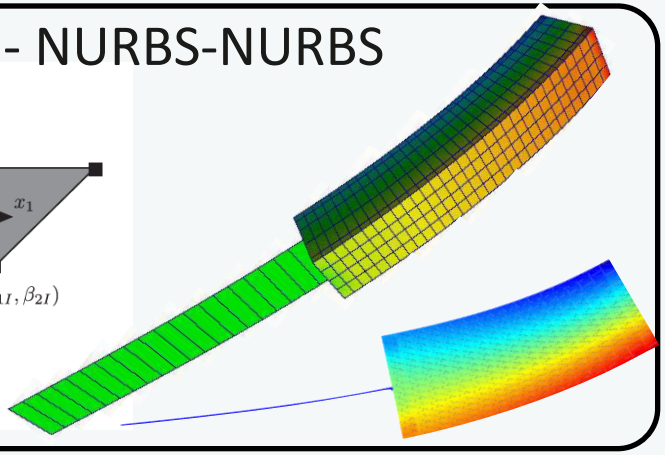

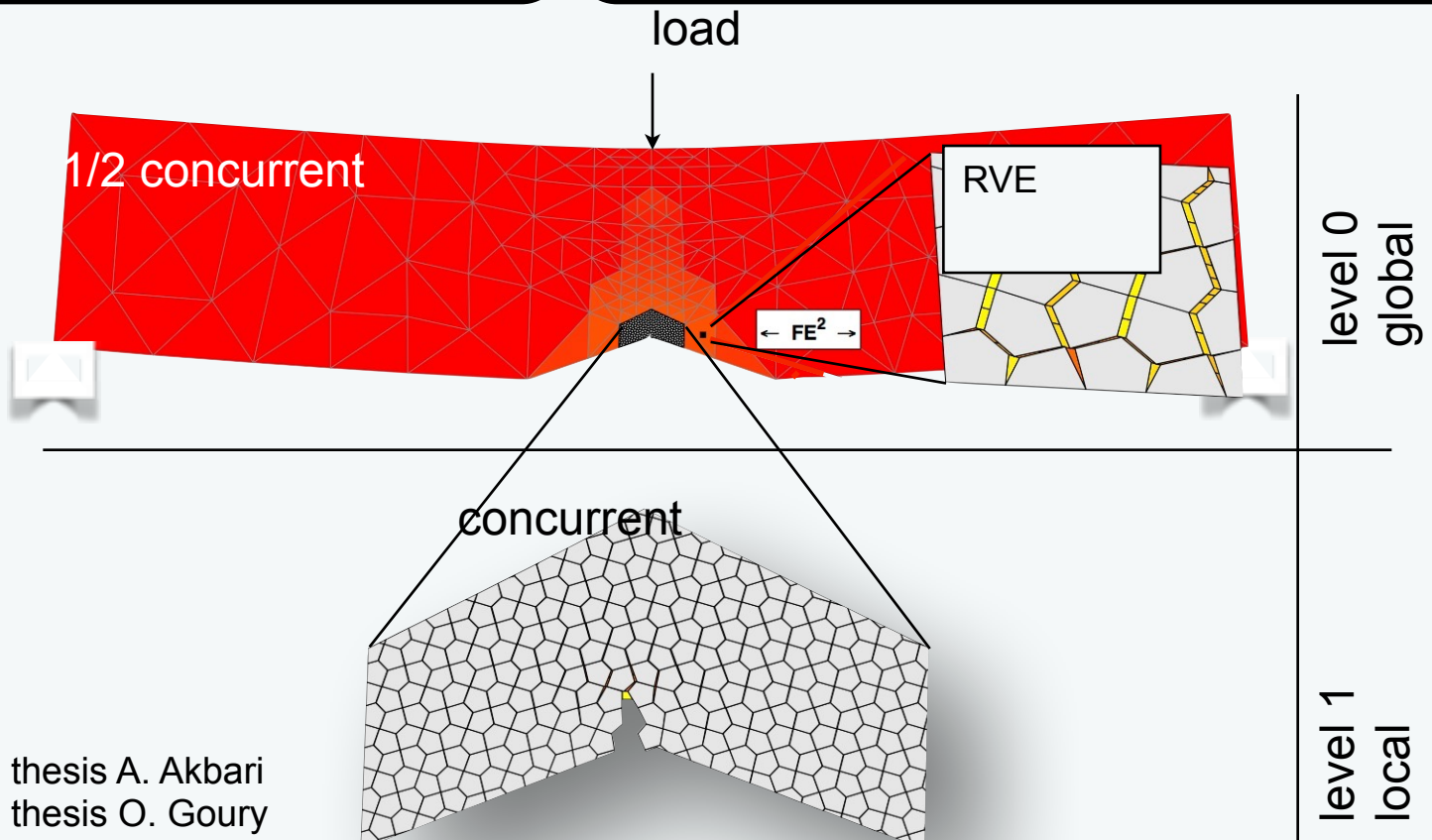

thesis A. Akbari
thesis O. Goury

Thank you for your attention!

International Centre
for Mechanical Sciences

CISM-ECCOMAS International Summer School on “Modelling, Simulation and Characterization of Multi-Scale Heterogeneous Materials” September 28, 2015 — October 2, 2015

OPEN SOURCE CODES

PERMIX: Multiscale, XFEM, large deformation, coupled 2 LAMMPS, ABAQUS, OpenMP -

MATLAB Codes: XFEM, 3D ISOGEOMETRIC XFEM, 2D ISOGEOMETRIC BEM, 2D MESHLESS
DOWNLOAD @ http://cmechanicsos.users.sourceforge.net/

COMPUTATIONAL MECHANICS DISCUSSION GROUP Request membership @
http://groups.google.com/group/computational_mechanics_discussion/about

CARDIFF UNIVERSITY
PRIFYSGOL CAERDYDD

Part III. Application to multi-crack propagation

with Danas Sutula, President Scholar

IMAM
Institute of Mechanics & Advanced Materials

Soitec

Numerical Modeling of SOI Wafer Splitting

Physical process

Manufacturing process: *SmartCut™*

- H^+ ionization of a thin surface of Si
- Bonding to a handle-wafer (stiffener)
- High temperature thermal annealing
- Nucleation and growth of cavities filled with H_2
- Pressure driven micro crack growth
- Coalescence and post-split fracture roughness

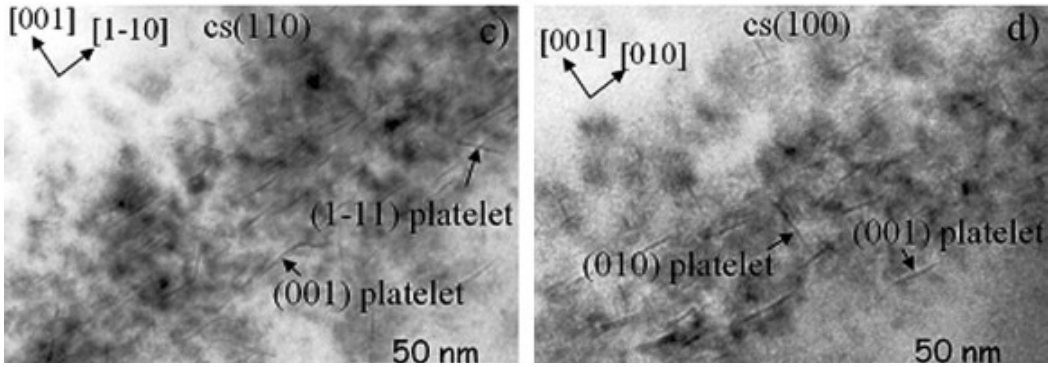

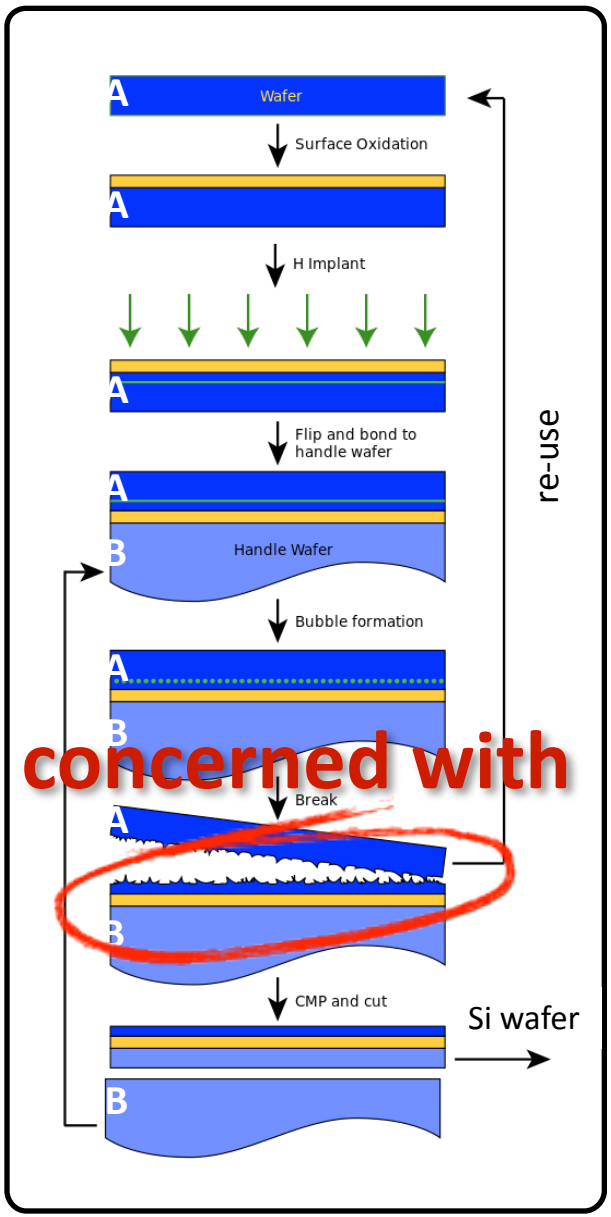

Objectives

Determine:

- micro crack nucleation points and direction
- multiple crack paths until coalescence
- time to complete fracture
- final surface roughness

Model

Modeling cavities by zero thickness surfaces

- discontinuities in the displacement field

Linear elastic fracture mechanics (LEFM)

- infinite stress at crack tip, i.e. *singularity*

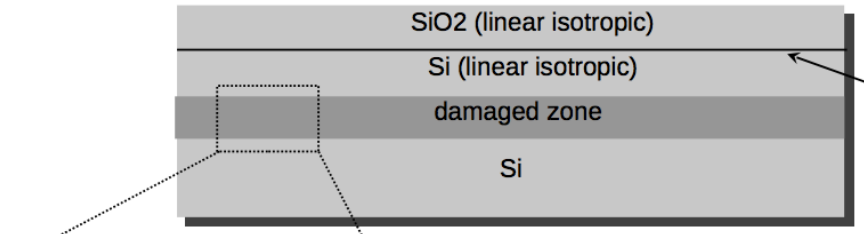

Cohesive interface with variation in surface energy

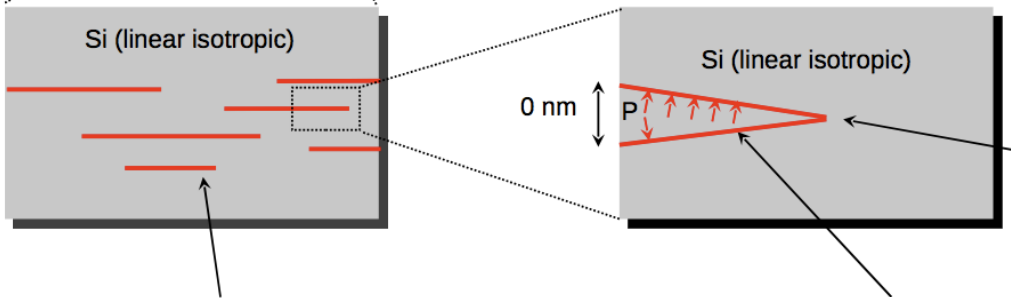

fracture criterion at the discontinuity tip

statistically distributed discontinuities

discontinuity subjected to H_2 pressure

XFEM formulation

Approximation function:

$$\mathbf{u}^h(\mathbf{x}) = \underbrace{\sum_{I\in\mathcal{N}_I} N_I(\mathbf{x})\mathbf{u}^I}_{\text{standard part}} + \underbrace{\sum_{J\in\mathcal{N}_J} N_J(\mathbf{x})H(\mathbf{x})\mathbf{a}^J}_{\text{discontinuous enrichment}} + \underbrace{\sum_{K\in\mathcal{N}_K} N_K(\mathbf{x}) \sum_{\alpha=1}^{4} f_\alpha(\mathbf{x})\mathbf{b}^{K\alpha}}_{\text{singular tip enrichment}}$$

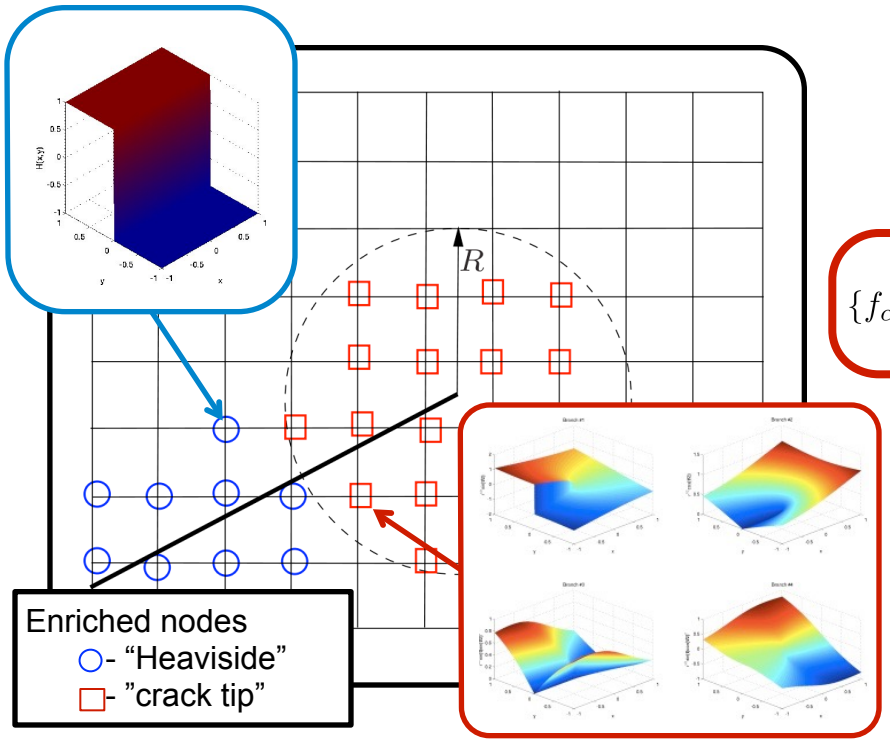

$$H(\mathbf{x}) = \begin{cases} +1 & \text{if } \mathbf{x} \text{ above crack} \\ -1 & \text{if } \mathbf{x} \text{ below crack} \end{cases}$$

$$\{f_\alpha(r,\theta), \alpha = 1,4\} = \left\{\sqrt{r}\sin\frac{\theta}{2}, \sqrt{r}\cos\frac{\theta}{2}, \sqrt{r}\sin\frac{\theta}{2}\sin\theta, \sqrt{r}\cos\frac{\theta}{2}\sin\theta\right\}$$

XFEM formulation

$$H(x) = \begin{cases} +1 & \text{if } x \text{ above crack} \\ -1 & \text{if } x \text{ below crack} \end{cases}$$

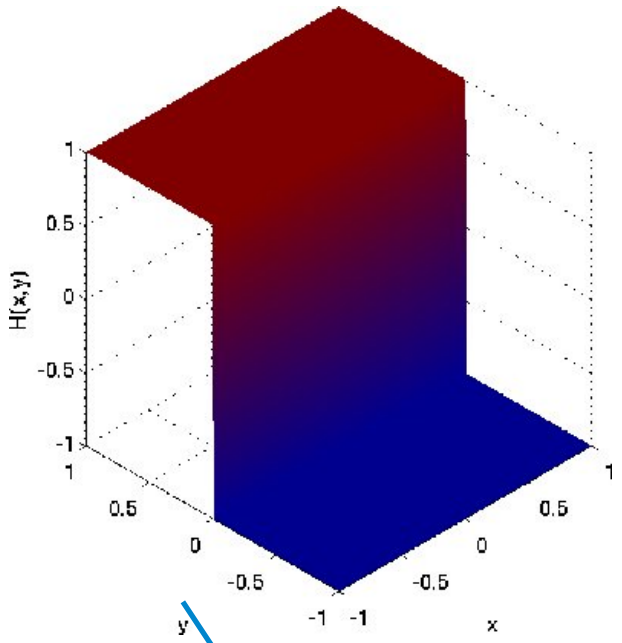

$$B(r,\theta) = \left\{ \sqrt{r}\cos\frac{\theta}{2} \quad \sqrt{r}\sin\frac{\theta}{2} \quad \sqrt{r}\sin\theta\sin\frac{\theta}{2} \quad \sqrt{r}\sin\theta\cos\frac{\theta}{2} \right\}$$

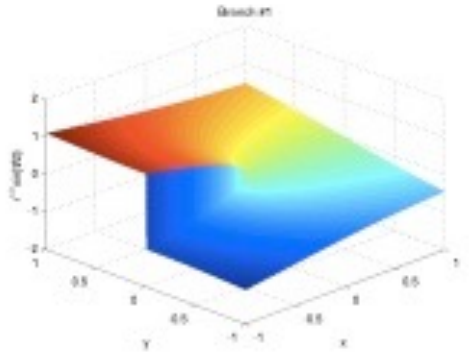

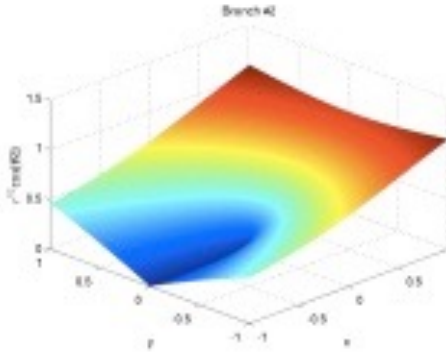

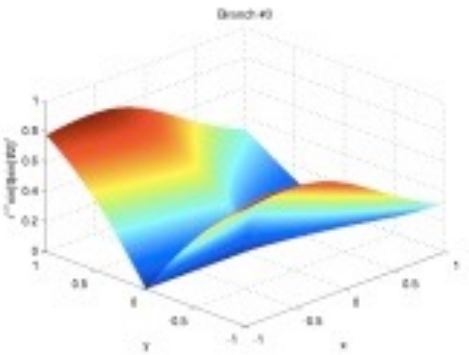

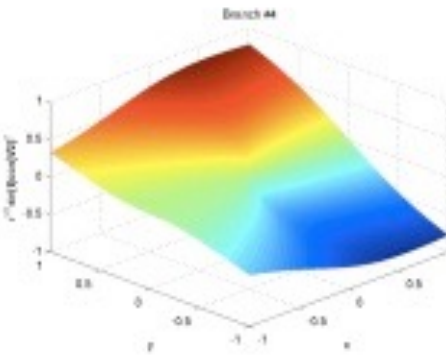

Discretization: XFEM

Extended Finite Element Method (XFEM)

- Introduced by Ted Belytschko (1999) for elastic problems

Fracture of “XFEM” using XFEM

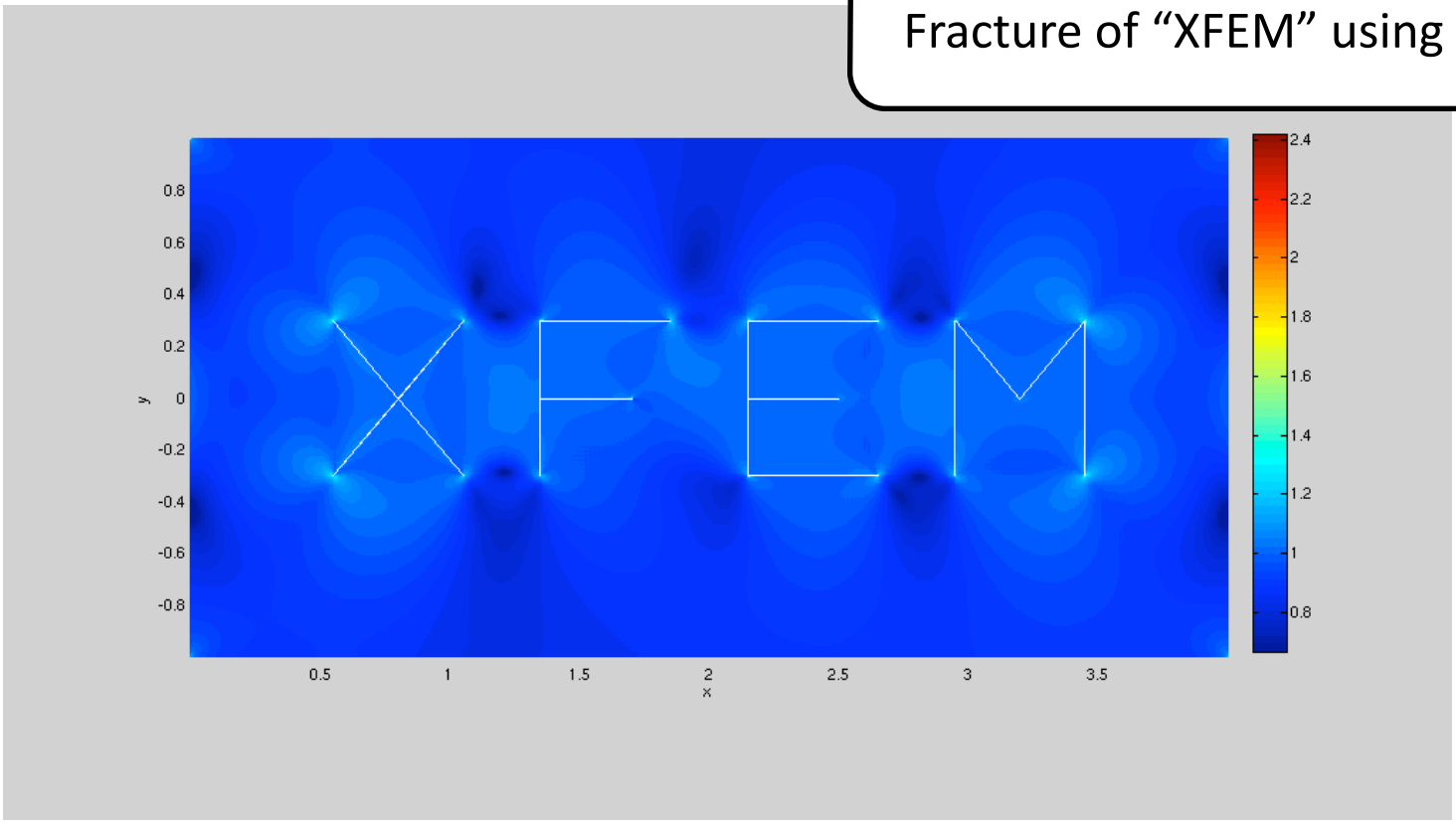

Plate with 300 cracks - vertical extension BCs

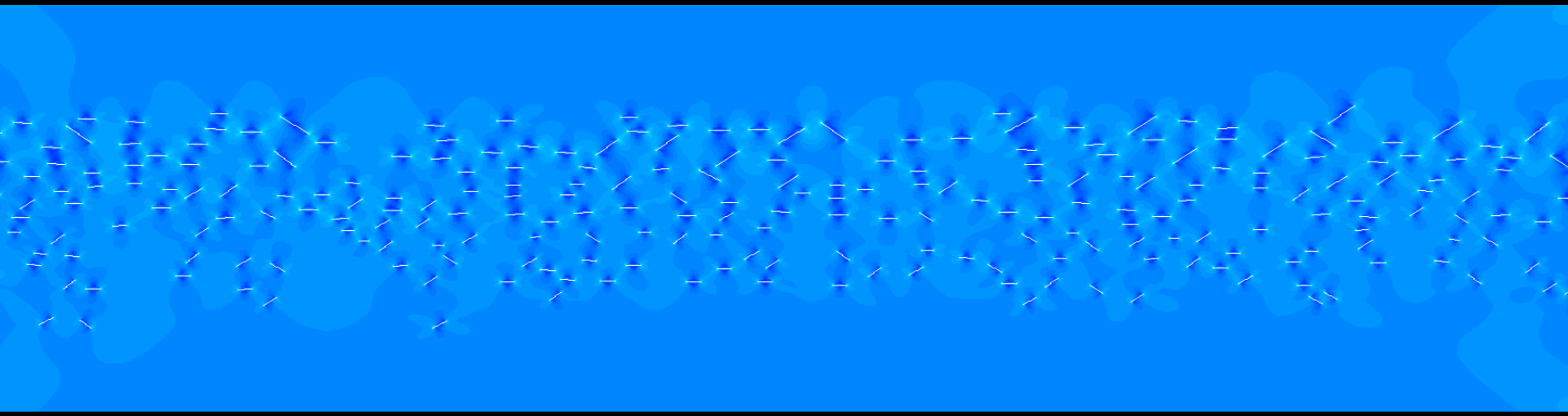

Example #1

Vertical extension of a plate with 300 cracks

Post-split roughness

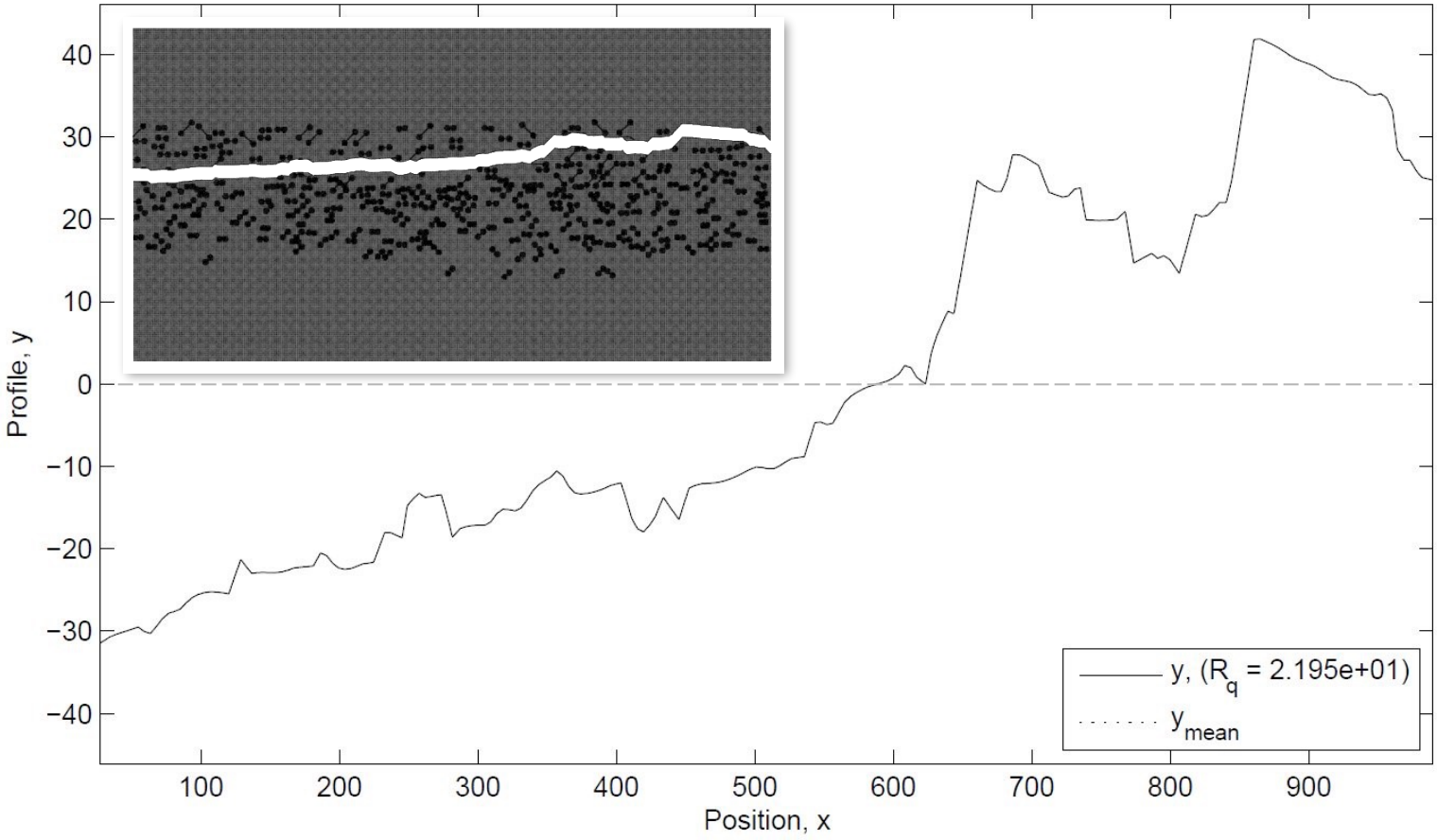

Example #2

Mechanical splitting of a wafer sample

- Post-split roughness as a function of micro crack distribution

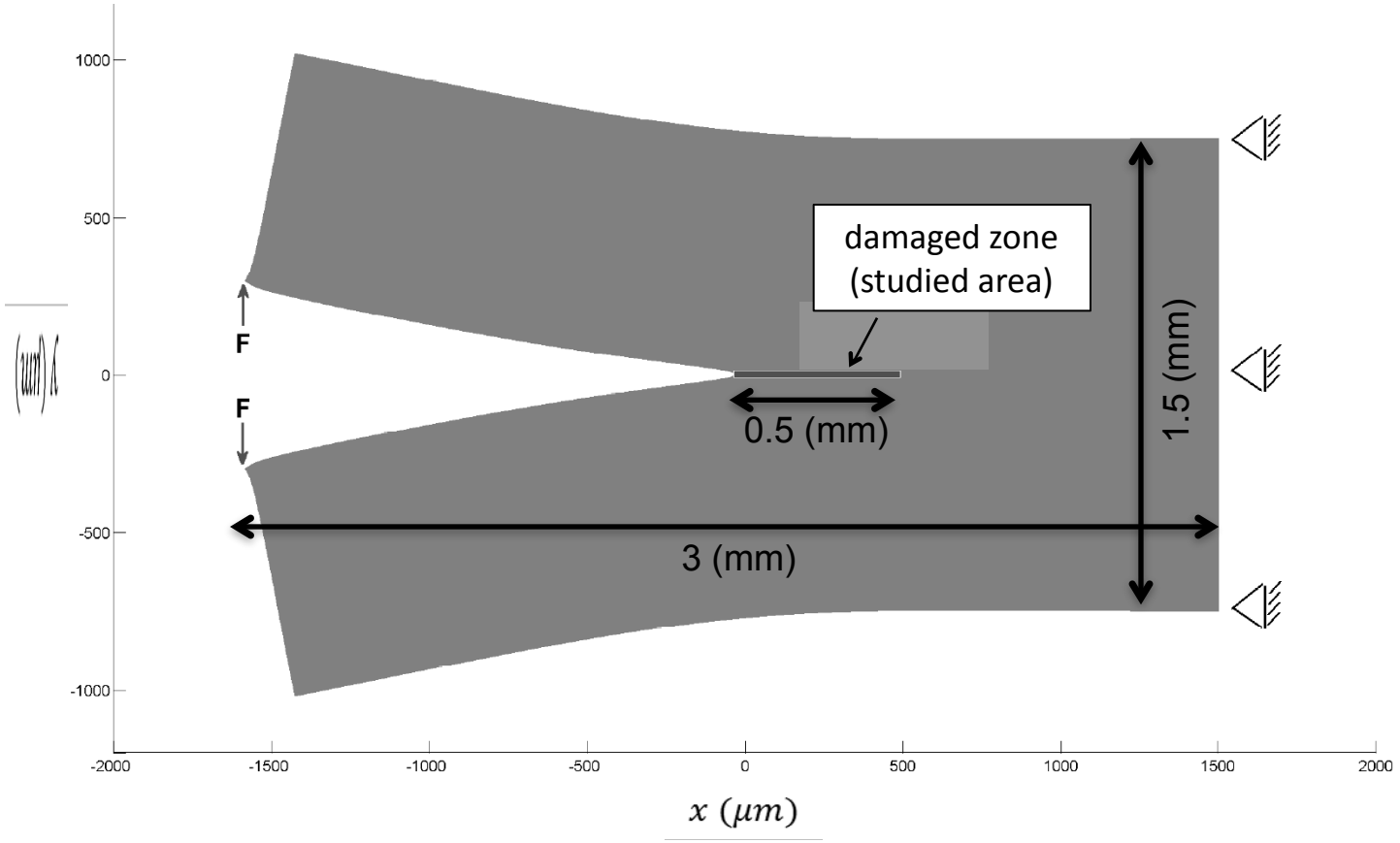

Example #2

Mechanical splitting of a wafer sample

- Discretisation (≈1mln. DOF, h_e = 150 nm)

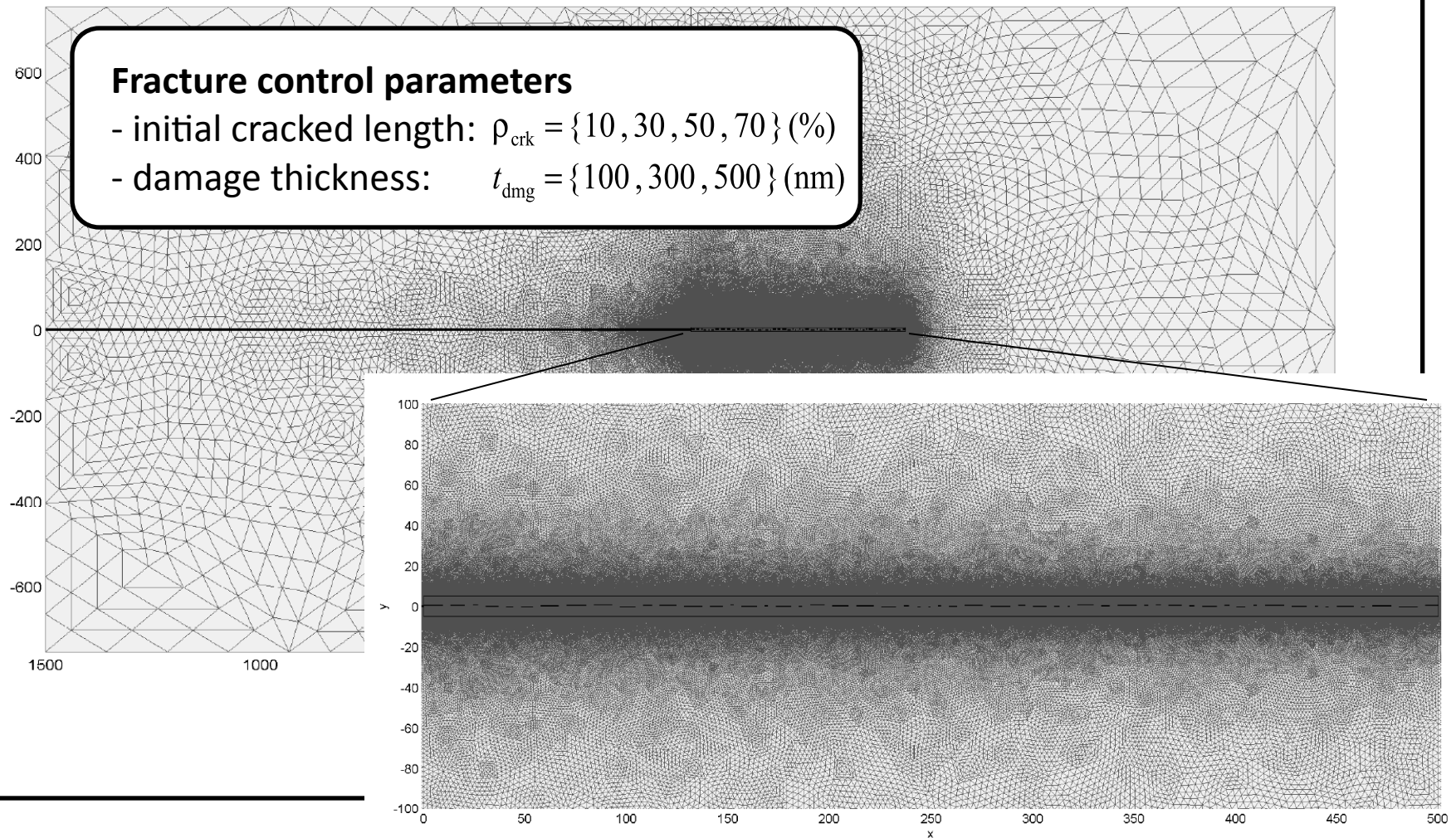

Example #2

Fracture ro

- Case exa

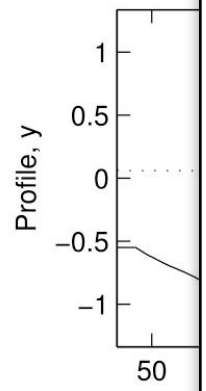

- Case exa

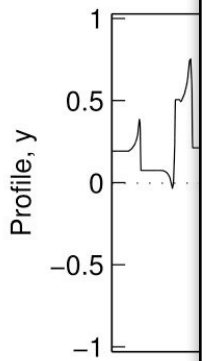

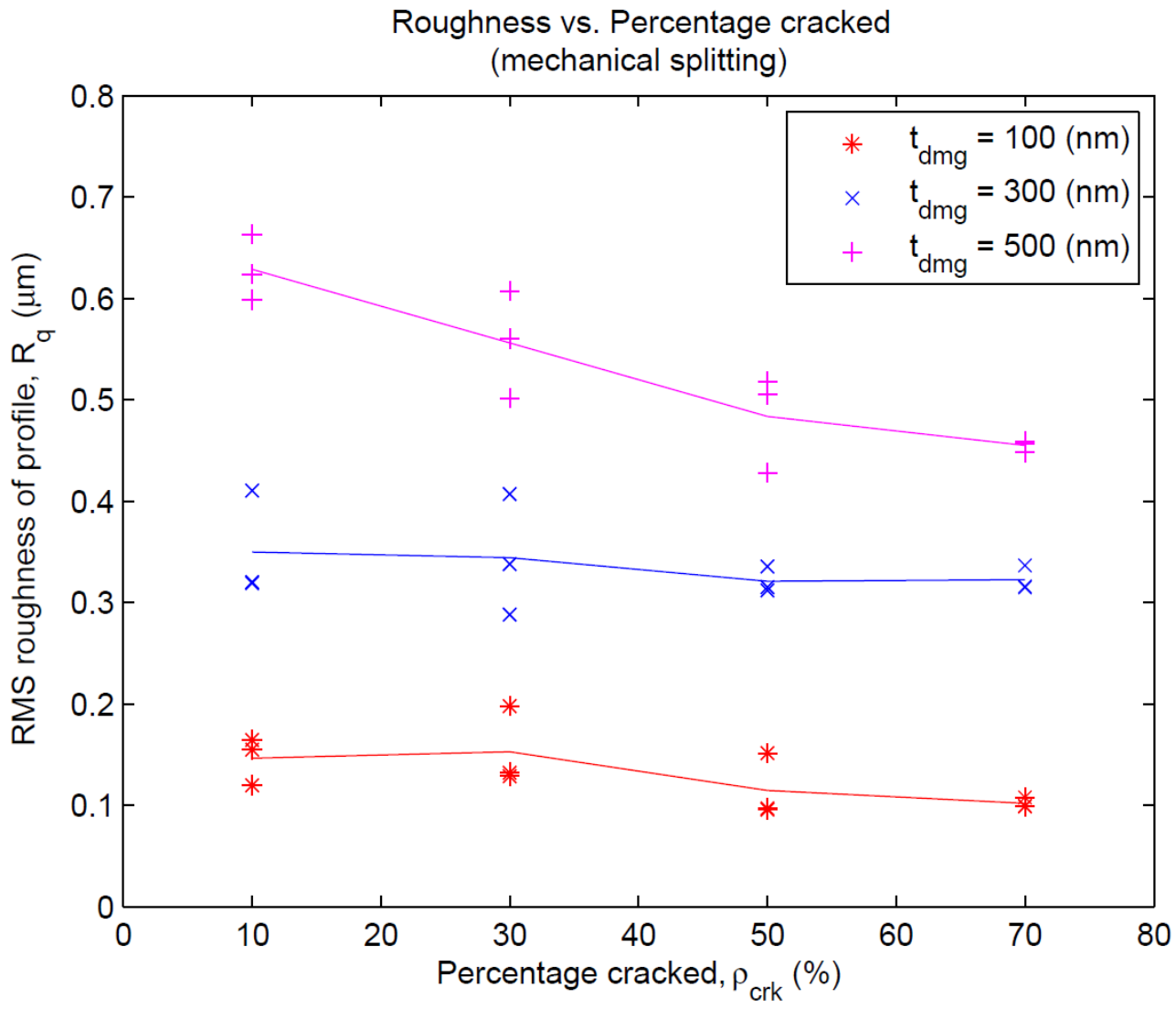

CARDIFF UNIVERSITY
PRIFYSGOL CAERDYDD

Part IV. Application to surgical simulation

with INRIA, France; Karol Miller, UWA.

erc

RealTcut

Interactive multiscale cutting simulations

IMAM
Institute of Mechanics & Advanced Materials

RealTcut

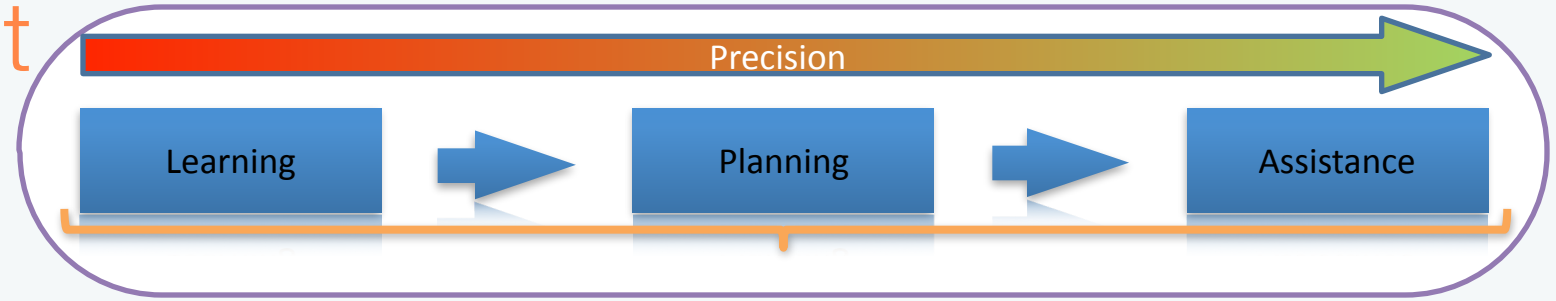

Surgical simulation (real time/interactivity)

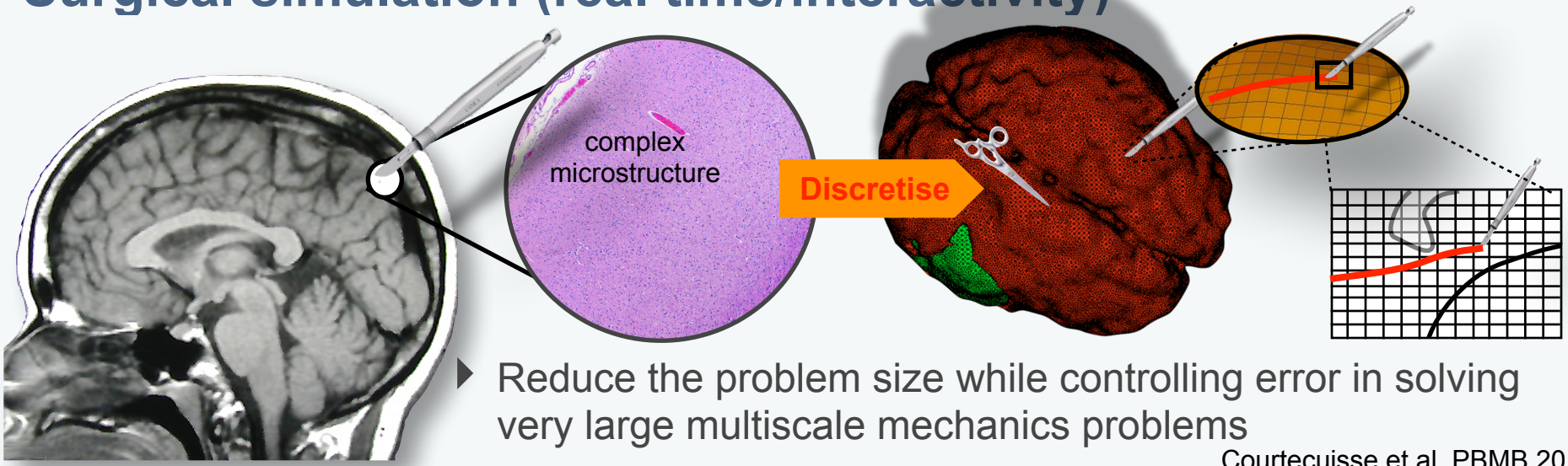

- Reduce the problem size while controlling error in solving very large multiscale mechanics problems

Courtecuisse et al. PBMB 2011

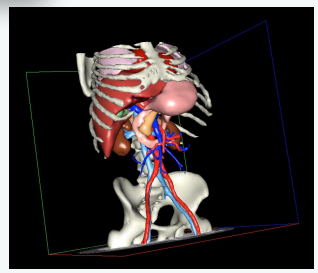

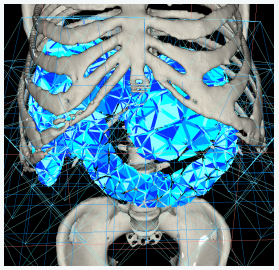

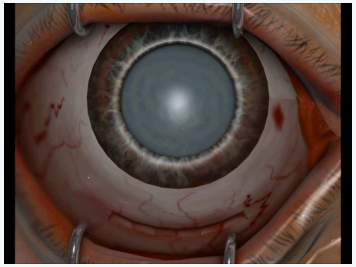

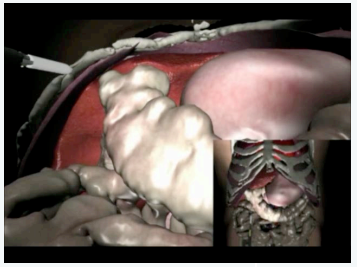

Approach

Concrete objective: compute the response of organs during surgical procedures (including cuts) in real time (50-500 solutions per second)

Two schools of thought

- constant time
  - ➡ accuracy often controlled visually only
- model reduction or “learning”
  - ➡ scarce development for biomedical problems
  - ➡ no results available for cutting

First implicit, interactive method for cutting with contact

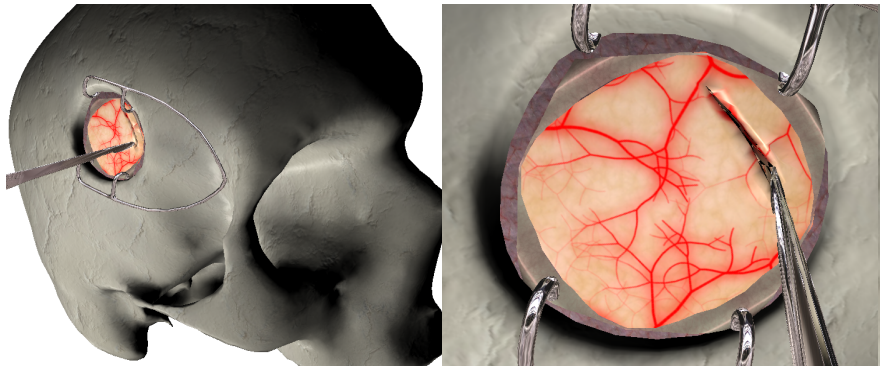

[Courtecuisse et al., MICCAI, 2013]
Collaboration INRIA

Proposed approach: maximize accuracy for given computational time. Error control

Four main difficulties

Complex geometries from medical images

segmentation

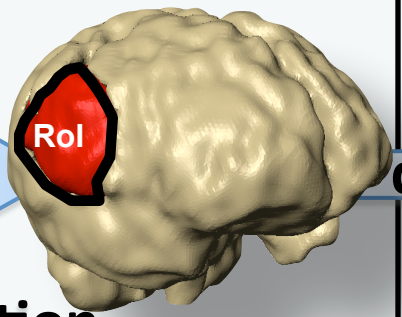

Region of interest (RoI)

Topological changes & contact

discretization

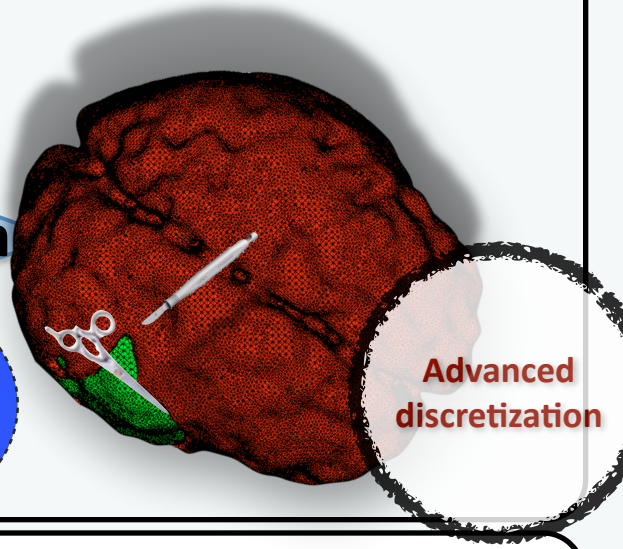

Model reduction

adaptivité

Error control

- interactivity
- space-time discretization?
- optimize use of compute resources

Verification & Validation

A semi-implicit method for real-time deformation, topological changes, and contact of soft tissues

Paper ID : 269

CARDIFF UNIVERSITY
PRIFYSGOL CAERDYDD

IMAM
Institute of Mechanics & Advanced Materials

SourceForge

TWO POST DOCS
TWO FACULTY POSITIONS AVAILABLE

OPEN SOURCE CODES

PERMIX: Multiscale, XFEM, large deformation, coupled 2 LAMMPS, ABAQUS, OpenMP - Fortran 2003, C++

MATLAB Codes: XFEM, 3D ISOGEOMETRIC XFEM, 2D ISOGEOMETRIC BEM, 2D MESHLESS
DOWNLOAD @ http://cmechanicsos.users.sourceforge.net/

COMPUTATIONAL MECHANICS DISCUSSION GROUP

Request membership @
http://groups.google.com/group/computational_mechanics_discussion/about